

## 4.6 Seismic Reflection

### 4.6.1 Seismic Reflection Profiling

#### 4.6.1.1 Scope and Objectives

The scope of the seismic program was to conduct source tests and other parameter tests during two walkaways and collect 1,500 feet of CDP data along two perpendicular lines 500 and 1000 feet long (see Plate 4-2). The CDP data was intended to test whether or not the seismic method could bridge the lithologic information gap between the trench and the boreholes especially in the upper 150 feet.

#### 4.6.1.2 Data Reduction

During the source tests and walkaways, very low signal-to-noise ratios were observed. Attempts to increase these ratios, including stacking and filtering, made small improvements. When such low ratios are inherent in seismic data, subsequent use of the data must be limited. The most major limitation, namely the inability to interpret laterally continuous beds, is due to the loss of coherency. Coherency is the most important aid to interpretation of seismic data and increases the confidence of the interpretation. Coherency of events or units is manifested on a seismic section as strong amplitude wavelets which align laterally to produce an easily recognized trend which, depending on the geology, may be curved or straight. Loss of coherency occurs due to near-surface inconsistencies or discontinuous geology. As the source energy passes through the earth, its strength is reduced. The more reduced or attenuated the signal strength becomes the less coherent the recorded signal. The Wake County site is characterized by a non-uniform near-surface, effectively reducing the coherency of recorded signal. Some of the non-uniformities include an irregular, deeply weathered layer; a large near-surface velocity gradient which produces strong refractions and reduces transmitted signal strength; and deeper units with similar acoustic properties.

As detailed in their Draft Report submitted under separate cover (Blackhawk, 1997), Blackhawk processed the seismic data using conventional techniques. Due to the low signal-to-noise ratio and narrow bandwidth of the data, enhanced processing was deemed necessary. The raw data was sent to Sterling Seismic Services, Ltd. (Sterling) for processing. Sterling processed the previous seismic data collected at the site by another contractor and has extensive experience with processing data acquired with the vibratory source used for this survey. Because of their experience, they were recognized as having the necessary capabilities to process this challenging data set.

The specific processing steps used by Sterling were as follows:

- Vibroseis sweep correlation
- Geometry and trace edit
- Gain recovery
- Surface consistent amplitude analysis and recovery
- Surface consistent deconvolution, spiking operator: 60 msec, noise: 0.01%
- Spectral enhancement (100 - 400 Hz)
- Green Mountain refraction statics, datum: 400 feet, velocity: 10,500 feet/sec, near-surface velocity: 1,500 feet/sec
- Common depth point gather
- Iteration 1 velocity/mute analysis and application
- Surface consistent automatic statics, 20 - 300 msec window
- Linear noise reject, f-k filter
- Iteration 2 velocity/mute analysis and application
- Surface consistent automatic statics, 10 - 400 msec window
- Bandpass filter (100/24 - 400/72 Hz/dB)
- Time variant scaling gates
- Common depth point stack
- Spectral enhancement (100 - 400 Hz)
- Post stack enhancement (100 - 400 Hz)
- Bandpass filter 0.0 - 0.5 sec (100/24 - 260/72 Hz/dB)
- Time variant scaling gates



Besides the application of the preceding processing steps, Sterling achieved good results by synthesizing a correlation wavelet rather than using the wavelet generated on the vibrator. The use of a synthetic wavelet has proved appropriate during previous work Sterling has performed for other contractors using the same vibrator.

Careful muting of the near-surface "noise" signals was a necessary step in the processing. Since these signals are of a much higher amplitude than other desired signals down the record, allowing them to remain in the data is counterproductive. The progressive application of processing steps and muting is presented in Appendix I. The plots in Appendix I represent progressive steps in processing the CDP data. The intent of presenting this data is to allow observation of the changes to the data that each significant processing step brings. Scaling and trace balance have been applied to all.

In order to convert reflections identified on the seismic section to depth, an average velocity function was calculated. This function was calculated by interpolating all of the stacking velocities to like times and mathematically averaging. Given the relative insensitivity of this data set to velocity, the calculated depths should be considered approximate and not corrected for dip. The calculated velocity-depth conversion function is shown in Table 4-9.

Since the overall quality of the seismic sections is fair at best, further processing in terms of migration to depth was deemed unnecessary due to the time and expense without expectation of gaining significant additional information. Relative depths of individual reflections can be calculated using the above velocity function.

The limits of resolution of the seismic data are subject to interpretation. The horizontal subsurface sampling in terms of trace spacing is 1 foot since the shotpoint spacing was 2 feet and each station was shot. However, considering the overall frequency of the data at approximately 125 Hz the Fresnel zone radius is approximately 80 feet. Therefore, the horizontal resolution around 80 feet at 150 feet. The vertical resolution is somewhat more difficult to calculate. Given the insensitivity of the data to changes in frequency and velocity, the errors in vertical resolution increase greatly with depth. From 0 to 200 feet the vertical resolution may be approximately 15 to 25 feet, but from 200 to 400 feet below ground surface the resolution is on the order of 70 to 80 feet. Since the useable data is largely below 125 feet, the vertical resolution is approximately 70 feet at best.

The data reduction steps for the refraction data are detailed in the Blackhawk report.

#### **4.6.1.3 Interpretation Results**

Interpretation of the seismic data was performed by identifying packages of reflections on the seismic section. Due to the need to reduce near-surface signals (muting) to eliminate unwanted returns such as refractions, ground roll and wide-angle reflections, the first interpretable reflections begin at approximately 40 msec or approximately 125 feet below ground surface. Rigorous and exact correlation of seismic reflections with known geologic units was difficult mainly

due to lack of coherency (caused by the non-uniform near-surface) and also due to the truncation of reflections at the 40 msec level (caused by the removal or muting of much of the data from 0 to 40 msec or so to remove unwanted noise). Without better correlation between the boreholes and the seismic section, individual reflections were not identified. The focus was placed then on identifying groups or packages of reflections that would indicate the overall dip of the beds, larger scale faulting, and other structural features such as folds. These packages are presented on Plate 4-2 and Figure 4-11. Each plate shows a seismic line without interpretation on the top and a line drawing of the interpretation on the bottom. The short line segments shown in the line drawing portion of the plates are meant to indicate the overall trend of the data and do not represent geologic interfaces.

Line 1 shows east-dipping reflections in the eastern section of the line and a small synclinal-anticlinal pair in the western section. Four packages of reflections have been interpreted on this line. Each package is differentiated by changes in trend or dip of the reflections. Packages A, B, and C are similar in that they are interpreted to represent somewhat steeply dipping beds with laterally discontinuous, but relatively similarly aligned reflections indicating the beds. A possible fault zone is indicated on the section and may correspond with the W-8 fault or a related splay thereof. It has been interpreted mainly by the discontinuity of reflections on either side, however there are small west-dipping reflections at shotpoints 300 to 320 and two-way travel times 90 to 100 msec which may be from the fault itself. Package D to the west has different dips than those to the east. This package is interpreted to represent a slight syncline/anticline pair with the syncline axis at shotpoint 450 and the anticline axis at shotpoint 370.

Line 2's reflections are much more discontinuous than Line 1's yet indicate generally flat-lying reflectors. Two packages have been interpreted, Package E to the north is unremarkable in its character with the exception of a possible bowl-shaped feature centered about shotpoint 1190 and more pronounced to the north (two-way travel times of 70 to 50 msec and shotpoints 1190 to 1240.) Package F is distinct from Package E only by the slight indication of reflections that dip somewhat steeply to the south. The cause of this dip is not understood. No fault zones have been interpreted on this line. Faults such as the W-8 would be imaged nearly flat-lying at this orientation. Lack of good signal coherency restricts the interpretation of such features on this line.

#### 4.6.1.4 Discussion

Given the challenging seismic character of this site, the seismic data interpretations are limited. Their usefulness is in corroborating the geologic interpretation and in delineating larger-scale structural features such as the syncline/anticline and the possible fault zones on Line 1. Since the data lack coherency and therefore continuity and confidence, even detailed work with synthetics would be limited in application to the area immediately adjacent to the borehole.

#### **4.6.1.5 Recommendations**

Given the objectives of the seismic survey, namely to bridge the data gap between the trench and the boreholes above 150 feet, continued seismic surveying is not indicated. The resolution of individual reflections and the initial depth of usable information obtained is not within the stated objectives of the survey. However, the larger scale information obtained below 150 feet indicate that the method may need to be reconsidered should any of the premises of the overall project change such as the location of the facility, changes to the design or newly identified hydrogeologic data gaps.

Collect of additional refraction data is not indicated.

#### **4.6.2 Vertical Seismic Profile (VSP)**

##### **4.6.2.1 Scope and Objectives**

The scope and objective of the VSP survey was to assist in the interpretation of the seismic data through the use of vertical seismic profile data collected from borehole W205CH1. A second objective of the VSP survey was to collect shear wave data to calculate engineering parameters.

##### **4.6.2.2 Processing and Results**

The processing and results are discussed in the Blackhawk report. In summary, the use of the vibratory source severely limited the first arrival identification and usefulness of both offsets in the VSP data. This limitation affected subsequent calculation of engineering parameters along with velocity and time data for processing the entire VSP data set. Processed VSP data yields few reflections; there are two that are notable - one at approximately 55 msec and one at 25 msec. Since the primary objective of the VSP was to tie the seismic sections to depth, no attempt was made to correlate these reflections to well logs since both of these reflections are above the zone of interpretable data on the CDP sections.

##### **4.6.2.3 Recommendations**

Further collection of VSP data is not indicated at this time.

#### 4.7 Recommended Site Investigation Tools

The results of this investigation indicate that a subset of the tools evaluated during the Pilot Study can be effectively utilized to acquire and to integrate sufficient hydrogeologic data to meet the objectives of the supplemental investigation program (SIP) and the intent of the LWP. The evaluation of the GM-1 Pilot Study results indicates that sufficient stratigraphic and lithologic data can be compiled using a reduced combination of geophysical and imaging tools for the purpose of hole to hole correlation, the identification of stratigraphic "packages", and the description of fracture and bedding orientation/character. The hydrogeologic character of the boreholes and the quantification of the hydraulic parameters associated with the inflow intervals can be established through the use of hydrophysical logging and systematic packer testing of the identified inflow intervals. This combination of all geophysical, image, and hydraulic testing techniques will provide a sufficiently detailed data set to characterize the hydrogeologic system(s) of the site.

To aid in the selection of the recommended geophysical and imaging tools, panel diagrams were prepared for each well which include individual log curves and interpretations based on the geophysical data along with image analyses and the hydrophysical inflow intervals and the packer test measurements. Geophysical logs and image tools can be utilized either singly or in combination. Interpretations of the individual logs can be made using the actual measurements or with values calculated from the measurements using certain assumptions which may or may not be valid in all cases. Furthermore, conditions in the hole (for example, hole enlargements associated with fractures) may affect log response. Geophysical logs can be used to identify boundaries between rock units with different properties, but because most of these logs have volumes of investigation with radii greater than one foot it is not possible to characterize fine-scale stratigraphy within a single well. All of these factors were taken into consideration in the selection of the recommendations of the logging tools to be utilized in the supplemental site investigation.

Table 4-10 is a matrix that qualitatively rates the actual performance of the selected suite of geophysical logging tools based on results of the GM-1 Pilot Study. This table also provides a comparison of the performance of these tools to the core and BIPS data. Performance is rated by identifying the usefulness of each tool in terms of data acquisition factors, and for providing a set of geologic and hydrologic parameters that may be important for characterizing the site. The order of importance of these parameters to the project has been broadly defined as critical, useful, or not applicable under the column labeled "Importance to Project Objectives". The performance of the geophysical techniques and imaging tools is compared to that information that would be collected from conventional core logging and analysis. In each case, the technique is identified as an excellent source of data, a fair source of data, or a technique that does not provide information on the particular geologic or hydrologic feature(s).

In most cases, actual performance met expectations. However, based on the analysis of geophysical log performance the following issues were noted:

- The time required to carry out the analysis was longer than anticipated due to the need for a more comprehensive approach in the pilot study than is likely required for the site characterization itself. Consequently, the log acquisition and analysis was somewhat more expensive than anticipated.
- There was a depth discrepancy between BIPS and FMI, and between the 3-arm caliper and the other logs. In no case was this discrepancy greater than about 1.5 feet. Although procedures were in place to identify the source of the discrepancy, these were not applied early enough in the analysis to correct the discrepancy. Therefore, these discrepancies were propagated throughout the work. This issue has been addressed by clarifying procedures for data validation prior to analysis. Because depth differences within a single log are not affected by this discrepancy, strata thickness and fracture frequency and spacing determinations met expectations.
- The log-derived hydraulic aperture is not considered effective because the electrical properties of clays and fluids in these materials are similar, and because it was not possible to isolate the effects of fractures from the effects of the accompanying hole enlargements. However, because direct hydrologic measurements are used to quantify these parameters, the log-based estimates are not necessary.

In combination with hydrophysical testing and the packer testing of specific intervals identified, the proposed log suite will allow for the compilation of pertinent hydrogeologic information that meets all supplemental investigation program objectives. This suite of logs and hydraulic tests provides for the identification and characterization of fractures, quantitative information on porosity, permeability and the thickness of hydraulically important features, and information which can be used to develop a structural model of the site. Furthermore, the data can be used to relate key lithologic, tectonic, or weathering processes and/or factors and their influence on individual hydrologic features.

As was demonstrated through the Geologic Integration Meeting on August 14, 1997, unique geophysical signatures and patterns were developed and correlated to both the corelogs from W205CH1, W208CH1, and the GM-series trench maps for the mapping units defined in Section 5.0, using a combination of the six geophysical and imaging logs recommended for use in the supplemental field program. From the Table 4-10 comparison, a combination of six standard logs can identify the hydrogeologic, structural, and lithologic characteristics of the subsurface units at the site. The six tools proposed for use as the standard logging suite during the supplemental investigation program include:

1. Spectral Gamma
2. Three-Arm Caliper
3. Neutron and Density
4. Resistivity

5. High Resolution, Electrical Imaging
6. Full Wave Form, Acoustic

Spectral gamma - This log provides better characterization of gamma activity than a standard gamma ray, and is available with higher vertical resolution.

Three-arm caliper - This log is essential to evaluate the effect of fractures on the other logs, and can help to identify those fractures which should be evaluated for hydrological testing.

Full Wave Form Acoustic - An accurate measurement of compressional wave velocity is required to determine the extent of the weathering zone. Acquisition of acoustic full waveforms is necessary to provide quality control.

Neutron / density - Neutron and density logs (with the addition of the PEF measurement which is provided by most modern gamma-gamma sondes) are critical to accurate evaluation of the relative volumes of clays, grains (quartz, feldspar) and porosity. It is important to remember that clay volume cannot be estimated from gamma alone. Additional logs are required in this environment.

Resistivity - Resistivity is necessary to calibrate the electrical image data. In addition, it provides valuable input to improve the accurate determination of clay volume and porosity.

High Resolution Electrical Image- The FMI or other imaging device with equivalent resolution can be used to identify, orient, and characterize fractures, to determine fine-scale (1-cm) bedding features, and to position and orient bed boundaries.

## 5.0 DATA INTERPRETATION AND INTEGRATION

This section describes the data interpretation performed during the GM-1 Pilot Study in the context of contribution to enhancing and refining the pre-existing hydrogeologic model of the Site. It also presents results of the integration of these data, which was accomplished through development of the GM Cross Section (Plate 5-1). Finally, it provides a summary of significant observations made as a result of this data integration.

### 5.1 Geologic Data

This section presents a discussion of components of the Site geology that have been updated using new information collected during the GM-1 Pilot Study. These components include stratigraphy, structure, and weathering.

#### 5.1.1 Stratigraphy

##### 5.1.1.1 Rocks

Except for thin (up to about 6 feet thick), scattered patches of Tertiary high-level sediment and Quaternary alluvium (Plate 5-1, Geologic Cross Section and Plate 5-2, Geologic Map), the Site is underlain by Triassic sedimentary rocks of the Sanford Formation (Reinemund, 1955). These strata consist of a sequence of claystones, siltstones, sandstones, and conglomerates that are representative of fluvial sequences, lacustrine deposits, and alluvial fan complexes. These rock units have been described in detail in the Safety Analysis Report (SAR) (Chem-Nuclear Systems, Inc., 1995, Revision 9).

During this study, rocks mapped in GM trenches 2, 3, and 4, and logged in core from the W200 series boreholes, were described and classified according to the Folk (1980) classification system and the Lexicon. The rock units identified include the following:

- Conglomerate (> 30 percent gravel), 3 percent of total
- Sandstone, coarse to very coarse-grained, 14 percent of total
- Sandstone, medium to very fine-grained, 23 percent of total
- Mudstone (including siltstone), 54 percent of total
- Claystone (>66 percent clay), 6 percent of total

Based on thin section analyses of core-plugs taken from 5 sandstones and conglomerates from W205CH1 and W208CH1 cores by Reservoirs, Inc., (1997), the sandstones are generally poorly sorted and range compositionally from feldspathic litharenites to litharenites. Metamorphic rock fragments (11 to 42 percent), both schistose and non-schistose varieties, dominate the framework constituents, followed by quartz (17 to 43 percent) and plagioclase feldspar (4 to 22 percent). For these sandstones, the amount of pore-filling material is relatively minor, ranging from 4 percent to 20 percent of the bulk volume. Hematitic clay matrix is the most common pore-filling phase although calcite and iron oxide cements are present locally. Based on thin section analyses and core logging, the bulk of the primary pore space in the sandstones appears to have been lost through mechanical compaction rather than cementation.

Thin section analyses of core-plugs taken from four mudstone and claystone samples from the W205CH1 and W208CH1 cores by Reservoirs, Inc., (1997), indicate that these rocks are sandy to silty and consist largely of micaceous, hematitic clay matrix with admixed silt to very coarse sand-sized quartz, metamorphic rock fragments, and feldspar. X-ray diffraction of 3 core samples and geophysical logs indicate that clay fractions are primarily illite with some smectite.

The ELAN logs produced by Schlumberger show results similar to that of the core analyses, with a few exceptions. For example, the ELAN log indicates more clay in the sandstone at 159 feet in W205CH1 than does the core sample. This may be a result of the small amount of sample taken from the core for analysis or of inaccuracies in the ELAN. In addition, the ELAN shows muscovite percentages up to 25 percent. This value is greater than what was estimated from thin section analysis or from core logging. Because the ELAN is an estimate of mineral percentages, the high muscovite percentages may be a result of the large percentage of schistose rock fragments in these rocks that were not considered to be "mica" by either core loggers or microscopists. Alternatively, the percentage of muscovite indicated on the ELAN may not be accurate. As discussed in Section 4.3.4.3, the precision implied with the ELAN technique is misleading and it cannot provide quantitatively accurate mineral volumes throughout the Site.

Results of the FMI stratigraphic analysis of rocks at the Site performed by Schlumberger (Appendix D-2) are consistent with observations made from the core and ELAN analyses. The FMI analysis showed that the rocks consist of poorly-sorted sandstones and conglomerates with subrounded clasts reflecting a short distance of transport. Although scour cuts are present locally, there are rarely large clasts at the base of these scours. Cross-bedding is not commonly seen in the FMI data, although it is locally present. Many of the conglomerates and sandstones are interpreted to be sheet sand or debris flow deposits. Evidence of sheet sands are horizontal flow structures indicating an upper flow regime such as parallel laminations, poor sorting, and the lack of cross-bedding. Debris flows were recognized by poorly-sorted, matrix-supported conglomerates/coarse-grained sandstones with large clasts distributed throughout the unit and often with larger clasts near the top of the unit. Other features identified on the FMI logs were zones interpreted to be representative of diagenetic mineralization (recognized by thin, homogeneous, very resistive layers or "blobs" interpreted by Schlumberger to be either calcite nodules or chert zones) and paleosols (recognized by the presence of



mud cracks and, in some cases, root structures). In general, the results of the core analyses and geophysical logging indicate an immature sediment dominated by sheet sands, debris flows and thick, floodplain deposits containing some well-developed channel sequences.

#### 5.1.1.2 Lithofacies

Lithofacies classification is a standard part of the analysis methodology for studying sedimentary rocks (Miall, 1996). Summaries of the principles and methods involved are presented in Reading (1996), Miall (1992, 1996), Walker (1986), and Walker and James (1992). The classification used in this study is based primarily on bedding characteristics, grain size, texture, and primary sedimentary structures (Collinson and Thompson, 1982; Pettijohn and Potter, 1964; Reineck and Singh, 1973; Ricci Lucchi, 1995). Biogenic structures such as burrowing and rooting have been used as additional descriptive attributes. Chemical sedimentary structures, such as pedogenic calcretes form minor components but were also considered in defining lithofacies. The scale of an individual lithofacies unit depends on the level of detail incorporated into its definition. Facies recognized in this study were defined broadly enough to: 1) identify mappable stratigraphic units, and 2) accommodate the level of detail required by the core logging procedures (TP-29). The goal was to examine all rock units in considerable detail to make possible complete, unbiased observations of all important lithofacies attributes.

The lithofacies scheme utilized in this study is summarized in Table 5-1 and is modified from one developed by Miall (1978, 1996) for fluvial deposits. The classification is based on detailed logging of 1,129-feet of drill core from boreholes W201ARIA through W208CH1 and careful examination of 1,035-feet of section (true stratigraphic thickness) mapped in the GM trenches. The capital letter in the facies code (Table 5-1) indicates the dominant grain size, where C = conglomerate, S = sandstone, and M = mudstone and claystone. The lowercase letters serve as a mnemonic for the characteristic texture or structure of the lithofacies (e.g., x = cross-bedded, cg = clast-supported, graded, m = massive). Detailed descriptions of these lithofacies types are given in Miall (1996, Chp. 5, p. 99-130).

Bed thickness minimum cutoffs of 0.2-feet were used to define lithofacies in core from boreholes W201ARIA through W208CH1 and in stratigraphic logs derived from detailed lithologic descriptions of the GM trenches. Some of the lithofacies types are gradational with others. For example, massive sandstones with matrix contents close to the 33.3 percent mud cutoff could be classed as Sm or Smm (Table 5-1) based solely on megascopic examination. Also, the degree of weathering in the GM trenches and core taken from the weathered zone in boreholes W201ARIA through W208CH1, present problems for lithofacies classification. Where weathering is intense it is difficult to distinguish individual lithofacies within major groups. For example, intense weathering may obliterate original structures such as lamination, burrows, and rooting, which are necessary for correct subdivision within the mudstone (M) lithofacies. Lithofacies have been annotated on the graphic core logs for W205CH1, W208CH1, and the requalified core. These annotated logs will be submitted under separate cover.

### 5.1.1.3 Map Units

Lithofacies associations are groupings of genetically-related lithofacies and form the basis for map units. Map units are based on the proportion of individual lithofacies within groups as well as the nature of their bounding surfaces and

vertical sequence. Each map unit is characterized by a distinctive lithofacies assemblage. Five map units are recognized based on data derived from core logging, trench mapping, and geophysical logging:

- 1) ( $U_f$ ) upward fining sequences, generally consisting of conglomerate and sandstone at the base with mudstone at the top;
- 2) ( $M_s$ ) massive mudstone with minor sandstone;
- 3) ( $S_m$ ) massive sandstone with minor mudstone;
- 4) ( $S_{wb}$ ) well-bedded sandstone with minor mudstone; and
- 5) ( $M_{wb}$ ) well-bedded mudstone with subordinate sandstone.

While map units are primarily based on lithofacies associations, they also incorporate geophysical response criteria. A fuller description of how map units were selected is presented in Section 5.4. Note that coarsening-upward sequences occur locally within the map units. Descriptions of these map units are presented below:

- $U_f$  (upward-fining) - Medium- to very coarse-grained, grayish-red and reddish-brown sandstone with subordinate conglomerate, fining upward through fine and very-fine sandstone and ending with reddish-brown siltstone or mudstone at the top. Basal units are commonly clast-supported and cross-bedded and rest in sharp contact with underlying siltstone or mudstone. The sandstone is moderately to poorly sorted lithic arkose, feldspathic litharenite and litharenite. Several upward-fining sequences may occur within one map unit. Lithofacies commonly include: conglomerate - Ccm, Ccg, Ccb, Ccx and sandstone - Sc, Scm, Sm, Smm, Sx, Sr, Sl in the lower part with mudstone - Mm, Ml, Mr, and Mb, and occasionally, claystone - Mc and Mbp in the upper portion. The gamma-ray log response is bell-shaped with low API values near the abrupt base (20-50), increasing upward to the top (100-120 API units). The type log for this unit with three upward fining sequences is W203AR1, from 34 to 85 feet (Figure 5-1). This unit is common west of the W8 fault and also occurs near the east end of the GM-4 trench (top of section).
- $M_s$  (mudstone/minor sandstone) - Interbedded grayish-red and reddish-brown, with occasional gray and purple intervals, generally massive mudstone and siltstone with subordinate, poorly-sorted, very fine- to coarse-

grained muddy sandstone. Claystone and very fine- to medium-grained sheet sandstone occur within the unit. Some mudstone, siltstone and fine sandstone may be laminated. Lithofacies in this unit are dominantly mudstone - Mm, Mb, Mr, Ml and claystone - Mc, Mbp with minor sandstone - Sm, Smm, Scm and conglomerate - Cmm. The gamma-ray log displays an irregular, serrated pattern that usually varies between 70 (muddy sandstone) and 120 (mudstone) API units. The type log for this unit is W202AR1, from 99 to 154 feet (Figure 5-2). This unit is most common west of the W8 fault.

- Sm (sandstone/minor mudstone) - Interbedded grayish-red and reddish-brown, generally massive, fine- to very coarse-grained sandstone and lithic conglomerate with subordinate sandy to pebbly mudstone. The sandstone is usually poorly-sorted arkose, lithic arkose, feldspathic litharenite or litharenite. Sandstone is the main lithofacies - Sc, Scm, Smm with subordinate conglomerate - Cmm and minor mudstone - Mm, Mp, Mb and claystone - Mc. The gamma-ray log response shows an irregular, serrated pattern that typically varies between 30 (sandstone) and 80 (sandy mudstone) API units. The type log for this unit is W203AR1, from 300 to 344 feet (Figure 5-3). This unit is most common east of the W8 fault.
- Swb (sandstone, well-bedded) - Gray, grayish-red, reddish-brown and brown sandstone with subordinate conglomerate and minor sandy and pebbly mudstone; individual lithologies commonly range from less than one to about three feet in thickness and often exhibit sharp contacts; planar- and cross-bedded intervals occur within this unit. The sandstone is usually fine- to coarse-grained, moderately to poorly-sorted arkose, lithic arkose and feldspathic litharenite. The Swb mapping unit begins with an overall coarsening-upward sequence in the lower portion of the map unit, changing to an overall fining-upward sequence in the upper portion of the mapping unit. Common lithofacies in this unit include sandstone - Sx, Sl, Sr, Scm, Smm and minor conglomerate - Ccx, Ccb, mudstone - Ml, Mb, and claystone - Mc. The gamma-ray log response displays a serrated, convex-outward (to left) symmetrical pattern that typically varies between 50 and 100 API units. It has a rounded base and top. The type log for this unit is W204AR1, from 54 to 80 feet (Figure 5-4). This unit is most common west of the W8 fault.
- Mwb (mudstone, well-bedded) - Predominantly grayish-red and reddish-brown mudstone and siltstone with subordinate very fine- to coarse-grained, poorly-sorted lithic arkose, feldspathic litharenite, and litharenite. Includes grayish-red purple and grayish mudstone and sandstone. Laminated mudstone (Ml) is the dominant lithofacies with subordinate sandstone - Sl, Sr, and Sx and claystone - Mc. The gamma-ray displays a serrated, convex-outward (to right) symmetrical pattern that varies between 100 and 150 API units. The type log for this unit is W104 from 90 to 112 feet (Figure 5-5). Note that the example given contains a laminated sandstone (Sl) near the midpoint of the mapping unit. These units are commonly observed within the Mwb mapping unit. The Mwb unit is well developed at the west end of GM-3, and west of drainage I in GM-1E and may be associated with Swb.

Strength

A designated HLA staff member actually at the work site with direct supervision over, and responsibility for subcontractor work in progress represents a solid activity controls approach.

- Observed packer testing performed by Earth Data under direction of Golder and evaluated related activity controls. This work was performed under HLA procedure TP-5 (Packer Testing). This surveillance reported the following:

Recommendation #1

The Work Instruction was incompletely filled out in that some spaces on the form were left blank. On any document such as this that will become a record of Project activities, all appropriate spaces on the form should be either filled in, or N/A marked in that space to provide for completeness or closure of that document. If the space in question is determined to be unnecessary, then consideration should be given to modifying the form.

Recommendation #2

Since the procedure for obtaining a water level measurement is a relatively simple one that is practiced by a number of disciplines, the steps for taking water level measurements for Packer Testing should be written directly into TP-5, taking into account the necessary allowances for site setup differences. TP-5 should be revised to incorporate this recommended change, and the reference to the Long Term monitoring procedure eliminated.

Recommendation #3

The additional calibration records available for the water level measuring tape add defensibility to the work product and should be requested from the sub to be part of the deliverable, if not already specified.

For each of these surveillances, any identified nonconformances, or opportunities for procedural or process improvements were communicated to the Project Management and tracked for resolution. Based on lessons learned from the GM-1 studies, the QA program and the procedures controlling site studies work activities have been further strengthened in preparation for site wide characterization.

Reanalysis of the data set following map unit definition indicates that three of the map units can easily be identified in boreholes using only calibrated gamma-ray logs at a scale of 1-inch equals 10-feet. These include the upward-fining ( $U_f$ ), mudstone/minor sandstone ( $M_s$ ), and sandstone/minor mudstone ( $S_m$ ) units. The well-bedded sandstone ( $S_{wb}$ ) and well-bedded mudstone ( $M_{wb}$ ) units are difficult to identify in boreholes using only the gamma-ray tool. However, when the gamma-ray is combined with the formation micro-imager log (FMI) at a scale of 1-inch equals 1-foot, these units can be readily identified.

Map Unit abundances along the GM-1 section are  $M_s$ -50 percent,  $U_f$ - 25 percent,  $S_m$ -16 percent,  $S_{wb}$ -6 percent and  $M_{wb}$ -3 percent.

#### 5.1.1.4 Comparison of Well Bore Logging Techniques (see pages 5-6a through 5-6c)

### 5.1.2 Structure

Structural data at the Site includes data collected during previous investigations and during the GM-1 Pilot Study. Data were collected during previous investigations during outcrop and trench mapping, and borehole core and ATV logging. During the GM-1 Pilot Study, structural data were collected from additional trenches and core, and from BIPS and FMI imaging tools. FMI and BIPS structural data, including stratigraphic and fracture orientations, are provided as tadpole plots on the montages for W205CH1 and W208CH1 and on panel diagrams for W201AR1A-W204AR1, W206AR1, and W207AR1 (Appendices D). These data, as well as the fracture data for the GM trenches, are also provided as stereonet plots provided in Appendix E.

#### 5.1.2.1 Faults

Previous studies at the Site have identified 3 primary faults: the W8 fault, the W82 fault, and the Borrow Pit Fault. The locations of these faults are shown on Plate 5-2, Geologic Map. The W8 fault trends generally north-south, and the W82 and the Borrow Pit faults trend generally east-west. Thus, the site is subdivided into a number of blocks separated by faults. The GM-1 Pilot Study was conducted across two of these fault blocks, separated by the north-south trending W8 fault. Revision of the site geologic conceptual model based on GM-1 Pilot studies is, therefore, restricted to portions of the W8 fault and the two blocks it separates. Contacts between rocks dominated by  $M_s$  and  $U_f$  map units and underlying rocks dominated by  $S_m$  units are located both east and west of the W8 fault (Plate 5-1, Geologic Cross Section GM-GM'). West of the fault, the contact is located in boreholes W202AR1 and W203AR1 at depths of 174 feet and 302 feet, respectively. East of the fault a similar contact is located in GM-4 trench at station 245 feet. Assuming that these two contacts are the same contact, projections to the fault show they are now separated along the dip by a distance of about 900 feet. Since this is the only feature found that may be correlatable across the fault, it appears that dip slip along the W8 fault is a minimum of 900 feet.

The W8 fault mapped in the GM-1E trench has a dip of approximately 55 degrees. By projecting a plane with a dip of 55 degrees from the surface to the W205CH1 corehole, the fault zone would intersect W205CH1 at approximately 420 feet. However, the W8 fault was penetrated during drilling of W205CH1 at a depth of 331 feet based on the geophysical logs. BIPS and FMI data analysis have indicated that the dip on this fault is approximately 56 degrees at this location. Projecting this dip to the surface, the fault would project west of the mapped location in the trench. Thus,

#### 5.1.1.4 Comparison of Well Bore Logging Techniques

Panel diagrams have been prepared that compare graphic core logs, well bore image logs (BIPS and FMI) and core photographs. The purpose of producing these diagrams is to compare, in a side-by-side format, the different techniques used to acquire and display lithologic information and sedimentary and structural features. To best illustrate this comparison, core intervals containing each of four types of geologic mapping units identified in W205CH1 were used. The four mapping units, each shown on a separate panel, are Uf, Ms, Sm, and Swb. These comparisons were used to assess the relative ability of each acquisition technique to provide the information needed to characterize the site. Keeping in mind that the primary goal of site characterization is to identify where and how groundwater is moving, the critical information required from the image logs is that which provides the ability to define and correlate both lithologic and mapping units, and structural features. (see Sections 5.4 and 6.0). The panel diagrams are presented in Appendix D as Plates D1 through D4.

Analyses of the four panel diagrams consisted of evaluating whether or not each acquisition technique adequately provides information on lithologic types and their boundaries, the nature of bedding and contacts, and secondary features such as rock structures and biogenic/epigenic markings. While geophysical logs (primarily gamma ray and resistivity) are not part of these panel diagrams, they (Figures 5-1 through 5-4) were used to provide additional confirmation of lithologic types and boundaries. Based on these analyses, the following conclusions can be made:

##### Graphic Core Logs

The combination of the rock classification column and the relative abundance curves developed during the core logging generally correlate well with the FMI logs. Note that in some cases, there is one or more feet of offset of contacts between the graphic core log and the images are noted. This likely results from errors in core depth measurement during drilling and/or logging, or mis-identification of the actual location of core loss zones. In this respect, the image logs provide more accurate data than the actual core.

It was also noted that, based on a comparison of the graphic core logs to the image and gamma logs, the graphic core logs tend to underestimate sand contents of rocks in the very fine sand to silt ranges. This results in intervals of very-fine grained sandstone not always being represented by the graphic core logs. As a result, Swb and Sm mapping units may be thicker, and associated Ms mapping units, may be thinner than what is shown on graphic core logs. Because of the difficulty in visually estimating sand content in fine-grained rocks, gamma and FMI logs provide a more objective and consistent characterization of the rocks at the site. However, it should be noted that the gamma logs can indicate a sandstone when the interval may actually be a silt-size unit composed of quartz. This is, in part, why multiple log types are proposed in each boring.

The graphic logs do provide information on biogenic and epigenetic features that can also be generally observed on the BIPS images. The FMI does not represent these features. However, correlations performed during the development of the

GM-1 cross section indicated that these biogenic and epigenetic features are widespread throughout the units at the site and provide little to no additional basis for correlations. As such, the lack of observed biogenic and epigenetic features on the FMI is not considered a serious problem.

### BIPS Images

BIPS images portray textures, structures and colors of borehole walls. In general, these features are not sharply defined and color is probably the least reliable feature. Reds and browns appear essentially the same. Important differences in shades of gray are generally lost. Part of the problem may be a result of processing the data to generate the color presented. Variations in processing probably accounts for color changes such as those at the 270.8 and 292.6 foot depths. The poor representation of color may also be related to data acquisition techniques. Medium to coarse-grained sandstone intervals on the BIPS logs compare very well to those on the graphic core logs and the FMI logs. However, subtle differences in color and textures on the BIPS logs make it difficult to define the finer-grained lithologic units. For example, the upper Swb mapping unit in the Swb panel diagram would probably go unidentified if BIPS were used alone. In addition, fine-scale features such as laminations do not show up well on the BIPS in comparison to the FMI logs. Fractures identified on the BIPS logs, where the log is clear, compare well with the location of fractures shown on the FMI logs and the core logs.

Although not specific to BIPS images on these panels, another problem identified with the BIPS data is the condition of the hole during acquisition. Portions of some BIPS logs are not clear because of either the murkiness of the water or poor condition of the hole (including lighting).

In conclusion, although Uf map units can be identified on the BIPS logs, they cannot be relied on to locate Ms, Sm, and Swb mapping unit boundaries, especially since these tend to be gradational.

### FMI Images

Measurement of the relative values of conductivity of rock provides data that generally portrays lithologies in shades ranging from pale yellow (sand and gravel) to dark brown (silt and clay). FMI logs are presented in two formats; dynamic normalization and static normalization. The static log best identifies lithology and relative grain sizes. The static normalization log portrays details of Uf, Sm and Swb mapping units very well and matches the associated gamma log curve best of all the four types of images shown on the panel diagrams. It allows for identification of the Swb units because it displays very finely layered sandstone units that do not show up very well on the BIPS logs. Ms mapping units are not so well defined by FMI because sand (quartz) contents of very fine grained lithologies apparently can vary considerably. However, when used in conjunction with gamma logs, Ms mapping units are accurately defined and located. The dynamic normalization log tends to show sharper images of fractures than does the static normalization log and indicates that the locations of fractures closely matches those identified on the BIPS logs. A discussion of the comparison of fractures between the BIPS and FMI image logs is presented in Appendix E.

### Core Photographs

Due to the small diameter of the core relative to the scale of the panel diagrams, the photographs do not clearly show small scale textures visible in the rock. However, they do show lithologic changes sandstone (light grey) to mudstone (grey-red to red) and some fractures. The locations of these lithologic changes and fractures compare very well to those indicated by the FMI and BIPS logs.

In conclusion, lithologies, contacts, structural features, and mapping units can most accurately and reliably be defined using the FMI images in combination with gamma ray logs. The graphic core logs are subject to the biases of the logging teams, and the geophysical logs suggest the current core logs underestimate the amount of fine-grained sand. Further, uncertainties in core depth due to measurement errors during drilling and logging, and difficulties in assigning core loss zones introduce errors in contact depths and unit thickness (although these errors are generally less than a few feet and are not considered critical at sitewide mapping scales). The BIPS images, even where clear, do not show fine-scale stratification as well as the FMI logs and do not accurately distinguish fine-grained sands from mudstones. Further, data acquisition issues with BIPS, including the need for clean water in the hole, appropriate lighting, etc., are not considerations with FMI, such that FMI is considered a more robust and consistent logging methodology.



the fault is not a planar feature but likely bends somewhere between the surface and W205CH1. An alternate interpretation may be that the W8 fault observed in the trench actually projects to a greater depth in W205CH1 and that the fault at 330 feet may be a splay associated with the W8 fault. There is a large fracture noted at about 520 feet on the FMI log for W205CH1 that could support this interpretation. However, this fracture does not have the attributes associated with major faulting, such as an associated fracture zone, higher rates of water inflow, <sup>nor</sup> a change in dip above and below this interval as observed at the 330ft depth.

The W205CH1 core log and FMI tadpole plot (Appendix D-1) indicate a significant increase in fracturing about 10 feet above the W8 fault at the 331 foot depth, and the FMI tadpole plot shows numerous fractures to about 30 feet below the fault. Thus, the W8 fault is not a discrete plane, but actually represents a zone along which displacement occurred (e.g., the W8 fault zone). This fault zone can be seen on both the FMI and the BIPS image logs. Localized drag in the fault zone is evident from the tadpole plots of the FMI and BIPS fracture data. These indicate a shift in the orientation of beds from an easterly dip to a westerly dip within the fault zone. Trenching and mapping conducted approximately 2000 feet west and more than 1700 feet east of the W8 fault outcrop have failed to find another fault similar in magnitude to the W8 fault.

In addition to the W8 fault, approximately 20 smaller faults (i.e., slip surfaces and breccias with little to no measurable offset) were observed in the trenches and borings. Most of the smaller faults are low-angle, and essentially parallel with bedding contacts. They are more commonly found near the contact between clast-supported sandstones and mudstones and may be traced downdip in boreholes. There is an increase in density of minor faulting at the east end of the GM-4 trench and a slight increase in density in the vicinity of the junction of GM-1W and GM-3 trenches and the nearby GT-5 trench.

#### 5.1.2.2 Bedding Orientation

Displacement along the Jonesboro Fault during evolution of the portion of the Deep River Basin in which the Site is located has resulted in the originally near-horizontal beds being tilted to the east at approximately 5 to 10 degrees with local dips of up to 25 to 30 degrees (Parker, 1979). During the GM-1 Pilot Study, bedding dip was interpreted based on trench data and FMI and BIPS structural data, and confirmed by correlation. Bedding dips west of the W8 fault range from approximately 20 to 25 degrees to the east and increase to approximately 40 degrees near the W8 fault. East of the fault, previous trench mapping has indicated that the beds form a very gentle anticline. The FMI and BIPS data for W206, which is located near the crest of this anticline, indicate essentially horizontal strata to a depth of 45 feet. The dip in this borehole gradually increases to about 10 degrees northeast at 165 feet and then continues to steepen to approximately 15 to 20 degrees at 400 feet. Trench and borehole data indicate that the northeastward dip gradually increases east of borehole W206 to about 20 degrees near the borrow pit. Similar orientation of bedding west and east of

the W8 fault had been reported previously (Geologic Map and Cross Sections of the License Area and Vicinity, January, 1996).

### 5.1.2.3 Fractures

Deformation during faulting has generated a network of fractures throughout the rock mass. Fractures in boreholes W205CH1 - W208CH1 were analyzed during the GM-1 pilot study with respect to orientation, aperture, and filling material using both electrical and optical image data. In addition, fracture data collected during GM-1 Pilot Study trench mapping (GM-2, GM-3, GM-4), and fracture data from previous trench mapping (GM-1W and GM-1E) were interpreted, in combination with the borehole data, to assess fracture characteristics in the GM-1 Pilot Study area. The borehole data used in the fracture study included electrical image data, optical image data and analysis of recovered core. A comparison of the fracture analysis based on the three data sources is presented in Appendix E. The results of the GM-1 fracture study are also compared with previous results of an analysis of acoustic televiewer data recorded at the site.

Based on the analysis of optical image data, two dominant fracture sets were identified from boreholes in the GM-1 Pilot Study area. One set is bedding parallel, striking roughly north-south and dipping predominantly to the east. This fracture set appears to correspond to internal bedding features detected in the electrical imaging data (see Appendix E). The other fracture set is orthogonal to the dominant bedding parallel fracture set and is comprised of more steeply-dipping fractures that are not parallel to bedding. Both optical and electrical imaging techniques detected this fracture set and provided similar determinations of their orientation and distribution. Although there is substantial scatter in the more steeply-dipping fracture set, they are also primarily north-south striking but dip steeply to the west. There is a slight change in orientation of the high angle fracture set in GM-1 and GM-4 where trend changes to slightly northwest to northwest. This is consistent with orientations of high-angle fractures in W208AR1. Stereonet plots of fracture orientations are presented in Appendix E.

The combined structural trends of the fractures and strata are quite similar for both of the imaging methods used. Borehole image analyses provide better and more complete information than the results of core analysis because the borehole samples a much larger fracture area, and also because the images allow determination of geographic orientation. The differences in interpretation of the bedding parallel features between optical and electrical imaging techniques are largely due to the different attributes these tools reveal. Internal laminations can generate mechanical discontinuities which in the optical data could be interpreted to be fractures. The electrical images revealed differences in the properties of the rock on either side of these discontinuities. Core analysts found that relatively few of these features were large enough to be called fractures, and therefore were effectively closed (impermeable). This is an important result of the GM-1 Pilot Study and is incorporated into permeability models. Thus, the differences between the results provided by these methods are due to differences in the physics of the measurements, and between the display

and analysis tools used to interpret the data. Differences in the classification of planar features may also be the result of different interpretations of these features by the analysts. See Appendix E for a more detailed discussion and for displays of data and results within a subset of depth intervals which highlight these differences.

As discussed in Section 4.2, fracture plots generated from the analysis of electrical image data (Appendix E) primarily represent the high-angle fracture set (i.e., the stereonet plots of fractures measured from electrical image data do not include bedding plane fractures). This high-angle fracture set is also consistent with the fracture data collected from the trenches, and in the optical image data, although in the stereoplots of this data it is somewhat obscured by the relatively large number of bedding parallel features. The stereonet plots of dipping strata derived from the electrical imaging data are consistent with bedding plane fracture orientations for the optical image data. These fractures may or may not be important hydrologically — this is revealed by Hydrophysical™ logging and packer testing.

Fracture orientations measured from the wellbore image data recorded during the GM-1 Pilot Study are consistent with those observed from previous analyses of fracture orientations based on acoustic televiewer image data (SAR, 1994 Section 2.3.1.3.5.3 and C. Barton, 1995). The data analyzed in Barton's report revealed three dominant subsets of fractures based on data from 19 drill holes. Most fractures were shallow to moderately east-dipping (bedding-plane) features. A second, less prominent set of moderately west-dipping fractures was also found as well as a steeply west dipping fracture set. An acoustic televiewer is better at detecting bedding parallel fractures than is an electrical imaging tool because it is sensitive to the mechanical character of macroscopic fractures. The acoustic televiewer generally detects fewer overall fractures than either electrical or optical imaging tools because of its lower feature-size detection threshold (approximately one centimeter).

Based on this analyses, fractures generally fall into two categories; high angle to near vertical fractures, and fractures oriented along and parallel to bedding planes. Some of the weaker, clay-rich rocks appear to also contain broken zones along bedding planes. These zones are classified as bedding parallel fractures from the analysis of optical image data and as strata based on analysis of the electrical image data. Comparison of fracture stereonet plots for boreholes W201ARIA through W205CH1 (Appendix E) shows that high-angle fractures are more commonly located in close proximity to the W8 fault, especially in its hanging wall. Examination of the same plots reveals that fracture density also increases in the hanging wall of the W8 fault. A similar increase in fracture density is seen in GM-2 and GM-1W data plots (Appendix I) and confirm earlier findings reported in the SAR (1994, Section 2.3.1.3.5.5, Fracture Domain Analysis).

A similar increase in occurrence of high-angle fractures and fracture density is observed in the stereonet plot for trench GM-4 where mapping has revealed many minor low- and high-angle faults. Greater than normal densities of manganese oxide-coated fractures are also observed near minor faults located near the junction of GM-1W and GM-3 and in the

nearby W202AR1 borehole. This suggests that fracture density may increase somewhat in the vicinity of minor faults as well as in the vicinity of major faults, an association not previously reported.

Fractures were also evaluated with respect to their distribution in specific lithologies. Based on this evaluation there does not appear to be a correlation between lithology and fracture orientation or lithology and fracture density. However, it should be noted that this is based on a limited data set collected in the GM-1 study area.

### 5.1.3 Rock Weathering

Previous studies showed that weathering effects on Triassic sedimentary rock at the Site range from complete at the surface, to slight at variable depths below the surface (Wake/ Chatham Safety Analysis Report, Section 2.3.1.3.4.2, Late Cenozoic Weathering). Those studies identified four zones of weathering. From the surface down, they are: (1) zone of complete weathering, (2) zone of severe weathering, (3) zone of moderate weathering and (4) zone of slight weathering. No completely unweathered or fresh rock was recognized at the Site. Figure 2-3-50 of the SAR (1995) summarizes major properties of the four weathering zones. In addition, the text of the SAR provided considerable data pertaining to the mineralogical, chemical and geophysical characteristics, and hydrologic properties of the four weathering zones. Discussions of the evolution of the completely, severely, and moderately weathered zones were also presented.

#### 5.1.3.1 Weathered Zone

Geological characteristics of the weathered zone at the Site were observed and measured during three GM-1 Pilot Studies activities; trench mapping, borehole soil and rock core logging, and borehole geophysical measurements. Earlier findings regarding textural and mineralogical changes to Triassic rocks due to weathering were generally confirmed. However, a number of refinements have been made based on data collected during the GM-1 Pilot Study. In this report, the term "weathered zone" is meant to include all its subzones, i.e., complete, severe, and moderate.

Geophysical measurements collected in boreholes drilled during the GM-1 Pilot Study have furthered our understanding of the depth and hydrologic nature of the zone of weathering. Based on the log results quantified using ELAN, this zone appears to be slightly more porous and softer than the unweathered rock. CMR porosity in this zone is lower than that determined using the other logs, whereas below this zone the ELAN porosity more closely matches the CMR porosity. The weathered zone has lower density and acoustic velocity and higher apparent neutron porosity than the unweathered zone. The geophysical log showing the largest change between the weathered and the unweathered zones is the acoustic velocity log (DTCO). The differences between the two zones recognized on the geophysical logs are interpreted to be due, in part, to the presence of stress-relief microcracks caused by mechanical unloading of the highly compacted sediments (particularly the claystones) in the weathered zone. These microcracks allow the movement of groundwater through this zone

and contribute to development of authigenic clay minerals (chemical weathering). Because the authigenic clays have not been compacted, they may have a lower density and slower sonic signature (and a different mineralogy, although this was not obvious from the log data) than clays at greater depth. Therefore the assumed clay properties used to compute the apparent effective porosity using ELAN may not be appropriate for these materials, resulting in an apparent effective porosity which is slightly larger than the CMR porosity. Alternatively, the CMR may simply undersample the microcrack porosity in this zone, as it may be associated with  $T_2$  times less than the cutoff time used to compute the CMR porosity. In either case, it is appropriate to use the CMR porosity as a lower bound, and the porosity derived using other logs or ELAN as an upper bound.

In many cases, the base of the weathered zone corresponds with a fracture or set of fractures, and a slight hole enlargement. The hole enlargement causes slightly decreased sonic coherence and a loss of pad contact which results in much higher neutron log values, lower density and an increased density correction at the contact. The fracture(s) at the base of the weathered zone may help to limit fluid circulation across the contact with the unweathered zone by allowing a pathway for preferential groundwater flow parallel to the contact.

The base of the weathered zone in boreholes 201-208 ranges from 40 to 80 feet bgs (Table 5-2). Figure 5.6 illustrates the vertical extent of the zone at each borehole using the DTCO curve. Figure 5.7 shows the differences in properties in this zone for W205 based on velocity and density data.

Different descriptions and depth criteria of the subzones within the zone of weathering have evolved depending on this particular study/technique being applied. Figure 5-8 shows the zone of weathering and its subzones and the criteria used for depth determination. Each of the subzones and depth criteria are described in the sections that follow.

#### 5.1.3.2 Subzone of Complete Weathering

The definition of the subzone of complete weathering was not changed during GM-1 Pilot Studies. This subzone, or soil zone, was continuously measured and described during the mapping of Trenches GM-2, GM-3 and GM-4, a total of approximately 1600 feet, and in logging shallow intervals of the eight, W200-series boreholes drilled in support of the GM-1 Pilot Study. Studies of soils performed during the GM-1 Pilot Study support findings of previous studies. For example, it was observed that the B horizon of the completely weathered subzone is the most clay rich of all the weathering zones, and thicknesses of the subzone of complete weathering were observed to generally fall within the range of thicknesses described during the previous studies. The thickness of the subzone of complete weathering was estimated to range between 2.0 and 6.5 feet during previous investigations and up to 8.0 feet during the GM Pilot Study investigation.

The potential for understanding the relationship of properties of the subzone of complete weathering to its parent material has been significantly increased during the GM-1 Pilot Study. Soil types and their properties were mapped at a

scale of one inch = five feet along with underlying lithologies and fractures in trenches GM-2, GM-3 and GM-4 (GM Cross Section). Such continuous mapping of soils had not previously been done at the Site. Detailed soil descriptions, recorded on electronic spreadsheets similar to those used for lithologies and fractures, make rapid sorting and correlation studies possible.

### 5.1.3.3 Subzone of Severe Weathering

Underlying the subzone of complete weathering is the subzone of severe weathering. The subzone of severe weathering is characterized by manganese, iron-oxide, and limonite staining. Manganese-coated fractures and manganese-stained, clast-supported sandstones appear to be largely confined to the severely weathered subzone but are not uniformly distributed over the Site. Hematite-filled fractures and stained rocks are occasionally present in the severely weathered zone but do not appear to be genetically related to modern weathering. Rather, they are interpreted to be related to Mesozoic-Jurassic diagenetic processes. These features, including hematite nodules, are observed at depths to several hundred feet in rock core.

The base of the subzone of severe weathering was defined in earlier studies as the depth at which power auger refusal occurred. During the drainage studies conducted in 1994, core drilling was instituted as soon as it was possible to retrieve core, generally at a depth shallower than power-auger refusal. A similar approach was taken during the GM-1 Pilot Study. The definition of the base of the subzone of severe weathering has been revised to correspond to the depth at which split-spoon sampling was abandoned, usually when the blow counts reached 50 per inch, and core drilling could be initiated. The depth of the zone of severe weathering based on split-spoon "refusal" for boreholes W201ARIA through W208CH1 ranged from 5.9 to 16.1 feet bgs. This depth is indicated in Figure 5-8 in the column titled "Core Logs".

The subzone of severe weathering was subdivided for mapping of trenches GM-2, GM-3 and GM-4 into two units; very severely-weathered and severely weathered. These zones are indicated on Figure 5-8 in the column titled "Trench Maps". Very severely weathered rock is defined as rock in which soil peds are beginning to develop such that rock structures and textures are locally absent. The depth of this very severely-weathered rock was found to be generally less than the depth of the trench which is approximately 5 to 8 feet. This depth would likely correspond to the depth of hand-auger refusal as described during previous investigations at the Site (Wake / Chatham Safety Analysis Report, 1994, Sections 2.3.1.3.4.3.2 and 2.3.1.3.6.3).

Immediately below the subzone of very severely-weathered rock is severely-weathered rock where rock has lost all strength, ie: is friable, but has not started developing peds. The top of this subzone was often observed in the lowest portion of geologic mapping trenches.

After split-spoon "refusal" (6-16 feet bgs), rock coring continued until competent bedrock was reached. Casing was installed at this depth. The depth of casing, which ranges from 24 to 36 feet bgs in boreholes W201AR1A through W208CH1., is shown in Figure 5-8 in the column titled "Driller's Log". Casing depth is, therefore, into the moderately weathered subzone.

#### 5.1.3.4 Subzone of Moderate Weathering

The subzone of moderate weathering underlies the subzone of severe weathering. Our understanding of the subzone of moderate weathering is little changed as a result of core logging during the GM-1 Pilot Study. The rock is generally moderately indurated to indurated. Manganese oxide and limonite coated fractures and rock staining are uncommon while local calcite cement and fracture filling may be found. The base of the zone of moderate weathering cannot be determined by examination of rock core. As in earlier studies, the base is determined largely by examination of geophysical logs and corresponds to the base of the zone of weathering described in Section 5.1.3.1.

### 5.2 Hydrogeologic Data

One of the main objectives of the GM-1 Pilot Study was to assess which geologic features are important for controlling groundwater flow beneath the Site. Observations of geologic features in the trenches and core (Table 5-3) provide indirect evidence of flow in the shallow subsurface. In addition, some of the geophysical logs also provide hydrologic information (i.e., the various porosity tools, caliper log, and Stoneley waveform log). However, the most diagnostic tool for assessing conductive intervals is direct testing. This was accomplished for the saturated zone using both hydrophysical logging and packer testing. This section presents a discussion of data that may be related to subsurface water occurrence and movement collected from the vadose zone and the saturated zone during the GM Pilot Study.

#### 5.2.1 Vadose Zone

Manganese oxide-coated fractures and manganese stained, clast-supported sandstones appear to be largely confined to the severely weathered zone, but are not uniformly distributed across the Site. These features often appear to be associated with near surface "seepage columns" observed during trench mapping. During the GM-1 Pilot Study, manganese oxide-coated fractures and open fractures were also observed to be associated with areas in which minor low- and high-angle faults (ie: slickensided surfaces with little or no measurable offset) are located and where weathering zones are somewhat deeper than normal (Plate 5-1, Geologic Cross Section GM-GM'). These features, suggesting the shallow circulation of water, may mark the locations of higher than normal groundwater infiltration. If so, they are very important features of the vadose zone. The best example of confluence of all these features is in the vicinity of the junction of the GM-1W and GM-3 trenches. Borehole W202AR1., located in the same vicinity, penetrated rock that contains abundant fractures, most of which are manganese oxide-coated.



Another important feature of the vadose zone are surface seeps. Sixteen seepage zones were identified in trenches that have been mapped prior to and during the GM-1 Pilot Study. These have been annotated on the GM-1 cross section. Available data used to identify the seeps included trench map spreadsheets, photographs, original field notes and sketches, and the annotated trench maps. Seepage zones were identified in trenches GM1E, GM1-ED, GM-2, GM-3, and GT-5. Trench GM-4 had no seeps, and trench GT-5 had the greatest number of seeps. Eight seeps occur in fine-grained sequences, and seven occur in coarse-grained units. Eight of the seepage zones identified in trenches GM-1 through GM-3 appear to be directly related to fracturing, rooting, or root-related fracturing. It is not clear what controls the seep that was photographed in GM-2, Unit 15, but it may be associated with the contact between Units 15 and 16 (i.e., bedding plane seep). Lithology does not appear to be an important factor controlling the occurrence of seeps. This observation is consistent with shallow core logs which indicate abundant fractures in all lithologies above approximately 30 feet. Additionally, there is no apparent relationship of seepage distribution to map units or to topography. Rather, seepage zones appear to be associated with fractures, roots, and root-induced fractures. Increased fracture density in near-surface units is probably due to a combination of 1) brittle behavior due to unloading/low confining pressure and 2) biogenice (i.e., root-induced) fracturing. Thus, most of the seeps are probably near-surface phenomena and may not be related to deeper pathways for groundwater flow.

### 5.2.2 Saturated Zone

Hydrologic data collected from the saturated zone include porosity data from geophysical logs, flow data from hydrophysical logging, and permeability data from packer testing.

#### 5.2.2.1 Porosity Data

The porosity curves are plotted on the montages for W205CH1 and W208CH1 and on the ELAN logs for boreholes W201AR1A through W204AR1, W206AR1, and W207AR1. These curves have also been included on the Panel Diagrams for W201AR1A through W208AR1 (Appendix D.3). The computed and edited CMR porosity is believed to represent a lower bound on formation porosity (see discussion in Section 4.3). Density porosity and ELAN-computed apparent porosity are also presented on the logs. As discussed in Section 5.1.3.1, the apparent porosity in the weathered zone is higher than that in the unweathered zone, and CMR porosity is lower than the other porosity curves. In the unweathered zone, the porosity curves more closely match the CMR porosity. From the various porosity curves, it is apparent that there are multiple zones of relatively higher porosity below the base of the weathered zone. The majority of these relatively higher porosity zones correspond to sandstone intervals for which porosities range from 2 to 8 percent. Less than 100 feet of logged depth have porosities above 10 percent. Although these porosities are still considered low, they stand out relative to the remainder of strata encountered in the GM-1 Pilot Study, for which porosities are less than 2 percent. Histograms of porosities which illustrate these observations are presented in Figure 5-9. A detailed discussion of the analysis and interpretation of the porosity curves is presented in Section 4.3.



### 5.2.2.2 Hydrophysical Logging Results

Hydrophysical logging is an excellent method for locating conducting features and providing an estimate of their flow capacities. Flow-rate values measured during hydrophysical logging range from 0.001 gpm to 1.06 gpm (Table 4-5). The distribution of conductive zones shows that they are concentrated in three primary areas; within the weathered zone as defined by geophysics, along strata-concordant fractures, and within the hanging wall of major faults. Most of the conductive zones were observed to occur within the weathered zone, except at W205CH1. W205CH1 is located on the hanging wall and in close proximity to the W8 fault.

Below the weathered zone, conductive intervals identified during hydrophysical logging occur primarily along bedding plane fractures or high-angle fractures in sandstones, except in W205CH1. In W205CH1, conductive features were also found to occur within some of the finer-grained units. Results of the hydrophysical logging have been plotted on the Geologic Cross Section (Plate 5-1).

### 5.2.2.3 Packer Testing

Packer tests were targeted at the conductive features or intervals that exhibited the highest yields during hydrophysical logging. Packer test transmissivities generally agreed well with the hydrophysical log results. The packer testing results from the GM-1 Pilot Study boreholes indicate values of  $T$  in the weathered zone of  $10E-6$  to  $10E-8$   $m^2/s$ , and generally lower values of  $T$  ( $10E-5$  to  $10E-9$   $m^2/s$ ) in the unweathered zone. The more transmissive features in the unweathered zone typically are strata-concordant fractures, or fractures on the hanging wall and adjacent to the W8 fault, with  $T$  values of  $10E-5$  to  $10E-6$   $m^2/s$ . Values of  $T$  calculated from packer testing have been plotted on the Geologic Cross Section (Plate 5-1).

## 5.3 Geochemical Data

Nineteen groundwater samples were collected from packer-tested intervals in boreholes W201AR1A through W207AR1, and from the two production wells used to supply water for drilling during the GM Pilot Study. The data were analyzed for major cations and anions. In addition, pH, temperature, and specific conductance data were collected. The results of the geochemical data analysis showed that there are two basic types of water in the GM study area: primarily sodium bicarbonate ( $Na-Cl-HCO_3$  or  $Na-HCO_3-Cl$ ), and sodium chloride ( $Na-Cl$ ). Piper diagrams for the various groundwater samples have been plotted on the GM Cross Section (Plate 5-1). Values of pH in site waters are slightly alkaline (i.e. greater than pH of 7) with the highest values reported from well W205CH1 in the hanging wall of the W8 fault.

A detailed discussion of the results of the geochemistry data collection activities is presented in Section 4.5. A discussion of the geochemistry data integration results is presented in Section 5.5.3.

## 5.4 Development of GM-1 Cross Section and Geologic Map

Prior to the GM-1 Pilot Study activities, a skeletal cross section was developed along the GM transect oriented east-west across the buffer zone. This cross section provided a vehicle for integrating all geologic, hydrologic, and geochemical data in the area of the existing and proposed GM trenches and boreholes to refine the hydrogeologic model for this area of the site. The ultimate goal of this integration effort was to assess the geologic features controlling groundwater flow. The cross section also provided a framework in which to plan additional data collection activities. This initial cross section was presented at the February 18-19, 1997, GM-1 Pilot Study planning meeting.

As additional geologic, hydrologic, and geochemical data were collected during the GM-1 Pilot Study program, this cross section was updated and revised. The cross section is located coincident with the location of the GM trenches shown on the Geologic Map (Plate 5-1). Data plotted on the cross section, or analyzed in conjunction with development of the cross section, to assist in the geologic interpretation and the integration of various data types, are summarized in Table 5-3. Table 5-4 summarizes how the geophysical logs were used in development of the cross section. These include data from core, trench maps, and geophysical logs. It should be noted that the W32 cluster and W8OW100 are located approximately 160 feet south and north of the cross section, respectively. The geophysical/graphic core logs for W32MP14 and W8OW100 appear to correlate along strike to geology shown on the cross section, but require projection in a direction that local strike data does not support. However, because the data from these borings provides additional information for the cross section, the locations were moved to a position where the data are consistent with that shown on the cross section (i.e., W32MP14 was moved 21 feet west and W8OW100 was moved 20 feet east). Borehole W97SW43 is located 170 feet northwest of the GM cross section and the correlations between the two are not readily apparent. Therefore, the requalified graphic core log is shown screened back, but was not used in constructing the cross section.

While data shown on Table 5-3 were used to construct and interpret the cross section, not all data listed are actually displayed on the cross section included in this report. Specifically, the graphic logs (both from core and interpreted from geophysics) are included separately in Appendix B. In addition, only fracture data that are important for understanding the nature of productive inflow intervals identified during hydrophysical logging have been noted. These include annotation as to whether the water-producing interval is characterized by strata-concordant fractures or high angle fractures. Fracture plots for each borehole and for the trench are included in Appendix E.

### 5.4.1 Stratigraphic Correlations

Correct correlation of stratigraphy is essential for construction of geologic cross sections and maps, and, ultimately, for development of a three-dimensional hydrogeologic model for the Site. Correlations were made using the gamma and resistivity logs, graphic logs of W205CHI, W208CHI, and the requalified core, trench maps, the trench columnar section, and dip information from both the FMI logs and the trench maps. In support of correlation, a graphic log of the

trench stratigraphic section was developed and is included in Appendix A. Currently, most geologists correlate along stratigraphic sections by matching log patterns (geophysical and core log), allowing for variations in lithology, thickness, and completeness of section. This method was also employed during the GM Pilot Study.

Two approaches were used for stratigraphic correlation: 1) using geophysical logs, the trench cross section, and the shallow core logs, and 2) using graphic core logs and the trench stratigraphic column. These two approaches were used to assess the reliability of using geophysical logs for correlation during the sitewide investigation. If correlations are similar using both approaches, the use of geophysical logs for correlation during the sitewide investigation is justified.

Correlation of lithologic units using geophysical logs was initiated by matching patterns on the gamma-ray and resistivity (primarily useful east of the W8 fault) logs between boreholes, followed by matching major (thicker) rock units between trenches and nearby boreholes. Prior to using this approach, the gamma logs were calibrated with the core logs for W205CH1 and W208CH1. Because the gamma logs run through casing did not appear to be reliable indicators of sandy lithologies, the core logs for the cased intervals were used for correlating to the shallow portions of the boreholes. More reliable gamma log signatures in the cased intervals can likely be obtained by using the appropriate type of casing and grout. Rock unit matching was constrained by bedding orientation data collected from the trenches and the FMI logs. Following the correlation of lithologic units, these lithologic units were grouped to define larger-scale map units that are associated with distinctive gamma-ray log patterns. It was observed that there are five distinctively different gamma-ray patterns on the cross section that are representative of these map units. Once map units were defined, it was found that they could be correlated more reliably than individual rock units.

In addition to correlation using the geophysical logs, correlations were also performed using the graphic logs for W205CH1, W208CH1, and the requalified logs in conjunction with the trench graphic log. Prior to correlation using this approach, lithofacies were added to the graphic logs for W205, W208, and the trench graphic log. Representative lithofacies have been annotated on the GM-1 hydrogeologic cross section. Correlations were made by pattern matching of various rock units in conjunction with their lithofacies designations. Using this graphic log approach, only minor revisions in correlations and map unit definitions, made using the geophysical logs, were required. Therefore, graphic core logs are not considered necessary for correlation of mapping units. Although lithofacies were initially helpful in defining mapping units, the addition of lithofacies is also not considered necessary for future defining of map units and correlating stratigraphy.

In addition to lithofacies, diagenetic features were also added onto the cross section to assess whether these features are important for correlating or whether they are diagnostic of water-producing intervals. These features include manganese staining, manganese nodules, iron staining, iron nodules, iron cement, calcite cement, carbonate nodules, silica cement (observed in trench), halo aureoles, and intense mottling. Diagenetic features such as manganese staining and nodules appear to be related to weathering and are confined to that zone, and their distribution may be an important characteristic

of the vadose zone. Mottling is generally ubiquitous throughout the section and not diagnostic of any one map unit. Other features, such as carbonate nodules, cements, and halos are present locally and do not appear to be confined to or diagnostic of one map unit. Based on these observations, diagenetic features do not appear to be a valuable aid in making correlations nor can they be used to predict the location of producing intervals.

Analysis of the distribution of biogenic features, burrowing, rooting and bioturbation, logged in core from W205CH1 and W208CH1, indicates that they are found in all lithologies except most claystone, very coarse sandstone, and conglomerate. Furthermore, biogenic features are not found to be restricted to nor indicative of any particular type of map unit. Thus, they do not appear to be important for making correlations.

Success in defining lithologic groups by means of borehole geophysical logs suggests that, during the sitewide investigation, stratigraphic interpretations and correlations can be made using only geophysical logs if boreholes are spaced closely enough. In addition, the existing and the limited core to be acquired in the supplemental field investigation will be used to calibrate the geophysical logging results.

Using the gamma logs and trench maps, correlations along the GM cross section (Plate 5-1) were readily apparent on the west side of the W8 fault, in part, because of the close spacing of the boreholes. In addition, the strata west of the fault consists of thicker, more continuous channel sands and conglomerates interbedded with thick siltstone/mudstone units that form more distinctive gamma log patterns. Some of the sandstones west of the fault can be correlated up to distances of 900 feet.

East of the fault the correlations were more difficult because of wider spacing of boreholes and less distinctive gamma log patterns. The strata in this area consists of relatively thin, discontinuous units of interbedded sandstones, siltstones, and minor conglomerates that are responsible for the less distinctive log patterns. With the exception of Ms and Uf map units near the east end of trench GM-4 (top of the section), map units east of the W8 fault are dominated by sandy packages. Because of this lithologic heterogeneity, correlation of boreholes W206AR1, W207AR1, and W208CH1 was extremely difficult using pattern matching. However, the gamma-ray and resistivity logs indicate excellent correlation with several clay-rich layers that occur in all three boreholes and which serve as marker beds (see Plate 5-1, GM Cross section). Dip data from the trenches and the FMI logs were also used to assist in the correlations. Correlations east of the W8 fault indicated that the section between 200 and 240 feet bgs in W207AR1 is missing in W208AR1 due to non-deposition or erosion. The remainder of the section in W208 above 324 feet bgs correlates with the section above 200 feet bgs in W207AR1 and the section in W208AR1 below 324 feet bgs correlates well with the section below 240 feet bgs in W207AR1. The missing section in W208AR1 is indicated on the cross section.

Stratigraphy could not be correlated across the W8 fault using available data. The lack of correlation across the fault is most likely due to offset that is too great to make correlations based on the stratigraphic sections available.

In addition to correlating units along dip parallel to the GM1 cross section, correlations were also performed along strike in a northerly direction from the GM1 cross section to assess the distance that map units may extend in the strike direction (see Geologic Map, Plate 5-2). These correlations are presented in the form of two cross sections: Plates 5-1A and 5-1B. The location map for these cross sections is presented in Figure 5-9a. These cross sections were first presented in the Discrete Fracture Modeling Report (Figures 3.3 to 3.5, HLA, 1995) and have been reproduced herein with minor edits to lithologic correlations and with the addition of mapping units. Cross section GMA-A' extends north from the GM1 cross section south of W74PM4 to W8OW61. Cross section GMB-B' begins at W8OW96 on cross section GMA-A' and extends northeast through W8PT4A to W8OW59.

Mapping units were identified on the basis of gamma logs primarily, but graphic core logs were also used, where available. However, as noted in Section 4.2.4, the graphic core logs often underestimate the amount of fine-grained sand and, therefore, do not always correlate with the corresponding gamma log. In these cases, the gamma log was used to identify the mapping unit.

Two sandstones that occur near the tops of both GMA-A' and GMB-B' cross sections have been designated as A and D. Sandstone A can be correlated all the way north to W8OW59. A facies change has been interpreted to occur along strike within sand A. In the area of W74PM4 and W8OW100, the sandstone is interpreted to be part of an Uf map unit, and a transition to an Swb map unit occurs between W8OW100 and W8OW96 then back to Uf between W8OW64 and W8MC12. Sandstone D can be correlated northward as part of an Uf map unit to W8DP4 then transitions to an Swb map unit at W8OW59. Correlations of these sandstones and map units indicate that both mapping units and some lithologic units can be correlated for distances of more than 600 feet along strike.

Mapping units identified along strike are similar to those recognized west of the W8 fault in the GM1 Pilot Study area. They are dominated by fluvial sequences (Uf) with minor Ms and Sm units near the GM1 Pilot Study area and dominantly by Ms and relatively thick Sm units with only minor Uf units to the north and northwest (i.e., north of W8OW65 on cross section GM-A-A' and north of W8MP3 on GM-B-B'). Thus, there are some facies changes occurring north and northwest of the GM1 Pilot Study area indicating that some fluvial sequences may be fairly limited in areal extent in that particular direction. A three-dimensional interpretation is required to assess the true extent and configuration of mapping units. These activities will be performed during further Site Characterization.

As discussed in Section 4.1, water level responses were noted in W8MC12 during drilling of W205CH1. Most of the responses were noted when drilling beneath the fault. However, a slight water-level increase was noted when coring between 140 to 156 feet (see Table 4-1). This interval corresponds approximately to the interval that had the highest yield during hydrophysical logging and where a strata-concordant conductor occurs (i.e., at 159 feet in W205CH1). A likely relationship may be that this conductor correlates

north to W8MC12. This hypothesis was examined by use of the two new cross sections. W8MC12 is screened within an interpreted conductive zone based on evaluations of the Aquifer Test 4 area by HLA (1995). Within this zone, one thin sand occurs which has been interpreted to be part of a Uf sequence. If the conductive zone identified in W8MC12 is related to a strata-concordant feature, it is likely that this feature would occur at the contact between a sandstone and an underlying mudstone. Therefore, an attempt was made to correlate the sandstone identified in the screened interval at W8MC12 to the GM1 Pilot Study area. This sandstone can be correlated as far south as W8OW96. However, it appears to pinch out just north of W8OW100 and, therefore, likely does not continue to W205CH1. The nature of the connection between W205CH1 and W8MC12 is not clear at this time, but could be through the enhanced fracture network associated with the W8 fault zone rather than through a specific strata-concordant conductor. Additional work is required to complete the correlation of map units and hydrologic conductors throughout the entire W8 area.

### 5.4.2 Scale and Detail

In comparing the various scales of data, it was found that lithologic correlations are best made at a scale of 1 inch = 10 feet using both the gamma logs and the graphic log of the trench. Resolution of the gamma logs (and other geophysical logs with the exception of the FMI) is lost at any greater scale and lithologic sequences are too stretched on the graphic trench log to identify correlatable units. In order to see detail in the trench maps, and to add a large amount of annotation data on the cross section, it was initially constructed at both a vertical and horizontal scale of 1 inch = 10 feet. However, a smaller scale (e.g., 1 inch = 20 feet) would be more workable for the sitewide characterization. This study also indicates that lithologic logging of core or trench exposures at a scale of 1 inch equals 5 feet provides sufficient detail for recognition of all map units. However, for the purposes of showing finer details observed in core, where necessary, and annotating fractures with respect to specific lithofacies, 1 inch equals 1 foot will be used when logging new core or relogging existing core.

### 5.4.3 Geologic Map

Bedding orientation shown on the previous geologic map of the Site (February 1996) has not been significantly changed. However, map units have been revised and additional minor faults have been added. All five map units occur both east and west of the W8 fault. Boundaries between map units were located on the geologic map (Plate 5-2) based on boundaries determined on the cross section. Bedding orientation and faults on the geologic map are based on trench mapping data. Stratigraphy west of the fault is dominated by mudstone with minor sandstone ( $M_s$ ) and closely associated upward fining ( $U_f$ ) map units, whereas the sandstone with minor mudstone unit ( $S_m$ ) dominates the area east of the fault. The portion of the Geologic Map revised as a result of GM-1 Pilot Studies is indicated on Plate 5-2 (Geologic Map) and is a 500-foot wide strip with the GM trenches located near its center.

One area of the map requiring explanation is the area where trench GM3 and GM1W tie. Two distinctive coarse-grained sandstones have been identified in this area during trench mapping conducted during previous investigations and the GM-1 Pilot Study investigation. One unit occurs at the eastern terminus of trench GM3, where it joins GM1W. The other unit has been mapped at the east end of trench GT5 about 60 feet north of the main trench system. Both sand units have been designated as  $S_m$  map units. However, although these two sandstones are in close proximity to each other, they do not appear to correlate. Rather, they are each of limited lateral extent and appear to have a lenticular geometry. Thus, they are shown to pinch out within a relatively short distance on the geologic map. The larger sand body at the east end of GM3 can be correlated to a thinner conglomerate unit that has been mapped in GT5 (see stratigraphic columnar section; Appendix A). However, the sandy conglomerate unit at the east end of GT5 has not been mapped at any other location.



Borehole W202AR1 is located about 30 feet east of the eastern edge of the GM3 sand. Examination of the shallow core log for this borehole indicates that it consists entirely of silt and clay. Therefore, the GM3 sand pinches out to the east prior to the location of W202AR1. The hypothesis that the GM3 sand is lenticular and may be of limited lateral extent is supported by its northwest strike and northeast dip, indicating that its orientation is anomalous with respect to regional strike and dip. The sand at the east end of GT5 is not present in W202AR1, nor can it be projected into the GM3 or GM1 trenches. Thus, it also appears to be lenticular, pinching out to the south and east.

The existing geologic maps of the Site show laterally continuous map units of uniform thickness striking NNE to SSW. This relatively simple map pattern is partly the result of the limited amount of outcrop and subsurface information that had been available prior to the GM-I Pilot Study. It now appears that the Sm map units may be much more laterally discontinuous than previously realized. In contrast, the Uf and Swb map units can often be correlated for relatively long distances across the site before pinching out. However, based on the GM cross section, it appears that the map unit which may be the most laterally continuous across the Site are the finer-grained sequences of the Ms unit.

## 5.5 Significant Observations Based on GM-I Cross Section Data Integration

During and after development of the GM Cross Section several significant observations were made with regard to geology, and the hydrogeologic, and geochemical data integration efforts. These have been summarized in the following subsections.

### 5.5.1 Geology

- The stratigraphy along the GM trench could be correlated using primarily the gamma ray log patterns, in conjunction with the FMI and trench stratigraphic orientation data. However, gamma curves within casing (as presently designed) may not be reliable indicators of sandy intervals. Core will be retrieved from the cased intervals during the sitewide investigation and will be used, in conjunction with the geophysical curves, to correlate stratigraphy.
- The stratigraphy west of the fault differs from the stratigraphy east of the fault. West of the fault the strata consist of thicker, more continuous channel sands and conglomerates interbedded with thick siltstone/mudstone units. These units were readily correlated because of the distinct gamma-ray signatures. The stratigraphy east of the fault consists of a greater percentage of sandstones, but which are thinner and less continuous than those west of the fault. Most of the individual sandstone units east of the fault could not be correlated for long distances. Additionally, the strata east of the fault (including the finer-grained units) are more quartz rich than the strata west of the fault. Thus, there are fewer extremely clay-rich intervals on the east compared to the west side of the fault (Figure 4-6). The clay unit in Drainage I is one such clay-rich unit. In borehole W205CH1, the



rock above the W8 fault is more similar to the strata west of the fault, and the interval below the fault is more similar to the data from boreholes on the east side of the fault.

- Gamma-ray logs and FMI logs indicate that core logging underestimated the sand/silt content of very fine lithologies east of the W8 fault. Thus, the Ms map units identified in W208CH1 based on core logging are, in some instances, probably Sm packages.
- The Ms map units comprise the greatest percentage of strata at the Site and are anticipated to be the most laterally continuous.

Based on experience gained in support of the GM Pilot Study activities, the data required for recognition of mapping units are geophysical logs (primarily gamma ray logs) and the FMI image data. These data sources provide lithology, relative grain size, percentage of clay versus quartz, contact type, primary sedimentary features, and the geophysical log pattern. Other lithologic features that were used to define map units during the GM Pilot Study, such as percent gravel-sand-mud, fabric, color, and biogenic and diagenetic features, are not considered necessary to define map units during the sitewide characterization. It should also be noted that a specific mapping unit recognized at one location on site does not necessarily correlate to the same type of mapping unit elsewhere on site. Rather, correlations made between closely-spaced boreholes using the geophysical logs are necessary to define the three-dimensional extent of a single mapping unit.

### 5.5.2 Hydrogeologic Data Integration

Based on hydrophysical logging, the distribution of conductive features shows that they are concentrated in three primary areas: 1) within the weathered zone as defined by geophysics (the base of Zone 1, See Section 4.0, Summary Report for Dp-1), 2) along strata-concordant conductors (bedding plane fractures), and 3) within the hanging wall adjacent to the W8 fault plane (approximately 50 feet above based on increase in fracturing noted on the FMI). In association with an analysis of the distribution of conductive features, hydrophysical and packer test data were also evaluated, in conjunction with the borehole image data and core data, to identify correlations between fluid flow indicators and geologic features that may be responsible for the flow anomaly. Because of possible depth tie mismatches between the different logging techniques, an interval  $\pm 3.0$  feet above and below a fluid flow anomaly was inspected for potentially permeable (open, eroded) fractures and/or structures that correlate to a producing zone. Note that BIPS data are not available past 100 feet depth for W204AR1 (TD 145 feet) and the Schlumberger fracture analysis results are required to analyze the lower part of this well. Also note that the BIPS data quality of W203AR1 was very poor below a depth of 100 feet where visibility was limited and the flow analysis for this well also requires the FMI fracture analysis results.

### 5.5.2.1 Fluid Flow in the Weathered Zone

The unsaturated portion of the weathered zone, the vadose zone, contains localized areas of manganese oxide-coated and open fractures associated with relatively deeper completely- and severely- weathered subzones. Seepages are often mapped in trenches at these locations. This association, which is not distributed uniformly over the site, may mark the locations of relatively greater surface water infiltration to subsurface water flow conduits.

The saturated portion of the weathered zone contains the greatest number of water producing intervals, except in W205CH1 which is located in the hanging wall of the W8 fault. The increased number of conductive intervals in the weathered zone is interpreted to be a result of enhanced secondary porosity/permeability due to chemical weathering or to enhanced fracturing as a result of isostatic unloading. A conductive zone was identified at or near the base of the weathered zone in every borehole except W206AR1, indicating that this contact may be a preferential pathway for groundwater flow. A caliper increase at the base of the weathered zone also suggests increased permeability at the base of this zone.

The base of the zone of weathering determined by geophysical logs appears to be more significant hydraulically than the base of the subzone of severe weathering determined by core and auger refusal. This suggests that a visual assessment of the depth of hydraulically significant weathering is difficult. Rather, the depth of hydraulically significant weathering can best be assessed by identifying a change in rock matrix based on the porosity logs, the density log, the sonic log, and the caliper log. The base of this zone ranges from 49 feet bgs in W204AR1 to 84 feet bgs in W208CH1.

### 5.5.2.2 Strata-Concordant Conductors

The results of the GM Pilot Study evaluation showed that almost every flow anomaly is associated with a fracture. At shallow depths (i.e., above 200 feet), most of these are parallel to bedding, while at greater depth most of these are steeply dipping. Table 5-5 presents the preliminary results of the correlation between fractures and producing zones. Three hydraulically significant strata-concordant fractures have been identified on the GM-1 cross section; at 129 and 159 feet bgs in W205CH, and between 159 and 161 feet bgs in W207AR1. These fractures yielded .265, 1.06, and 0.69 gpm, respectively, during the hydrophysical logging program. The fractures at 159 feet in W205CH1 and at 159 - 161 in W207AR1 were the highest producers identified during the GM1 Pilot Study program. The sandstones with which these fractures in W205CH1 are associated have been correlated across the GM-1 Pilot Study area as shown on the GM-1 cross section. The strata-concordant fractures at 159-161 feet in W207AR1 do not continue to boreholes each side of W207AR1. Groundwater elevation monitoring during drilling indicated that the strata-concordant fracture at 159 feet in W205CH1 is hydraulically connected to well W8MC12, and may be one of the strata-concordant conductors identified in the vicinity of the W8 well cluster during HLA's 1996 evaluation of Aquifer Test 4. Additional evaluation of this hypothesis will be conducted during the SIP.

Hydraulically-significant strata-concordant fractures generally occur at the contact between coarse-grained to conglomeratic sandstones and underlying siltstones or claystones (i.e., where large contrasts in physical properties occur across the contact). It is difficult to determine whether fluid flow at a given location is more dependent on strata-concordant fractures or on the overlying lithologic unit that appears to be relatively more permeable than others; for example in borehole W205CH1 near 161.5 feet depth. The sandstone interval including this feature is relatively more permeable (0.259 md) relative to the sandstone unit 5 feet higher (0.157 md). The highest T values below the weathered zone ( $10\text{E}-5\text{m}^2/\text{s}$ ) were measured in W205CH1 at 159 and 270 feet bgs. T values elsewhere in the unweathered zone ranged from  $10\text{E}-5$  to  $10\text{E}-9\text{m}^2/\text{s}$ . The sandstones above the bedding plane fracture at 159 feet has an estimated effective porosity of up to 8 percent based on the CMR and ELAN logs. The higher T value in this zone may be a result of both fracture porosity and secondary porosity in the sandstone. Thin section analysis of this sandstone during the GM-1 Pilot Study and performed during previous investigations at the Site indicates that the porosity is secondary and is a result of the dissolution of feldspar and, in some cases, intergranular cement. Of interest is that some of the fractures with relatively high T values ( $10\text{E}-5\text{m}^2/\text{s}$  at 270 feet in W205CH1) have flows during hydrophysical testing as low as 0.005 gpm as compared to 1.06 gpm at 159 feet in W205CH1. The higher T value at 270 feet is likely a result of increased fracturing approaching the W8 fault. Both bedding plane and high angle fractures were noted in this sandstone. Thus, the higher producing intervals appear to be associated with bedding plane fractures that are in contact with a relatively higher permeability sand. The bedding plane fractures are most likely a result of slip along these surfaces to accommodate stress associated with faulting and are mechanically more likely along fold limbs. Thus, these features may become less important with increased distance away from the major fault zones.

There are also examples of significant bedding plane fractures identified through geophysics that did not produce during the hydrophysical logging. An example is at 90 to 100 feet in W204AR1. This sandstone correlates to the sandstone in W205CH1 at 159 feet. Although these sandstones correlate and are both characterized by bedding plane fractures at their base, the sandstone in W204AR1 did not produce. The hydrophysical logging indicated a producing zone from 103 to 138 feet. It may be possible that it was actually producing from the fracture at the base of the sandstone (i.e., at 100 feet). Alternatively, the sandstone in W204AR1 may not have produced because it has a higher clay content (based on the geophysical logs) than the sandstone in W205CH1. This would suggest that the location of the "clean" sandstones may be predictors of producing intervals. Although the CMR porosity in the sandstone in W204AR1 is 14 percent, this value is likely a result of borehole enlargement rather than matrix porosity.

### 5.5.2.3 Hanging Wall of W8 Fault

In addition to the weathered zone and bedding plane fractures in the unweathered zone, the hanging wall of the W8 fault zone is also interpreted to be a zone of higher conductivity. The W8 fault is clearly visible in image data. Intensely fractured rock associated with the fault, especially its hanging wall side, appear to be fluid flow conduits. In support of this conclusion, W205CH1, located on the hanging wall and adjacent to the W8 fault, had the highest number of

producing features and higher porosity intervals (as interpreted from the ELANs) in the GM-1 pilot study area. Although several conductive features were identified in the weathered zone in W205CH1, several conductive features were also identified below this zone. These occur above the W8 fault both along strata-concordant fractures and as high-angle fractures within sandstones and claystones. As indicated from the BIPS, FMI, and Stoneley waveforms, this borehole exhibits has a high density of fractures approaching the W8 fault and for some depth beneath it.

#### 5.5.2.4 Other Potential Controls on Groundwater Flow

Fractures inclined to bedding may also play an important role in controlling groundwater flow if they connect one bedding-plane fracture to another. These are likely to be confined to individual units and to be truncated at bedding contacts. One such feature crosses W205CH1 within the sand above 165 feet. It is associated with a large thorium anomaly, possibly suggesting that it has carried, or is, carrying large amounts of fluids. The hydrophysical anomaly at 158 feet may be associated with this high-angle fracture as well as the fracture at the base of the sandstone and the sandstone itself. Open, high angle shear fractures are also responsible for permeability at depth, particularly in W205CH1. A large, high-angle fracture in a sandstone at 317 feet bgs in W205CH1 had a relatively high flow rate at 0.05 gpm. This fracture occurs approximately 23 feet above the W8 fault. In some cases the permeable zones correspond to the depth location of the intersection of the two orthogonal fracture sets. However, it should be noted that these fractures all occur in W205CH1 which is located in the hanging wall and adjacent to the W8 fault. The importance of these high-angle fractures away from fault zones will continue to be evaluated during the sitewide investigation.

At greater depth, the more steeply dipping fracture set associated with high-angle faults may assume a more important hydraulic role. Based on fracture data from W205CH1, the hydrologic importance of the bedding parallel fractures appears to decrease with depth. Most of the conductive intervals identified below 200 feet in this borehole (4 out of 5) are associated with high-angle fractures. This is likely a result of the increase in lithostatic load with depth. Producing intervals in other boreholes were not identified below 200 feet. Therefore, this hypothesis is based on a very limited data set.

#### 5.5.3 Geochemical Data Integration

##### DP-2 Geochemical Site Conceptual Model Summary

The geochemical site conceptual model has been revised based on the results of the GM-1 program. The essential observations used in the development of the geochemistry site conceptual model for major ion chemistry include the following:

- Three basic types of groundwater have been identified thus far as a result of the review of historical and recently collected data and include Na-Cl-HCO<sub>3</sub> or Na-HCO<sub>3</sub>-Cl, Na-Cl, and production mixed cation-HCO<sub>3</sub>

waters. The total dissolved solids (TDS) content of these waters range from several hundred to nearly 5000 milligrams per liter (mg/l) with the highest TDS waters found in the most highly weathered rocks in the proximity of surface drainages.

- Surface-waters are mostly dilute Na-SO<sub>4</sub> to dilute Na-Cl waters with TDS values typically less than 50 mg/l.
- Precipitation is dilute Na-SO<sub>4</sub> water with TDS values less than 50 mg/l .
- The dominance of Cl over HCO<sub>3</sub> and the range of TDS values observed in groundwater may be related to weathering, residence time, amount of groundwater circulation, changes in lithology, and the presence of faulting and fracturing. Specific conductance is strongly correlated with chloride and TDS. This makes for the easy distinction of waters within the system based on major ion chemistry.

Stable isotope chemistry data for oxygen and deuterium presented in the DP-2 information package and the recently collected packer test data collected in support of the GM Pilot Study indicate the following:

- Groundwater is not evaporatively enriched and surface-waters are moderately enriched.
- No evidence of isotopic enrichment by thermal exchange.
- No evidence of depletion associated with paleotemperature effects.
- Isotopic compositions of waters are consistent with post-pleistocene precipitation in central north America.

These finding indicate that stable isotope signatures will be a very useful tool in distinguishing water types at the site.

Radon-222 results indicate the following:

- Groundwater values are higher than in surface water and range from 230 to 2,100 picocuries per liter (pCi/l).
- Generally surface-water radon concentrations are less than the method detection limit of 50 pCi/l.

Radon-222 results suggest that low levels observed in surface-waters may be the result of dilution, diffusion across air-water interfaces, or the absence of groundwater discharge to surface-water within the footprint of the site. The utility of radon as a tool to identify discharge of groundwater to the surface is considered to be limited unless lower method reporting limits can be obtained.

Unstable isotope analyses for carbon-14 and tritium indicate that groundwater at the site may not be as old as model ages indicate and correction of the data may be necessary. However, they do indicate a general downward flow of groundwater with increasing age with depth.

### GM Pilot Study Geochemistry Site Conceptual Model Update

The results obtained during evaluation of the geochemical data collected during the GM Pilot Study confirm the previous findings detailed in the DP-2 Information Package concerning the geochemical site conceptual model. The results also provide some additional insights that will be used in moving forward towards site characterization activities. Packer test analytical results indicate the following:

- Production water is low in sodium, chloride and TDS, and high in magnesium.
- East of the W-8 fault rocks in borehole W207AR1 are higher in quartz and lower in clay content and fewer permeable water bearing zones exist. Waters in this environment are dominated by the anion chloride relative to bicarbonate even at depths below the weathering zone. Tighter, less productive boreholes (insufficient flow during packer testing to support pump testing) west of the fault from which samples were collected from the weathering zone are also dominated by chloride over bicarbonate, while tighter boreholes tested below the weathering zone show bicarbonate dominating over chloride.
- In the hanging wall of the W8 fault groundwater samples collected from corehole W205AR1 are dominated by bicarbonate over chloride and TDS values are lower.
- Oxygen/deuterium results from the packer tests plot with groundwater from elsewhere at the site and show no sign of enrichment.
- Radon concentrations in groundwater collected during the packer tests appear to crudely increase with depth and are similar to those obtained during the DP-2 groundwater sampling program.

The analytical results collected during the GM Pilot Program confirm previous DP-2 observations used in the development of the initial geochemical site conceptual model with one exception. It also appears that waters higher in chloride than bicarbonate, and higher in TDS, exist at depths below the weathered zone in areas east of the W-8 fault. This occurs in less productive zones where the mineralogy of the sequence is less clay-rich and more quartz-rich.

Time series results also provide interesting results relative to the current geochemical site conceptual model and include the following:

- A gradual decrease in specific conductance and rapid decrease in temperatures were observed in test intervals from well W207CH1. The pH values were relatively constant and moderately basic (pH ~ 8) and less than 200 gallons total were produced from any one interval.

- The pH values from the deepest interval tested in well W205CH1 increased with time from approximately 8 to 9 and temperatures were relatively constant throughout the tests. As much as 1450 gallons of water were produced in a 3 hour period.

Constant and relatively lower specific conductance, and constant temperatures, suggest uniform groundwater composition and more rapid circulation in corehole W205CH1. Variable and relatively higher specific conductance suggest higher residence times, lower circulation, and more mature weathering in borehole W207CH1. Increases in pH with time suggest that carbonate sequences found below the W8 fault may be influencing water chemistry.

### Geologic, Climatic, and Physical Factors Influencing the Geochemical Site Conceptual Model

Clay mineralogy was found to be predominantly smectite and illite based on analysis of samples collected from core and analysis of the geophysical logs run during the GM Pilot Program. Previous analyses conducted by Rust (1995) also indicate the presence of some kaolinite clays (primarily in samples collected from the weathered zone). Mineralogical information from rocks present at the site is incomplete, as is the water chemistry data. However, preliminary indications based on the available data are that the mineralogy of the rocks is simple; composed primarily quartz, plagioclase feldspars, and clay, with variable amounts of potash feldspars, micas, and oxides. Rain and surface-waters are acidic with a pH of around 4.5 and vegetation (evapotranspiration) relatively prolific across the site. These and other factors are the result of, or control the processes that are responsible for, the geochemistry of the waters present at the site.

### Summary and Conclusions

At present, insufficient data of a known quality is available to refine our understanding of the geochemical processes that control the water chemistry and related mineral-forming processes at the site. Geochemical modeling using several of many codes (e.g. PHREEQC, WATEQ4F, NETPATH) will need to be used to analyze the available data once it has been compiled and verified. The overall nature of the system and the processes controlling the system can, however, be examined briefly given the currently available and verified data.

Rock-dominated waters are those in relatively closed systems, out of contact with fresh, diluting recharge. Such waters can approach equilibrium with respect to contacting silicates and aluminosilicates, and so tend to have relatively high pHs and high major ion and silica concentrations (Langmuir, 1997). High pH values may also result from the concentrating impact of evapotranspiration. Clay types and content reflect differences in the maturity of weathering, rock composition, and fracturing that has enhanced water circulation.

The early weathering products of complex silicate rocks, such as plagioclase feldspars to clays, result primarily in the release of sodium and bicarbonate (Andrews, 1996). Chlorine and the related anion chloride is found to occur in



gneissic rocks, similar to those which are found as lithic fragments throughout the sedimentary section at the site at concentrations as high as 200 micrograms per kilogram (Johns, 1966). Chlorine in these rocks is likely to have substituted for hydroxyl ions in micas or occur in late magmatic fluid inclusions in quartz and potash feldspars. As weathering reaches a mature stage, chlorine is released when micas and quartz breakdown. This explains the presence of Na-Cl waters in the weathered zone and in rocks containing elevated percentages of weathered micas. Diabase rocks are inherently higher in magnesium than those relatively more acid parent rocks from which most of the sedimentary rocks found throughout the stratigraphic sequence were derived. This explains the mixed cation composition of the production water.

In addition to the release of sodium and bicarbonate into the system as a result of the initial weathering of complex silicates to form clays, hydronium ions ( $\text{OH}^-$ ) are also released to the system acting to raise the pH (Langmuir, 1997). Time series plots of pH versus time discussed in Section 4 indicate that pHs are highest in the vicinity of well W205CH1. This is consistent with the upper portion of W205CH1 in the hanging wall of the W8 fault where rock - water interactions are likely enhanced due to increased circulation and aquifer capacity.

Figure 5-10 shows the pathways for the development of clay minerals and iron oxides under various degrees of maturation and parent rock composition. From this figure it is easy to conclude why the dominant clay types found at the site are illite and smectite. Magnesium and potassium contents of rocks and waters at the site are low and cation removal likely slow throughout most of the system although in areas where cation removal is high it is anticipated that substantial kaolinite should be present. It is suspected because of its relatively high solubility that in areas where circulation is low (because of less fracturing), weathering more complete (weathered zone), or where rocks contain a larger abundance of lithic fragments containing micas, that chloride would dominate over bicarbonate as the primary anion. This hypothesis, however, must be confirmed through more detailed analyses of the distribution of micas and the actual source of chloride in the system. The high solubility of chloride and the higher relative abundance of complex silicates in most of the rocks at the site would suggest that, under conditions that enhance circulation (i.e., fractured zones) and where weathering is not as complete, that bicarbonate would be found at higher concentrations. This conclusion is further supported by the fact that waters found to have higher TDS, which are generally associated with longer residence times or more complete weathering, are dominated by chloride (W206AR1, W202AR1, W201AR1), while waters with lower TDS which generally occur below the weathered zone, or in areas that are more highly fractured, contain substantial quantities of bicarbonate.

Figure 5-11 shows how the bulk chemistry of most systems can be tied into the processes responsible for the dominance of chloride over bicarbonate and result in a range of TDS concentrations in groundwaters. While this is a gross over simplification of the geochemical system likely present at the site this same general diagram can be applied to most water types found across the globe. During site characterization these relationships will be examined in detail and specific mechanisms and reactions identified. This information will then be funneled into facility performance assessment.



## 6.0 SIGNIFICANT FINDINGS OF THE GM-1 PILOT STUDY

During the GM-1 Pilot Study, a large volume of information and data was compiled for the geologic, geochemical, and hydrogeologic conditions within the investigation area. The analysis and integration of this comprehensive data set has resulted in an increased knowledge and understanding regarding the hydrogeologic conditions along the GM-1 Pilot Study Area. This Section presents a summary of the most significant findings of this GM-1 Investigation:

1. This field investigation evaluated a number of investigative techniques, tools and protocols for the compilation of data required to characterize the hydrogeologic, hydraulic, and geochemical conditions at the Wake site. From this study, a series of six downhole geophysical tools and two hydraulic testing tools have been identified as best suited to site conditions and the project needs for site characterization and analysis. These tools include: three arm caliper, full wave form sonic, high resolution electrical imaging, density and neutron, spectral gamma, and resistivity. In addition, hydrophysical and packer testing techniques provide delineation and quantification of the important hydrogeologic features. Comparison of the information gained from these techniques to that from rock core, when used in combination with trench maps and existing site data, indicates that the selected geophysical and hydraulic testing tools significantly improve the accuracy, repeatability, consistency, and reliability of measurement, while reducing uncertainty in the results and interpretations. The proposed combination of geophysical, imaging, and hydraulic tools allows:
  - direct identification of hydraulically conductive discrete features or zones,
  - rapid evaluation of the relative magnitude of flow through each feature or zone,
  - quantitative analysis of conductive-feature geometric and hydraulic parameters,
  - *in-situ* images of the conductive features or zones for geologic classification,
  - a range of associated physical characteristics of the feature or zone and surrounding rocks,
  - the ability to collect water samples directly from the feature or zone for geochemical analysis, and
  - the identification of mapping units for correlation and geologic data integration.
2. Development of the geologic cross section along the GM-1 trench has provided valuable insights into the scale and detail of investigations needed for site-wide studies. Work along the GM-1 trench included logging two deep cores and selected existing cores at a scale of 1 inch=1 foot. This scale allowed definition of fine-scale features in these cores and comparison of fine-scale features to geophysical logs and images. The trench mapping was done electronically by surveying points along contacts and fractures. As such, this mapping can

be considered scale-independent. Similarly, the geophysical logs have resolutions ranging from less than an inch to approximately one foot. The hydrophysical testing allows direct and accurate location of conductive features, which can then be correlated to images and geophysical data. Correlation of map units with those exposed in the GM trenches was done primarily by pattern matching using the graphic log of the trench with the resultant graphic logs for each borehole. This comparison indicated that the correlations made using only the gamma log patterns for map units, in combination with the trench maps, provided the same results as using the trench graphic log in combination with borehole graphic logs.

3. The basic geologic information evaluated in the GM-1 Pilot Study was collected at very fine scales. As part of the integration and correlation studies, lithofacies were identified which ranged from a few inches to a few feet in thickness. Associations of lithofacies were assembled into mappable rock units ranging in thickness from about 10 to about 60 feet. These mappable units have characteristic physical properties, geologic attributes and geophysical signatures that are distinctive across the GM-1 Study Area. As such, this scale of geologic units appears appropriate and usable for correlation between trenches, surface exposures, and borings at the site for the SIP. This scale of mappable units is also appropriate to meet the regulatory requirements for geologic mapping of the site at a scale of 1 inch=100 feet. Lithologic correlations were readily made over distances of 800 ft and for thickness on the order of 60-90 ft.
4. The GM-1 Pilot Study results indicate that groundwater occurs in three principal locations: 1) within and at the base of the weathering zone, 2) along inclined bedding plane (strata-concordant) conductors near the lithologic contacts of sandstones and mudstones, and 3) within the enhanced fracture zone of the W8 fault, approximately 150 to 200ft from the fault plane in the hanging wall. The weathered zone contains the greatest number of producing intervals, except in W205, which is in the hanging wall of the W8 fault. A producing feature is generally present at or just above the base of the weathered zone. The geophysical log analysis indicates this zone is higher in porosity, lower in acoustic velocity, and contains lower density geologic materials. Analyses of both the geophysical and image tool results, in combination with the hydrophysical logging, indicate that fluid flows appears to be dominated by open strata-concordant fractures, particularly at shallow depth. Where data are available from some of the deeper boreholes, there is evidence that the hydraulic importance of the strata-concordant fractures decreases with depth as the lithostatic load increases. At greater depth, the more steeply dipping fracture sets associated with high-angle faults may assume a more important hydrologic role in groundwater occurrence and movement. In many cases, the strata-concordant fractures occur at the contact between an upper, more permeable, unit (usually sandstone) and a lower, impermeable, unit (usually mudstone or siltstone). These coarse sandstones are relatively clean, well-sorted, and are often conglomeratic. It is difficult to determine whether inflow at a given location is more dependent on bedding plane fractures, or on a lithologic unit that is relatively more permeable than others. In its hanging wall, the W-8 fault contains

intensely fractured rock associated with the fault and acts as a fluid flow conduit. Fractures inclined to bedding may also play an important role if they connect one bedding-plane fracture to another.

5. Significant understanding has been compiled regarding the structural geology along the GM-1 Pilot Study Area. The combination of trench mapping and oriented downhole imaging provide in-situ fracture data, including fracture density, orientation, and apparent aperture. The dominant fracture directions in the GM-1 area include generally north-trending high-angle fracture sets as well as low-angle fractures parallel to the east-dipping stratigraphy. The high angle fracture set is more prevalent in the hanging wall of the W8 fault. Strata-concordant fracture zones tend to occur at the boundaries of units with significantly different mechanical properties, such as coarse-grained sandstone in contact with mudstone. This relationship is consistent with preferential slip along these zones to accommodate movements during ancient faulting and tilting episodes. Downhole imaging provides oriented bedding directions throughout each boring, so that variations in bedding orientation due to changes in depositional environment or structural deformation can be recognized. Dips west of the W8 fault are on the order of 20 degrees to the east, increasing to about 40 degrees approaching the fault. Immediately east of the W8 fault, a gentle anticline has been mapped, with nearly horizontal beds at the surface near the fault and dips systematically increasing to about 20 degrees NE both with depth near the fault and eastward.
6. The location of drainages across the site was hypothesized to be controlled by the presence of major faulting. Comparison of the revised geologic map and the trench maps in the GM-1 Pilot Study Area, and the apparent absence of faults in the topographic lows, indicate that the topography in this area is more likely controlled by stratigraphy than by structure. A correlation does exist between topographic saddles and strike-parallel drainages which are underlain by fine-grained units such as mudstones within the GM-1 Pilot Study Area (Plate 5-2, Geologic Map). The topographic saddle at GM-3 Trench Station 150 feet and Drainage 1 are both underlain by Ms map units. Similarly, topographic highs and ridge-lines tend to correlate with lithologic intervals dominated by sandstone units mapped in the trenches (Plate 5-1, Geologic Cross Section) and on the geologic map. The southeastern trending ridge at GM-2 Trench Station 250-350 feet is held up by an Sm unit, and the topographic high with associated northerly trending ridges at GM1-W Trench station 500 to 765 feet can be correlated with a lithologic interval dominated by sandy map units. At a smaller scale, isolated zones of deeper weathering and minor topographic lows tend to correlate with the occurrence of small faults or increased fracturing observed in the trenches. An example is located in GM-1 Trench at Station 510 feet.
7. Analysis of the GM-1 Pilot Study, review of the existing data, and review of the data collection methodologies provided a technically strong foundation upon which to design theSIP. A combination of previously applied techniques along with the recommended geophysical and imaging tools will be implemented. These methodologies include but are not limited to:
  - Trenching and scraping to expose near-surface soils, rock, and geologic structures;

- Continuous sampling in all borings from the surface to an appropriate depth for setting casing, including standard penetration testing in the upper zone for geotechnical evaluation;
  - Percussion drilling to provide boreholes for geophysical logging and hydrologic testing;
  - Downhole imaging and geophysical logging using the proposed suite of tools from the GM-1 Pilot Study;
  - Hydrophysical logging to identify significant groundwater conductors;
  - Targeted packer testing of these discrete features or zones;
  - Collection of samples from groundwater, surface water and soil and rock for geochemical analysis;
  - Infiltration testing at or near final design grade;
  - Interference testing in paired wells to develop additional hydrologic parameters, and;
  - Natural gradient tracer testing, and use of tracers during aquifer and infiltration testing.
8. The analysis and integration process of this GM-1 program demonstrate that integration of multiple lines of evidence does lead to a more complete and internally consistent understanding of the site conditions in the GM-1 area. This observation is based, in part, on:
- Direct observation and measurement of water level responses in wells along the W8 fault and along strata-concordant conductors perpendicular to the fault during drilling and packer testing at well W205CH1;
  - Successful packer testing and modeling of geometries and hydraulic characteristics of discrete conductors identified through hydrophysical logging, and the consistency of those geologic analysis models with the current understanding of the relationships of high angle fractures to strata-concordant conductors;
  - Hydraulic responses and analyses of packer tests that are consistent with earlier observations at the site, including the results of Aquifer Tests 1 and 4;
  - The ability to geologically classify discrete hydraulic features by downhole imaging and geophysical techniques, and recognition that these features are related to specific geological characteristics;

- Demonstration that uncontaminated formation water can be collected for geochemical analyses even after drilling and geophysical and hydrophysical logging of new borings, and;
- Trends in the geochemical data that are consistent with water movement and geochemical evolution laterally and downward from the potentiometric high along the W8 fault towards both the east and west.

#### 6.1 Significant Findings Regarding the Applicability of the Proposed Field Testing and Analysis Techniques

Many technical issues regarding the protocols and the sequence of testing methods were addressed during the GM-1 Pilot Study. The following summarizes some of the pertinent findings related to field methods, protocols, and data analysis techniques:

- Continuous sampling from the surface to the depth of casing provides geological information related to the weathered portion of the geologic section. This information is lacking from most previous investigations at the site.
- Downhole geophysical data provide a reliable and unbiased indicator of the top of slightly weathered rock. In contrast, visual observation of core or observations during drilling appear to be inconsistent and highly variable.
- Information from trenching, coring and downhole geophysics and imaging in the GM-1 area allowed definition of five mappable geologic units generally ranging from 10 to 60 feet in thickness. Each map unit has characteristic geological (lithofacies) components, physical properties, and geophysical signatures. These mapping units were correlable for distances approximately on the order of 500 ft along strike and dip. The geology underlying the GM portion of the site is comprised of alternating combinations of these units.
- Correlations of map units from the trench to and between boreholes were successfully accomplished, both by pattern matching of geophysical signatures and by geologic correlation of individual map units. Each approach yielded the same correlations along the GM-1 cross section.
- Fine descriptive details of rock characteristics, such as the presence or absence of nodules, burrows and root traces, color mottling and small variations in composition or physical characteristics were found to be of little use in correlating between boreholes and to the trenches.
- Downhole imaging and geophysical data provide true orientations of bedding and fractures. This allows resolution of changes in the strike and dip of map units both laterally and with depth, and

provides actual fracture orientations. Additionally, in-situ fracture apertures can be estimated from the images, and the in-place characteristics of faults and broken zones can be determined. None of this information is available from rock core.

- Hydrophysical testing of boreholes allows direct measurement of conductive features. Once conductive features are identified, targeted packer testing provides information on geometry and properties and provides samples for geochemical testing. This approach is more efficient and superior to fixed interval packer testing and bulk geochemical sampling.
- Water-level monitoring using pressure transducers in nearby wells during the drilling and testing programs provided valuable information with respect to delineating the connectivity of conductive features in the subsurface.
- The techniques and sequencing of borehole drilling and testing evaluated in the GM-1 Pilot Study demonstrate that reliable samples of formation water can be extracted from individual hydrologic conductive features in boreholes for geochemical analysis. This was demonstrated by comparison of major ion chemistry of tested waters with the production well and surface water and the stability of field geochemical parameters with time during pump-out packer testing.
- The suite of geochemical parameters proposed for analysis provides information useful for flow and transport modeling of the site and for estimation of groundwater residence time and rock/water interaction. Information from the groundwater testing program will be enhanced once the rock geochemistry program is instituted.

## 6.2 Significant Findings Related to Refinement of the Site Conceptual Model

The GM-1 Pilot Study provided significant information and data resulting in the refinement of both the GM-1 cross section and the hydrogeologic conceptual model along the study area. This section briefly summarizes some of the more pertinent findings relating to the conceptual understanding of the hydrogeologic setting:

- Five major map units have been identified in the GM-1 area, based on trench mapping, core, and geophysical signatures: 1) Uf: upward fining sequences, 2) Ms: massive mudstones with minor sandstone, 3) Sm: massive sandstones with minor mudstone, 4) Swb: well bedded sandstone with minor mudstone, and 5) Mwb: well bedded mudstone with subordinate sandstone. Each map unit is characterized by distinctive lithofacies, physical characteristics and geophysical signatures. Map units range in thickness from about 10 to 60 feet. The geology underlying the GM-1 portion of the site is

composed of alternating combinations of these units. Approximately 75 percent of the rocks along the GM-1 cross section area are within the Uf and Ms units.

- Along the GM-1 trench, correlations of map units were readily made over distances exceeding 500 feet in the dip direction. Extension of map units to the W8 well cluster area and other borings indicates similar correlation distances along strike.
- Stratigraphy west of the W8 fault differs from that to the east of the fault. No clearly correlatable units were identified across the fault. As such, a preliminary estimate of the vertical displacement on the W8 fault appears to be in excess of 900 feet.
- During the drilling of boring W205CH1 along the W8 fault, hydrologic responses were observed in the W8 well cluster, about 650 feet to the north. Responses to packer testing at W205CH1 were also observed at the W8 cluster and at the original deep VSP boring W109SV3, about 125 feet to the west. These observations are consistent with the concept of enhanced connectivity along the hanging wall of the W8 Fault and/or the lateral extent of a strata-concordant conductor.
- During packer testing at W205, hydrologic responses were also noted at well W203AR1, about 525 feet west. This connection is interpreted to be along a strata-concordant conductor and is consistent with the conceptual model of flow along these features.
- A total of 27 conductive features were identified in the W200 well series by hydrophysical testing. Conductive zones occurred in the lower portion of the weathered zone which includes the contact between moderately weathered and slightly weathered rock defined by the geophysical data. This observation is consistent with enhanced secondary porosity in at least the lower portions of the weathered zone due to weathering and possibly fracturing related to unloading.
- Conductive features were also associated with strata-concordant fractures, and, particularly near the W8 fault, with individual high angle fractures. These observations are consistent with the current conceptual model of two classes of conductors in slightly weathered to fresh rock (bedding plane and high-angle fractures), and enhanced connectivity and conductivity in the hanging wall of faults.
- Inflow rates from the conductive features during hydrophysical logging ranged from 0.001 to 1.06 gallons per minute. The highest yields came from boring W205CH1 in the hanging wall of the W8 fault, where over 1500 gallons of water were extracted in a three-hour packer test. This is consistent with the current conceptual model of enhanced hydraulic conductivity in the hanging wall of the fault.

- During the analysis of the packer test data, modeling of the packer test response data indicated that the conductors exhibit finite sources of water, which is consistent with the expected physical characteristics of the conductors at the site. Both high angle fractures and strata-concordant conductors likely vary in aperture, effective porosity, storage and transmissivity both laterally and vertically. The packer test data provide valuable insights into the geometries of these features.
- Major ion and isotope geochemical data from groundwater samples analyzed as part of the GM-1 Pilot Study are consistent with those obtained during earlier site-wide geochemical sampling activities.
- The major ion chemistry is consistent with the current conceptual model in the vicinity of the W8 fault. For example, samples from W205CH1 are relatively lower in chloride than samples from wells to the east and west. This observation is consistent with a model of lateral movement and evolution of groundwater from the potentiometric high along the hanging wall of the W8 fault outward to the east and west. The single exception is well W204AR1, which has significantly lower TDS and chloride content and may represent local recharge.
- Time series geochemical sampling for field parameters during packer testing at W205CH1 and W207AR1 yielded generally stable results, suggesting that single geochemical samples from earlier sampling programs are likely representative of the formation waters in the area of the sampling well.
- During the drilling of boring W205CH1 along the W8 fault, water-level responses were observed in Well W206AR1, located approximately 350 feet east of W205CH1 and approximately 30 feet east of the W8 fault trace. This response suggests that there is hydraulic connection across the W8 fault, despite the large apparent throw on the fault (greater than 900 feet) and despite the significant difference in the type of mappable geologic units on either side of the fault. This response implies the following: (a) the W8 fault along the alignment of GM-1 activities (trench and boring locations) does not apparently serve as a barrier to hydraulic response; and (2) different, but hydraulically connected conductors occur on both sides of the W8 fault.



## 7.0 REFERENCES

- Barker, J.A., 1988. *A generalized radial flow model for hydraulic tests in fractured rock*. Water Resource Res., 24(10), 1796-1804.
- Back, W., 1960. Origin of chemical facies of groundwater in the Atlantic Coastal Plain: Internat. Geol. Cong., Copenhagen, Proc., p. 87-95.
- Back, W., 1961. Techniques for mapping of chemical facies: U.S. Geol. Surv. Prof. Paper 424-D, p. 380-382.
- Blackhawk, 1997. Interim Final Report, Seismic Surveys at the North Carolina Low Level Radioactive Waste Disposal Facility (NCLLRWDF), prepared for Harding Lawson Associates, July 10,
- Bourdet, D., J.A. Ayoub, and Y.M. Pirard, 1984. *Use of pressure derivative in well test interpretation*. SPE Paper #12777.
- Cant, D. J., 1992. Subsurface facies analysis, in Walker, R. G., and N. P. James, eds., *Facies models: response to sea level change*, 3rd ed.: Geological Association of Canada, St. John's Newfoundland, p. 27-45.
- Chakrabarty, C. and C. Enachescu, 1996. *A new approach for slug test analysis using deconvolution - theory and application*. Groundwater, in print.
- Chem- Nuclear Systems, Inc., 1995. Safety Analysis Report, North Carolina Low-Level Radioactive Waste Disposal Facility, Wake/Chatham County Preferred Site, March.
- Collinson, J. D. and D. B. Thompson, 1982. *Sedimentary structures*: Boston, Allen and Unwin, 194 p.
- Colog, 1997. *Hydrophysical logging results for Harding Lawson Associates Raleigh, North Carolina*.
- Freeze, R.A., and Cherry, J.A. 1979. *Groundwater*: Prentice Hall, Inc., Englewood Cliffs, NJ. Ch. 3, p. 81 - 143.
- Hem, J.D. 1985. *Study and interpretation of chemical characteristics of natural water*, 3rd ed., USGS Water Supply Paper 2254.
- Harding Lawson Associates, 1997a. *Work plan for the GM-1 pilot study for the North Carolina Low-Level Radioactive Waste Management Facility, Wake County North Carolina, 42 p., March 27.*

- Harding Lawson Associates, 1997b. *Graphic Logs: Re-Qualified Cores Along GM-1 Trench in Support of DP-1 Activities. Wake County North Carolina, 113 p., August 21.*
- Major, E. 1991. *Applied chemical and isotopic groundwater hydrology*: Halstead Press.
- Miall, A. D., 1978. Lithofacies types and vertical profile models in braided river deposits: a summary, *in* Miall, A. D., ed., *Fluvial Sedimentology*: Calgary, Canadian Society of Petroleum Geologists Memoir 5, p. 597-604.
- Miall, A. D., 1992. Alluvial deposits, *in* Walker, R. G., and N. P. James, eds., *Facies models: response to sea level change*, 3rd ed.: Geological Association of Canada, St. John's Newfoundland, p. 119-142.
- Miall, A. D., 1996. *The geology of fluvial deposits*: New York, Springer-Verlag, 582 p.
- Nuclear Regulatory Commission. 1989. *Quality assurance program. Procedure 370-QA-001.*
- Parker, J.M., III, 1979. *Geology and mineral resources of Wake County: North Carolina Geological Survey Bulletin 86, 122p.*
- Peres, A.M.M., M. Onur, and A.C. Reynolds, 1989. *A new analysis procedure for determining aquifer properties from slug test data. WRR 25(7), 1591-1602.*
- Pettijohn, F. J. and P. E. Potter, 1964. *Atlas and glossary of sedimentary structures*: New York, Springer-Verlag, 370 p.
- Ramey, H.J., R.G. Agarwal, and I. Martin, 1975. *Analysis of slug test or DST flow period data. Can. Pet. Jour., July 1975.*
- Reading, H. G.; ed., 1996. *Sedimentary environments and facies*, 3rd ed., Blackwell Science, Ltd., Oxford, 688 p.
- Reineck, H.-E. and I. B. Singh, 1973. *Depositional sedimentary environments; with reference to terrigenous clastics*: New York, Springer-Verlag, 439 p.
- Reinemund, J.A., 1955. *Geology of the Deep River coal field, North Carolina*: U.S. Geological Survey Professional Paper 246, 159p.
- Ricci Lucchi, F., 1995. *Sedimentographica: photographic atlas of sedimentary structures*, 2nd ed.: New York, Columbia University Press, 255 p.
- Straltsova, T.D., 1988. *Well testing in heterogeneous formations - An Exxon Monograph*, 413 p.
- Tchobanoglous, G., and Schroeder, E.D., 1987. *Water Quality*: Addison-Wesley Pub. Co., p. 43 - 162.

- U.S. Environmental Protection Agency, 1986. *Test methods for evaluating solid waste, physical/chemical methods, SW-846*. September.
- U.S. Environmental Protection Agency, 1992. *Test methods for evaluating solid waste, final update I, SW-846*. July.
- U.S. Environmental Protection Agency, 1994a. *Contract laboratory program national functional guidelines for inorganic data review*, February.
- U.S. Environmental Protection Agency, 1994b. *Test methods for evaluating solid waste, final update II, SW-846*. September.
- Walker, R. G., and James, N. P., eds., 1992, *Facies models: response to sea level change*, 3rd ed.: St. John's, Newfoundland, Geological Association of Canada, 409 p.
- Walker, R. G., ed., 1986, *Facies models*, 2nd ed.: Toronto, Geological Association of Canada, St. John's, Newfoundland, Geological Association of Canada, 317 p.

Table 1-1. Topical Meetings Held Related to the GM-1 Pilot Study

NCLLRWDF  
Wake County, North Carolina

Date	Topic
February 18, 19, 1997	Planning meeting for GM-1 pilot studies ✓
March 12, 1997	Discussion of GM-1 work plan
April 21, 1997	Field progress meeting
May 29, 1997	First topical meeting to discuss imaging techniques
August 7, 8, 1997	Trench walk through and review
August 14, 1997	Geologic integration and cross-section review
September 10, 1997	Second topical meeting on comparison of rock core with imaging and geophysical results
September 17, 1997	Vadose zone status report
September 17, 1997	Geochemistry status report
September 18, 1997	LWPSC meeting on proposed strategy for supplemental field investigation "D"

LWPSC - Licensing Work Plan Steering Committee

Table 1-2. Summary of Borehole Geophysics and Imaging Tool Runs

NCLLRWDF  
Wake County, North Carolina

Borehole	BIPS	CPR	AIT	CMR	ECS	FMI	NGT	PEX
W201AR1A	X	X	X	X	X	X	X	X
W201AR1B	X	X						
W202AR1	X	X	X	X		X	X	X
W203AR1	X	X	X	X		X	X	X
W204AR1	X	X	X	X		X	X	X
W205CH1	X	X	X	X	X	X	X	X
W206AR1	X	X	X	X		X	X	X
W207AR1	X	X	X	X		X	X	X
W208CH1	X	X	X		X	X	X	X

BIPS - Borehole Imaging Processing System  
CPR - 3 Arm Caliper  
AIT - Array Induction Tool  
CMR - Combinable Magnetic Resonance Imager  
ECS - Elemental Capture Spectroscopy Tool  
FMI - Formation Micro Imager  
NGT - Natural Gamma Ray Spectrometry Tool  
PEX - Platform Express Tool

Table 3-1. Summary of Borehole Construction

NCLLRWDF  
Wake County, North Carolina

Borehole Number	Start Drilling Date	End Drilling Date	Ground Surface Elevation (feet above MSL)	Top of Surface Casing Elevation (feet above MSL)	Total Split-Spoon Sampling Depth	Total Depth of Non-Competent Bedrock (feet bgs)	Total Depth of Cored Competent Bedrock (feet bgs)	Depth of Surface Casing (feet bgs)	Total Borehole Depth (feet bgs)	Drilling or Reaming Bit Type
W201AR1A	4/2/97	4/5/97	251.3	252.81	9.8	36.0	NA	36.0	115.0	Tri-cone bit
W201AR1B	4/3/97	4/4/97	251.2	252.97	NA	NA	NA	36.0	115.0	Button bit
W202AR1	4/6/97	4/12/97	258.5	260.29	4.9	30.0	NA	31.0	215.0	Tri-cone bit
W203AR1	4/3/97	4/10/97	272.1	273.48	5.6	32.0	NA	32.0	365.0	Button bit
W204AR1	4/3/97	4/9/97	270.9	272.48	11.2	32.0	NA	32.0	145.0	Button bit
W205CH1	4/1/97	4/22/97	268.8	270.03	12.4	31.0	562.0	31.0	715.0	Button bit
W206AR1	4/4/97	4/16/97	271.3	273.14	7.4	32.0	NA	33.0	415.0	Tri-cone bit
W207AR1	4/7/97	4/14/97	249.3	251.66	9.4	22.5	NA	24.0	465.0	Button bit
W208CH1	4/5/97	4/18/97	249.7	251.02	7.0	32.0	501.1	32.5	515.0	Tri-cone bit

MSL - Mean sea level

bgs - Below ground surface

NA - Not applicable

Table 3-2. Soil and Rock Core Logged During GM-1 Pilot Study

NCLLRWDF  
Wake County, North Carolina

Borehole		Soil (by Split Spoon)		Rock (by Coring)	
Number	Total Depth (ft)	Depth (ft) Sampled	Recovered/Logged Footage	Depth (ft) Cored	Recovered/Logged Footage
W201AR1A	115	0-9.8	7.85	10.2-36.0	24.35
W202AR1	215	0-4.9	3.35	5.85-30.0	23.05
W203AR1	365	0-5.6	3.25	5.95-32.0	23.75
W204AR1	145	0-11.2	8.6	11.5-32.0	16.45
W205CH1	715	0-12.4	9.25	12.5-562.0	513.05
W206AR1	415	0-7.4	4.05	8.0-32.0	23.1
W207AR1	465	0-9.4	4.6	10.0-22.5	12.05
W208CH1	515	0-7.0	5.6	8.0-501.1	490.6

Table 3-3. Borehole Imaging and Geophysical Log Mnemonics

NCLLRWDF  
Wake County, North Carolina

Tool	Acronym	Units	Measurement
AIT	AHT10	ohm-m	AIT-H Two Foot Resistivity A10
	AHT20	ohm-m	AIT-H Two Foot Resistivity A20
	AHT30	ohm-m	AIT-H Two Foot Resistivity A30
	AHT60	ohm-m	AIT-H Two Foot Resistivity A60
	AHT90	ohm-m	AIT-H Two Foot Resistivity A90
	AHIMR	ohm-m	AIT-H Input Borehole Mud Resistivity To AIT Processing
CMR	CMFF	decimal	CMR Free Fluid
	CMRP	decimal	CMR Porosity
	KCMR	mDarcy	Permeability from CMR
DSI	DTCO	10-6 sec/ft	Compress. wave inverse velocity (1/Vp)
	DTSM	10-6 sec/ft	Shear wave inverse velocity (1/Vs)
	DTST	10-6 sec/ft	Stoneley wave inverse velocity
ECS	CFE	no units	ECS Capture Iron Relative Yield
	CTI	no units	ECS Capture Titanium Relative Yield
	CGD	no units	ECS Capture Gadolinium Relative Yield
	CCA	no units	ECS Capture Calcium Relative Yield
	CSI	no units	ECS Capture Silicon Relative Yield
	CSUL	no units	ECS Capture Sulphur Relative Yield
NGT	SGR	API units	Total Gamma Ray
	CGR	API units	Computed Gamma Ray (Total minus URAN)
	THOR	ppm	Thorium
	POTA	decimal	Potassium
	URAN	ppm	Uranium
PEX	HCAL	inches	HRCC Cal. caliper SC
	TNPH	decimal	Thermal Neutron Porosity
	NPPI	decimal	Thermal Neutron Porosity (RatioMethod)
	NPOR	decimal	Enhanced Thermal Neutron Porosity
	HNPO	decimal	HiRes Enhanced Thermal Neutron Porosity
	PEFZ	Barnes/e	HRDD Formation Photoelectric Factor
	PEF8	Barnes/e	HRDD HiRes Formation PEF
	RHOZ	g/cm	HRDD Formation Density
	RHO8	g/cm	HRDD HiRes Formation Density
	HDRA	g/cm	HRDD Density Correction
	DPHZ	decimal	HRDD Density Porosity
	DPH8	decimal	HRDD HiRes Density Porosity
	RXOZ	ohm-m	MCFL Invaded Zone Resistivity
	RXO8	ohm-m	MCFL HiRes Invaded Zone Resistivity

ohm-m - Ohm \* meters

Mdarcy - milli Darcy (flux)

sec - second

ft - feet

API - American Petroleum Institute

ppm - parts per million

e - electrons

g - grams

cm - centimeter

Vp - Velocity of primary wave

Vs - Velocity of secondary wave

HRCC - High Resolution Common Cartridge

HRDD - High Resolution Density Detector

MCFL - Micro Cylindrically Focused Log

CMR - Combinable Magnetic Resonance

ECS - Elemental Capture Spectroscopy



Table 3-4. Borehole Imaging and Geophysical Log Field Activity Chronology

NCLLRWDF  
Wake County, North Carolina

Borehole No.	Date	Tool	Activity
W201AR1A	4/7/97	BIPS	With ambient water
W201AR1A	4/7/97	BIPS	Borehole pumped dry
W201AR1A	4/7/97	BIPS	Borehole refilled with clear water
W201AR1A	4/8/97	BIPS	Borehole jetted and pumped dry
W201AR1A	4/9/97	3-Arm Caliper	
W201AR1A	4/10/97	BIPS	Additional testing
W201AR1A	4/11/97	BIPS	Additional testing
W201AR1A	4/24/97	BIPS	FINAL LOG: First log after furlough, using new calibration tank and color-adjusted tool
W201AR1A	4/24/97	3-Arm Caliper	FINAL LOG
W201AR1A	4/29/97	Schlumberger	Minor acquisition problems were resolved and successful logs obtained in the following order: NGT, FMI, PEX, AIT, CMR, DSI. DSI dipole data poor (see above and comment for W205CH1)
W201AR1A	4/30/97	ECS	Run to test tool performance and acquisition software - test successful
W201AR1B	4/7/97	BIPS	With ambient water
W201AR1B	4/8/97	BIPS; logged twice while borehole refilled	Borehole jetted clean and pumped dry
W201AR1B	4/10/97	3-Arm Caliper	
W201AR1B	4/12/97	BIPS	
W201AR1B	5/8/97	BIPS 3-arm caliper	FINAL LOG
W202AR1	4/12/97	BIPS 3-arm caliper	To test borehole conditions
W202AR1	4/25/97	BIPS 3-arm caliper	FINAL LOG
W202AR1	5/2/97	Schlumberger:	<16:42-18:55> Data were acquired in the following order: FMI, DSI, AIT/NGT, DSI dipole data poor (see above and comment for W205CH1)
W202AR1	6/3/97	Schlumberger CMR log	<9:25-10:25> Station measurement acquired at 115 ft
W203AR1	4/10/97	BIPS	Water murky at depth
W203AR1	4/11/97	3-Arm Caliper	
W203AR1	4/25/97	BIPS	Aborted at 40 feet - opaque water
W203AR1	4/27/97	BIPS	Suspended solids observable in water
W203AR1	4/28/97	3-Arm Caliper	
W203AR1	5/2/97	Schlumberger:	<11:34-15:30> Data were acquired in the following order: FMI, DSI, NGT/AIT, PEX (a high gamma reading at 295' was attributed to having stopped there prior to logging to perform electrical checks) DSI dipole data poor (see above and comment for W205CH1)

Table 3-4. Borehole Imaging and Geophysical Log Field Activity Chronology

NCLLRWDF  
Wake County, North Carolina

Borehole No.	Date	Tool	Activity
W203AR1	6/2/97	Schlumberger CMR log	<16:45-18:13> Station measurements were obtained at 261.3 and 229.5 ft
W204AR1	4/9/97	BIPS	
W204AR1	4/9/97	3-Arm Caliper	
W204AR1	4/25/97	BIPS	Halted at 32.4 m due to high suspended solids beginning at 30 m.
W204AR1	4/26/97	3-Arm Caliper	Carried out after attempting BIPS log of W208CH1
W204AR1	5/3/97	Schlumberger	<9:45-12:44> Data were acquired in the following order: FMI, DSI, AIT/NGT, PEX.DSI dipole data poor (see above and comment for W205CH1)
W204AR1	6/2/97	Schlumberger CMR	<14:00-15:24>A station measurement was obtained at 95 ft
W205CH1	4/27/97	BIPS	from water level to 280 feet
W205CH1	4/27/97	3-Arm Caliper	
W205CH1	4/30/97	Schlumberger: FMI/DSI/AIT/NGT	DSI dipole data poor - due to the shallow depth of the borehole and operational requirement for finite pressure (see above) - monopole data is sufficient here to measure shear-wave velocity.CMR failed while running stations -<11:35-21:30>
W205CH1	5/7-5/8	BIPS	From TD to 267 feet: repeated logs, borehole flushed and filled with DI water prior to logging.An exception was allowed to record BIPS data moving uphole, rather than downhole as the TP requires - this allows fluid replacement from TD with tool below, and
W205CH1	6/2/97	Schlumberger CMR	This was the first log acquired with the CMR in June. A calibration was obtained prior to logging using a borehole simulator containing a gel with known properties.Two runs; Repeat stations were acquired at 167.1 ft using carbonate and sandstone settings.
W206CH1	4/26/97	BIPS3-arm caliper	FINAL LOG
W206CH1	5/1-5/2	Schlumberger	<16:48-18:15><08:45-10:35> Data were acquired in the following order: on 5/1: FMI, DSI (repeat halted for thunderstorms); On 5/2: AIT/NGT, PEX.DSI dipole data poor (see above and comment for W205CH1)
W206CH1	6/3/97	Schlumberger CMR	<10:40-14:02>3 stations were obtained

Table 3-4. Borehole Imaging and Geophysical Log Field Activity Chronology

NCLLRWDF  
Wake County, North Carolina

Borehole No.	Date	Tool	Activity
W207AR1	4/24/97	BIPS	FINAL LOG: Second log after furlough below about 124 m (406 ft) there was a slight decrease in image quality due to suspended sediments
W207AR1	4/25/97	3-Arm Caliper	
W207AR1	5/1/97	Schlumberger wireline	<10:00-15:40> Data were acquired in the following order: FMI, DSI, AIT, PEX, NGT. NGT was run only two hours after PEX w/ nuclear source. DSI dipole data poor (see above and comment for W205CH1)
W207AR1	5/4/97	Schlumberger wireline	<9:00-10:20> NGT re-run to obtain better data than acquired during the earlier run. That run may have been contaminated due to running immediately after the PEX chemical nuclear sources.
W207AR1	6/3/97	Schlumberger CMR	<14:10-16:30> No stations were obtained
W208CH1	4/26/97	BIPS	BIPS in dry borehole - log stopped due to glare at 85 feet
W208CH1	4/28/97	BIPS 3-arm caliper	FINAL LOGS - borehole filled with water
W208CH1	5/3/97	Schlumberger wireline logging	<15:45-21:30> Data were acquired in the following order: FMI, AIT/NGT, ECS, PEX, DSI. DSI dipole data poor (see above and comment for W205CH1) NO CMR log was obtained in W208CH1

BIPS - Borehole Imaging Process System  
 NGT - Natural Gamma Ray Spectroscopy Tool  
 FMI - Formation Micro Imager  
 PEX - Platform Express Tool  
 AIT - Array Indicator Tool  
 CMR - Combinable Magnetic Resonance  
 DSI - Dipole Sonic Imager  
 ECS - Elemental Capture Spectroscopy

Table 3-5. Rating of Conductive Features Encountered in the  
Hydrophysical Logging

NCLLRWDF  
Wake County, North Carolina

Category	Inflow Rate (gpm)
Very Low	<0.01
Low	0.01 - 0.05
Moderate	0.05 - 0.1
Medium	0.1 - 0.5
High	>0.5

Values based on a maximum drawdown of <10 ft.  
gpm - gallon per minute

Table 3-6. Summary of Test Intervals and Hydrophysical Logging Results

NCLLRWDF  
Wake County, North Carolina

Borehole	Test No.	Top of Interval (ft. BGS)	Bottom of Interval (ft. BGS)	Type of Test	Hydrophysical Category
W201AR1A	1	44.6	64.1	Slug	Low
W202AR1	1	31.0	215.0	Constant Rate	1 @ Low, 2@ Very Low
W203AR1	1	117.0	126.3	Slug	Low
	2*	58.0	67.3	Slug	Low
	3	61.0	70.3	Pulse	Low
	4*	38.8	52.2	Slug	Very Low
W204AR1	1	38.8	55.2	Slug	low
W205AR1	1*	145.2	166.2	Constant Rate	High
	2	148.2	169.2	Constant Rate	High
	3*	313.0	334.0	Constant Rate	Moderate
	4	301.1	715.0	Constant Rate	Moderate
	5*	262.9	283.9	Constant Rate	Moderate
	6	258.9	279.9	Constant Rate	Moderate
	7	195.6	216.6	Pulse	Very Low
	8	118.1	139.1	Slug	Low
	9	72.0	93.0	Slug	Low
W206AR1	1	41.7	57.1	Slug	2 @ Low
W207AR1	1	35.0	44.3	Slug	Moderate
	2	67.5	76.8	Constant Rate	Moderate
	3	153.1	465.0	Constant Rate	Medium
	4	41.5	50.8	Slug	Low

\* Tests prematurely ended due to packer bypass.

bgs - below ground surface

Table 4-1. Hydrogeologic Responses to Field Activities

NCLLRWDF  
Wake County, North Carolina

Hydrogeologic Response No.	Location of Response	Start Date	End Date	Magnitude of Response (feet of head change)	Suspected Cause
0	W203AR1	4/12/97	4/14/97	41.6	Natural recharge after air rotary drilling at W203AR1 and response to rock coring at W205 at depths of 476 to 546 feet bgs
1	W203AR1	4/14/97	4/15/97	-22.2	Reaming at W205CH1 (at depths of 31 to 556 feet bgs, 8,050 gallons of groundwater produced from formation) and Air rotary drilling at W206AR1
2	W203AR1	4/15/97	4/17/97	12.99	Natural recovery of formation groundwater after/during reaming at W205CH1, and a potential rise in head resulting from the installation of casing at W205CH1
3	W203AR1	4/17/97	4/18/97	9.7	Rock coring at W205CH1 (at depths of 556 to 562.5, 10 gallons of water lost to formation)
4	W203AR1	4/21/97	4/22/97	7.8	Recovery after air rotary drilling at W205CH1
5	W203AR1	4/22/97	4/23/97	-4.7	Air rotary drilling at W205CH1 (at depths of 585 to 715 bgs, 12,200 gallons of water produced from formation)
6	W203AR1	5/21/97	5/21/97	At Least -14.0	Packer testing at W203AR1
7	W205CH1	4/16/97	4/18/97	At Least -65.4	Reaming of W205CH1 (at depths of 500 to 556 feet bgs, 3,270 gallons of water produced from formation)
8	W205CH1	4/18/97	4/20/97	At Least 91.3	Natural recovery of formation groundwater
9	W205CH1	4/22/97	4/22/97	At Least -49.3	Air rotary drilling at W205CH1
10	W205CH1	4/23/97	4/27/97	At Least 56.5	Natural recovery of formation groundwater
11a	W205CH1	5/16/97	5/19/97	At Least -7.8	Packer Testing at W205CH1
11b	W109VS3	5/16/97	5/19/97	-21.7	Packer testing at W205CH1
11c	W203AR1	5/16/97	5/19/97	-4.7	Packer testing at W205CH1
12	W206AR1	4/20/97	4/21/97	-7.3	Air rotary drilling at W205CH1 (at depths of 556 to 585 bgs, 2,300 gallons of water produced from formation)
13	W206AR1	4/21/97	4/22/97	53.1	Natural recharge
14	W206AR1	4/22/97	4/22/97	At Least -9.4	Air rotary drilling at W205CH1 (at depths of 585 to 715 bgs, 12,200 gallons of water produced from formation)
15	W206AR1	4/22/97	4/26/97	At Least 34.4	Natural recharge
16	W206AR1	5/14/97	5/14/97	At Least -3.1	Packer Testing at W206AR1
17	W8MC12	4/6/97	4/13/97	1.3	Rock Coring at W205CH1 at a depth of 140 to 156 bgs; 13,110 gallons water lost to formation
18	W8MC12	4/14/97	4/17/97	-3.2	Reaming at W205CH1 at a depth of 546 to 562.5 bgs; 11,680 gallons water produced from formation
19	W8MC12	4/17/97	4/21/97	0.7	Natural recharge after air rotary drilling at W203AR1 and response to rock coring at W205 at depths of 476 to 546 feet bgs
20	W8MC12	4/21/97	4/25/97	-2.6	Air rotary drilling at W205CH1 at a depth of 585 to 715; 15,300 gallons water produced from formation
21a	W201ARIA	5/15/97	5/15/97	-2.4	Packer testing at W201ARIA
21b	W201AR1B	5/15/97	5/15/97	0.6	Packer testing at W201ARIA

Table 4-1. Hydrogeologic Responses to Field Activities

NCLLRWDF  
Wake County, North Carolina

Hydrogeologic Response No.	Location of Response	Start Date	End Date	Magnitude of Response (feet of head change)	Suspected Cause
22	W202AR1	5/15/97	5/16/97	-3.0	Packer testing at W202AR1
23	W202AR1	5/20/97	5/20/97	-2.2	Geochemical Sampling at W202AR1
24	W204AR1	5/20/97	5/20/97	-2.9	Packer Testing at W204AR1
25	W207AR1	5/10/97	5/13/97	-4.6	Packer testing at W207AR1

bgs - Below ground surface

Table 4-2. Boreholes With Hydrogeologic Connections

NCLLRWDF  
Raleigh, North Carolina

Location of Field Activity	Borehole With Hydraulic Response	Hydrogeologic Response Numbers	Open Interval Of Borehole With Hydraulic Response (feet bgs)	Relative Location of Borehole With Hydraulic Responses
W205CH1	W203AR1	1, 2, 3, 5, and 11c	32 to 365	530 feet west (updip) on the hanging wall block
W205CH1	W206AR1	12 and 14	33 to 415	350 feet east (downdip) across the W8 Fault on the foot wall block
W205CH1	W109VS3	11b		110 feet west (updip) on the hanging wall block
W205CH1	W8MC12	17 through 20	94.9 to 125	500 feet north along strike of the W8 Fault
W201AR1A	W201AR1B	21b	36 to 115	10 feet west (updip)

bgs - Below ground surface



Table 4-3. Summary of Hydrophysical Logging Results

NCLLRWDF  
Wake County, North Carolina

Borehole	Type of Test	Drawdown (feet)	Hydraulically	Inflow Rate:	
			Conductive Intervals (feet bgs)	Simulated <sup>1</sup> (gpm)	Inflow Rate Rating <sup>2</sup>
W201AR1A	Slug	3.80	45.28	0.0048	Very Low
			48.88	0.0098	Very Low
W201AR1B	Slug	2.80	46.92 - 47.90	0.004	Very Low
			56.76 - 62.34	0.001	Very Low
W202AR1	Slug	6.16	33.79 - 39.37	0.013	Low
			53.15	0.006	Very Low
			91.86	0.001	Very Low
W203AR1	Slug	6.53	44.95	0.002	Very Low
			53.15 - 80.05	0.011	Low
			108.27 - 141.08	0.009	Very Low
W204AR1	Slug	5.60	42.98	0.0106	Low
			103.02 - 138.45	0.0077	Very Low
W205CH1	Pumping Test	5.64	61.02	0.013	Low
			80.05	0.053	Moderate
			82.02	0.053	Moderate
			128.94	0.265	Medium
			158.14	1.059	High
			206.04	0.008	Very Low
			270.01	0.005	Very Low
W206AR1	Slug	8.53	316.93	0.050	Moderate
			36.09 - 41.01	0.0025	Very Low
			42.98 - 43.96	0.0120	Low
W207AR1	Pumping Test	10.83	46.92	0.0080	Very Low
			38.39 - 39.37	0.1060	Medium
			46.92	0.0397	Low
			70.54 - 76.44	0.1393	Medium
			159.12 - 161.09	0.6860	High

1) Inflow Rate simulated by numerical modeling using code BORE. Inflow Rates reported for late time data.

2) Inflow Rate Rating:

Very Low -	< 0.01 gpm
Low -	0.01 - 0.05 gpm
Moderate -	0.05 - 0.1 gpm
Medium -	0.1 - 0.5 gpm
High -	> 0.5 gpm

bgs - Below ground surface  
gpm - Gallons per minute

Table 4-4. Physical Input Parameters

NCLLRWDF  
Wake County, North Carolina

Borehole radius	$r_w$	6.75	[inch]	nominal
Test string radius	$r_t$	2.0	[inch]	measured
Interval length	$h$	-	[ft]	test specific
Interval volume	$V_i$	-	[ft <sup>3</sup> ]	test specific
Formation porosity	$\phi$	0.05	[-]	assumed
Water viscosity	$\mu_w$	1.00E-03	[Pa s]	PVT correlation
Water density	$\rho_w$	1000	[kg m <sup>-3</sup> ]	assumed
Total compressibility (formation)	$c_t$	7.00E-06	[Psi <sup>-1</sup> ]	assumed
Duration of borehole history	$t_h$	0	[h]	assumed

ft - Feet

Pas - Paschal \* second

kgm - Kilogram \* meter

Psi - Pounds per square inch

h - Height

Table 4-5. Summary of Results for Packer Tests

NCLLRWDF  
Wake County, North Carolina

Borehole	Test	Depth [ft bgs]	Main Test Phase	Tool Arrangement	Inner Boundary	Formation Model	Outer Boundary	T [m <sup>2</sup> /s]	Logging Rating	Head [ft bgs]
W201ARIA	1	44.6 - 64.1	Slug	Double Packers	W.S.	Homo.	Infinite	8.51E-07	Low	22.9
W202ARI	1	31.0 - 215.0	Production (analyzed as a slug)	Open Borehole - No Packers	W.S.	Composite	Infinite	Ti = 6.04E-07 To = 6.04E-06	1 @ Low, 2 @ Very Low	N/A
W203ARI	1	117.0 - 126.3	Slug	Double Packers	W.S.	Composite	Infinite	Ti = 5.95E-06 To = 1.98E-07	Low	38.8
	3	61.0 - 70.3	Pulse	Double Packers	W.S.	Homo.	Infinite	T = 9.42E-09	Low	38.0
W204ARI	1	38.8 - 55.2	Slug	Double Packers	W.S.	Homo.	Infinite	T = 3.32E-07	Low	25.5
W205ARI	2	148.2 - 169.2	Production	Double Packers	W.S. & Skin	Homo.	Open Ended Rectangle <sup>1)</sup>	T = 4.97E-05	High	34.3
	4	301.1 - 715.0	Production	Single Packer	W.S. & Skin	Dual Porosity	Infinite	T = 2.34E-06	Moderate	36.5
	6	258.9 - 279.9	Production	Double Packers	W.S. & Skin	Homo.	Open Ended Rectangle <sup>1)</sup>	T = 7.14E-05	Moderate	37.9
	7	195.6 - 216.6	Pulse	Double Packers	W.S.	Composite	Infinite	Ti = 2.13E-09 To = 3.55E-09	Very Low	33.3
	8	118.1 - 139.1	Slug	Double Packers	W.S.	Composite	Infinite	Ti = 5.29E-07 To = 5.29E-05	Low	33.1
	9	72.0 - 93.0	Slug	Double Packers	W.S.	Composite	Infinite	Ti = 7.70E-07 To = 1.60E-06	Low	32.8
W206ARI	1	41.7 - 57.1	Slug	Double Packers	W.S.	Composite	Infinite	Ti = 9.54E-07 To = 1.91E-07	2 @ Low	27.6
W207ARI	1	35.0 - 44.3	Slug	Double Packers	W.S.	Composite	Infinite	Ti = 2.33E-06 To = 3.33E-08	Moderate	9.8
	2	67.5 - 76.8	Production	Double Packers	W.S. & Skin	Dual Porosity	Infinite	T = 1.86E-06	Moderate	10.4
	3	153.1 - 465.0	Production	Single Packer	W.S. & Skin	Homo.	Open Ended Rectangle <sup>1)</sup>	T = 3.09E-05	Medium	12.4
	4	41.4 - 50.8	Slug	Double Packers	W.S. & Skin	Homo.	Channel Boundaries <sup>2)</sup>	T = 4.94E-07	Low	11.0

1) Open-ended rectangle model contains three no flow boundaries

2) Channel boundaries model contains two no flow boundaries

W.S. - Wellbore Storage

T - Transmissivity

Ti - Inner zone transmissivity

To - Outer zone transmissivity in a composite flow model

ft - Feet

bgs - Below ground surface

pro-only/formatb/Sect-4.xls

10/24/97 8:25 PM

Table 4-6. Comparison Between Hydrophysical Logging and Packer Test Results

NCLLRWDF  
Wake County, North Carolina

Group	Transmissivity [ $\text{m}^2/\text{s}$ ]	Relative Rating from Hydrophysical Logging
1	9.42E-09	Very Low
1	2.13E-09	Very Low
2	8.51E-07	Low
2	6.04E-07	Low
2	5.95E-06	Low
2	3.32E-07	Low
2	5.29E-07	Low
2	7.70E-07	Low
2	9.54E-07	Low
2	4.94E-07	Low
3	2.34E-06	Moderate
3	7.14E-05	Moderate
3	2.33E-06	Moderate
3	1.86E-06	Moderate
4	3.09E-05	Medium
5	4.97E-05	High

The transmissivity is derived from either a homogenous model or from the inner zone in composite formation model.

Table 4-7. Geochemical Results Reviewed in Support of DP-1

NCLLRWDF  
Wake County, North Carolina

Sample Designation	Sample Date	Time Sampled	Interval	HCO <sub>3</sub> (mg/l)	Ca (mg/l)	K (mg/l)	Mg (mg/l)	Na (mg/l)	Cl (mg/l)	SO <sub>4</sub> (mg/l)	O18 %	Deut %	Radon	Comment
PRODUCTION-01	4/21/97	12:05	NA	250	55.2	1.33	18.4	37	18	12	-5.9	-39	230	
PRODUCTION-02	4/21/97	13:55	NA	260	54.4	1.31	18.1	36.2	21	12	-5.8	-37	610	
W207AR1-67.5-77.9-1	5/11/97	12:50	67.5 -77.9	130	47.3	6.53	27.6	286	470	5U	-5.7	-30	NA	
W207AR1-67.5-77.9-2	5/11/97	16:20	67.5 -77.9	190	42.9	4.18	16.3	364	510	7.5	-5.7	-32	NA	
W207AR1-67.5-77.9-3	5/11/97	16:30	67.5 -77.9	200	36	3.78	13.3	334	470	5	-5.6	-29	NA	
W207AR1-67.5-77.9-4	5/11/97	16:45	67.5 -77.9	190	34.5	3.72	12.6	331	460	5.1	-5.6	-31	NA	
W207AR1-67.5-77.9-5	5/11/97	17:00	67.5 -77.9	200	30.3	3.49	10.9	309	280	5U	-5.8	-28	NA	
W207AR1-156-166-1	5/12/97	13:55	156-166	150	27.5	3.29	7.84	254	370	6.2	-5.6	-34	NA	
W207AR1-156-TD	5/12/97	14:05	156-TD	120	NA	NA	NA	NA	340	28	-5.8	-28	NA	
W207AR1-153-3	5/12/97	17:20	153-TD	150	18.3	2.17	3.46	244	310	18	-5.5	-32	1400	
W207AR1-153-4	5/12/97	17:35	153-TD	160	19.8	2.21	3.24	270	310	22	-5.5	-31	1400	
W207AR1-153-5	5/12/97	17:45	153-TD	170	20.7	2.28	3.21	289	310	24	-5.5	-30	1350	
W206AR1-42-57	5/14/97	14:00	42-57	76	18.9	4.63	9.6	80	120	5	-5.8	-34	100	
W201AR1B-44.58-65.08	5/15/97	12:25	44.58-65.08	81	92.2	5.4	26	205	500	5U	-6.3	-34	70	
W205AR1-145.18-166-1	5/16/97	15:45	145.18-166	39	3.59	1.52	1.24	60.1	82	5U	-5.7	-34	NA	
W205AR1-145.18-166-2	5/16/97	16:01	145.18-166	190	10.5	1.75	1.91	177	160	5U	-5.5	-35	NA	
W205AR1-145.18-166-3	5/16/97	16:31	145.18-166	250	9.97	1.59	1.72	173	130	13	-5.3	-29	NA	
W205AR1-145.18-166-4	5/16/97	17:00	145.18-166	240	9.75	1.54	1.69	174	140	16	-5.3	-31	NA	
W205AR1-148.2-169.2-1	5/16/97	18:30	148.2 - 169.2	220	10.2	1.76	1.8	177	120	5U	-5.4	-28	NA	
W205AR1-148.2-169.2-2	5/16/97	19:09	148.2 - 169.2	240	9.58	1.63	1.71	177	120	5.8	-5.3	-30	NA	
W205AR1-148.2-169.2-3	5/16/97	19:41	148.2 - 169.2	240	9.35	1.59	1.64	171	120	8.2	-5.4	-30	NA	
W205AR1-148.2-169.2-4	5/16/97	20:13	148.2 - 169.2	250	9.2	1.47	1.62	170	120	5U	-5.4	-31	NA	
W205AR1-148.2-169.2-5	5/16/97	20:50	148.2 - 169.2	250	9.34	1.66	1.64	172	120	5U	-5.3	-29	NA	
W205AR1-148.2-169.2-6	5/16/97	21:32	148.2 - 169.2	240	9.43	1.96	1.68	165	120	7.3	-5.3	-32	NA	
W205AR1-Annulus	5/17/97	14:57	Open Hole	130	14.1	2.29	3.97	170	220	NA	NA	NA	NA	
W205AR1-313-334-1	5/17/97	15:01	313-334	170	8.58	1.52	1.47	145	120	5U	-5.4	-33	NA	
W205AR1-313-334-2	5/17/97	15:21	313-334	140	5.11	1.01	0.632	108	87	5U	-5.5	-34	NA	
W205AR1-301-715-1	5/17/97	18:42	301-715	130	5.61	1.24	0.819	111	87	10	-5.5	-27	NA	
W205AR1-301-715-2	5/17/97	18:49	301-715	140	5.49	1	0.591	114	89	16	-5.7	-31	NA	
W205AR1-301-715-3	5/17/97	19:13	301-715	150	5.9	1	0.556	123	96	24	-5.6	-26	NA	
W205AR1-301-715-4	5/17/97	19:45	301-715	150	5.94	0.891	0.532	124	100	30	-5.5	-29	NA	
W205AR1-301-715-5	5/17/97	20:16	301-715	140	6.3	0.877	0.544	130	100	38	-5.6	-28	NA	
W205AR1-301-715-6	5/17/97	20:36	301-715	140	6.24	0.884	0.548	132	100	34	-5.5	-30	NA	
W205AR1-262.88-283.88-1	5/18/97	9:33	262.88-283.88	140	6.14	0.884	0.532	132	99	32	-5.6	-31	740	
W205AR1-262.88-283.88-2	5/18/97	9:37	262.88-283.88	140	6.17	0.921	0.558	131	110	33	-5.5	-32	1260	
W205AR1-266.88-287.88-1	5/18/97	11:03	266.88-287.88	200	9.52	1.37	1.11	160	140	15	-5.4	-30	660	
W205AR1-266.88-287.88-2	5/18/97	11:13	266.88-287.88	200	9.48	1.42	1.15	164	130	17	-5.5	-31	700	

Table 4-7. Geochemical Results Reviewed in Support of DP-1

NCLLRWDF  
Wake County, North Carolina

Sample Designation	Sample Date	Time Sampled	Interval	HCO <sub>3</sub> (mg/l)	Ca (mg/l)	K (mg/l)	Mg (mg/l)	Na (mg/l)	Cl (mg/l)	SO <sub>4</sub> (mg/l)	O18 %	Deut %	Radon	Comment
W205AR1-266.88-287.88-3	5/18/97	11:47	266.88-287.88	180	8.51	1.15	0.935	155	130	21	-5.4	-32	630	
W205AR1-266.88-287.88-4	5/18/97	12:15	266.88-287.88	180	8.11	1.12	0.858	153	130	25	-5.5	-28	680	
W205AR1-266.88-287.88-5	5/18/97	12:45	266.88-287.88	180	7.74	1.06	0.789	149	130	27	-5.6	-29	610	
W205AR1-266.88-287.88-6	5/18/97	13:15	266.88-287.88	170	7.68	1.05	0.774	149	130	30	-5.5	-31	570	
W205AR1-266.88-287.88-7	5/18/97	13:30	266.88-287.88	170	7.8	1.06	0.774	152	130	31	-5.5	-32	710	
W205AR1-195.6-216.6-1	5/19/97	9:40	195.6-216.6	170	7.835	1.12	0.8	152.5	125	32.5	-5.4	-30	560	
W205AR1-195.6-216.6-ML	5/19/97	9:40	195.6-216.6	1.0U	7.76	1.12	0.79	151	130	32	-5.6	-33	540	Duplicate
W205AR1-RH-ML	5/19/97	10:45	NA	1.0U	57.6	0.061	15	138	1.0U	5U	-7.6	-45	30U	Trip Blank
W205AR1-EB	5/19/97	10:50	NA	1.0U	88.1	0.061	0.012	132	1.0U	5U	-7.7	-43	50U	Equipment Blank
W205AR1-118.1-139.1-1	5/19/97	12:15	118.1-139.1	180	9.02	1.27	1.19	156	150	27	-5.5	-34	690	
W205AR1-71.98-92.98-1	5/19/97	14:48	71.98-92.98	170	13.9	1.9	3.11	178	230	15	-5.5	-31	590	
W205AR1-71.98-92.98-2	5/19/97	17:20	71.98-92.98	150	17.7	2.52	5.1	194	280	12	-5.5	-29	500	
W202AR1-1	5/20/97	7:40	38.78 - 55.18	200	25.9292	3.91	10.6074	64.0183	240	5U	-5.6	-31	240	
W202AR1-ML-RH	5/20/97	10:15	NA	1.0U	50.3	61	17.4	38.3	1.0U	5U	-7.6	-46	40U	Trip Blank
W202AR1-ML	5/20/97	10:20	NA	1.0U	58.4	62	14.8	36.6	1.0U	5U	-7.6	-45	40U	Equipment Blank
W202AR1-RH	5/20/97	10:25	NA	1.0U	101	63	19.7	84.5	1.0U	5U	-7.6	-45	30U	Pump Blank
W204AR1-1	5/20/97	12:05	33.78-55.18	56	4.3	1.44	2.05	17.9	5.1	5U	-5.5	-32	70	
W204AR1-2	5/20/97	14:30	33.78-55.18	59	4.7	1.52	2.01	17.4	4.9	5U	NA	NA	NA	
W203AR1-117-126.4-1	5/21/97	10:05	117-126.4	50	1.79	0.818	0.543	44.9	46	5U	-5.7	-35	120	
W203AR1-117-126.4-ML	5/21/97	10:05	117-126.4	48	1.8	0.742	0.543	46	46	5U	-5.4	-34	130	Duplicate
W203AR1-117-126.4-TU	5/21/97	11:25	NA	1.0U	29	61	12.3	65.2	1.0U	5U	-7.5	-46	40U	Trip Blank
W203AR1-117-126.4-RF	5/21/97	11:40	NA	1.0U	41.5	61	12.3	47.8	1.0U	5U	-7.6	-43	40U	Equipment Blank
W203AR1-117-126.4-SSB	5/21/97	12:25	117-126.4	1.0U	29.4	61	12.3	42.5	1.0U	5U	-7.5	-44	40U	Equipment Blank
W203AR1-117-126.4-PPT	5/21/97	13:25	117-126.4	1.0U	38.7	61	12.3	51.6	1.0U	5U	-7.6	-46	50U	Pump Blank
W203AR1-117-126.4-2	5/21/97	14:05	117-126.4	57	1.18	0.614	0.216	43.5	32	5U	-5.5	-33	320	
W203AR1-58-67.4-1	5/21/97	16:00	58-67.4	46	1.63	0.869	0.403	40	39	5U	-5.5	-33	100	
W203AR1-61-70.4-1	5/21/97	17:45	61-70.4	51	2.32	1.07	0.817	47.1	52	5U	-5.6	-35	170	

U - Not detected at or above the Method reporting Limit

NA - Sample Not Analyzed for the parameter indicated or data not applicable to the sample type

Table 4-8. Chemical Compositions of Groundwater from Sampled Intervals

NCLLRWDF  
Wake County, North Carolina

Well ID	Interval Sampled	No. of Samples	Composition
W201AR1B	44.8 - 65.08	1	Na-Ca-Mg-Cl
W202AR1	Grab Sample	1	Na-Ca-Mg-Cl-HCO <sub>3</sub>
W203AR1	58 - 67.4	1	Na-Cl-HCO <sub>3</sub>
W203AR1	61 - 70.4	1	Na-Cl-HCO <sub>3</sub>
W203AR1	117 - 126.4	2	Na-Cl-HCO <sub>3</sub>
W204AR1	38.78 - 55.18	2	Na-Ca-Mg-HCO <sub>3</sub> -Cl
W205AR1	71.98 - 92.98	2	Na-Cl-HCO <sub>3</sub>
W205AR1	118.1 - 139.1	1	Na-Cl-HCO <sub>3</sub>
W205AR1	145.18 - 166	4	Na-Cl-HCO <sub>3</sub>
W205AR1	148 - 169.2	6	Na-HCO <sub>3</sub> -Cl
W205AR1	195 - 216.6	1	Na-Cl-HCO <sub>3</sub>
W205AR1	262.88 - 283.1	2	Na-Cl-HCO <sub>3</sub> -SO <sub>4</sub>
W205AR1	266.88 - 287.88	7	Na-Cl-HCO <sub>3</sub>
W205AR1	313 - 334	2	Na-Cl-HCO <sub>3</sub>
W205AR1	301 - 715	6	Na-Cl-HCO <sub>3</sub>
W206AR1	42 - 57	1	Na-Ca-Mg-Cl-HCO <sub>3</sub>
W207AR1	67.5 - 77.9	5	Na-Ca-Cl-HCO <sub>3</sub>
W207AR1	156 - 166	1	Na-Ca-Cl-HCO <sub>3</sub>
W207AR1	156 - TD	3	Na-Cl-HCO <sub>3</sub>
Production Well	N/A*	2	Ca-Na-Mg-HCO <sub>3</sub> -Cl

\* Not available

\*\* Cations listed in order of abundance followed by anions listed in order of abundance

Table 4-9. Velocity Function

NCLLRWDF  
Wake County, North Carolina

Two-way travel time (msec)	Average Stacking Velocities (ft/sec)	Calculated Depths (feet) Below Ground Surface from Stacking Velocities
0	7,932	-
25	10,182	127
50	12,039	301
75	13,665	512
100	14,630	732
125	15,408	963
150	15,907	1,193
175	16,272	1,424
200	16,631	1,663
225	16,993	1,912
250	17,260	2,158
275	17,539	2,412
300	17,828	2,674
325	18,117	2,944
350	18,407	3,221
375	18,718	3,510
400	19,030	3,806



Table 4-10. Comparison of Core with Actual Performance of Geophysical and Imaging Tools used in the GM-1 Pilot Study

NCLLRWDF  
Wake County, North Carolina

	Importance to Objectives	Core	BIPS	Selected Logging / Imaging Techniques						
				High Resolution Electrical Image	Spectral Gamma	Full Wave Form Sonic	3-Arm Caliper	Density Neutron	Resistivity Induction	Combined Set of Tools
Data Acquisition Factors										
Recovery of Information										
Reproducibility										
Time Factor										
Economic Factor										
Geologic and Hydrologic Features										
FRACTURES / FAULTS										
Fracture Depth										
Fracture Dip										
Fracture Dip Direction										
Hydraulic Aperture										
Fracture Spacing										
Fracture Frequency										
Fracture Type										
Fracture Descriptor										
Fault Fabric										
Apparent Fracture Aperture										
Cumulative Mean Hydraulic Aperture										
Apparent Electrical Fracture Porosity										
Fracture Origin										
Fracture Fit										
Fracture Shape										
Effective Fracture Length										
STRATA										
Contact Depth										
Strata Dip										
Strata Dip Direction										
True Stratigraphic Thickness										
Lithology										
Porosity										
Permeability										
Relative Grain Size										
Degree of Weathering										
Induration										
Grading										
Lithologic Modifiers										
True Grain Size										
Clast Percent										
Clast Size										
Primary Bedding Features										
Bedding Marks										
Contact Type										
Roundness										
Sorting										
Coarse Fraction Accessories										
Soft Sediment Deformation										
Sandstone/Coag Composition										
Epigenetic/Diagenetic Descriptors										
Biogenic Descriptors										
Rock Color										
Rock Color Modifiers										

Measure of Importance

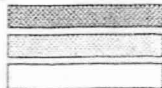


Critical - Can be used by itself to satisfy project requirements for this item.

Useful - Addresses project requirements in a qualitative way, by inference, or with insufficient precision, may be used in combination with other data to satisfy project requirements.

Not Useful - Does not address project requirements for this item.

Source of Data



Excellent

Fair

Poor

Table 5-1. Lithofacies Classification

NCLLRWDF  
Wake County, North Carolina

<u>Conglomerate</u>	
Cmm	Matrix supported, massive
Cmg	Matrix supported, normal or inverse graded
Ccm	Clast supported, massive
Ccg	Clast supported, normal or inverse graded
Ccb	Clast supported, crude horizontal bedding
Ccx	Clast supported, cross-bedded
<u>Sandstone</u>	
Sm	Massive, very fine to very coarse grained
Smm	Massive, muddy (> 33% mud matrix), very fine to very coarse grained, may be burrowed, bioturbated, or rooted
Sc	Massive, conglomeratic (trace to 30% gravel), very fine to very coarse grained
Scm	Massive, conglomeratic (trace to 30% gravel), muddy (> 33% mud matrix), very fine to very coarse grained
Sx	Cross-bedded, fine to very coarse grained, may be pebbly
Sr	Ripple cross-laminated, very fine to coarse grained, may be pebbly
Sl	Horizontal laminated, very fine to coarse grained, may be pebbly
<u>Mudstone</u>	
Mp	Massive, pebbly (trace to 30% gravel), may be sandy
Mm	Massive, may be sandy
MI	Laminated, may be sandy and micaceous
Mr	Rooted, may be sandy and bioturbated
Mb	Burrowed, bioturbated or texturally mottled; may be sandy
Mn	Massive, with calcareous nodules; may be sandy
<u>Claystone</u>	
Mc	Massive, may display minor root structure, lamination, burrows, or bioturbation
Mbp	Waxy, blocky or platy structures, may contain root traces, and small-scale slickensided surfaces

Table 5-2. Base of "Weathered Zone" based on Geophysics

NCLLRWDF  
Wake County, North Carolina

Well/Boring	Base of "weathered zone" based on ELAN or acoustic velocity change	Casing Depth - (near base of severe weathering in feet)
W201	62	36
W202	53	31
W203	53	32
W204	49	32
W205	82	31
W206	68	33
W207	79	24
W208	84	32.5
W104MP18	50 (AVL)	17.5
W74PM4		
W73PM3		
W32MP18	54 or 66 (AVL)	53
W97SW43		15
W112MP22		5
W8OW100	66 (AVL)	41

AVL - Acoustic velocity log

Table 5-3. Data Used to Construct the GM Cross Section

NCLLRWDF  
Wake County, North Carolina

Boring/Well ID	BOREHOLE DATA		
	Geologic	Hydrologic	Geochemical
W201AR1A	Spectral Gamma Log	Hydrophysical Data	Groundwater Sample from packer
	ELAN log *	Packer Test Data	test interval(s)
	FMI log*	Water level (4/97)	Stiff diagrams
	Integrated graphic log *		
	Fracture Data		
	Stoneley anomalies		
W202AR1A	Spectral Gamma Log	Hydrophysical Data	Groundwater Sample from packer
	ELAN log *	Packer Test Data	test interval(s)
	FMI log*	Water level (4/97)	Stiff diagrams
	Integrated graphic log *		
	Fracture Data		
	Stoneley anomalies		
W203AR1A	Spectral Gamma Log	Hydrophysical Data	Groundwater Sample from packer
	ELAN log *	Packer Test Data	test interval(s)
	FMI log*	Water level (4/97)	Stiff diagrams
	CMR log*		
	Integrated graphic log *		
	Fracture Data		
W204AR1	Spectral Gamma Log	Hydrophysical Data	Groundwater Sample from packer
	ELAN log *	Packer Test Data	test interval(s)
	FMI log*	Water level (4/97)	Stiff diagrams
	CMR log*		
	Integrated graphic log *		
	Fracture Data		
W205CH1	Spectral Gamma Log	Hydrophysical Data	Groundwater Sample from packer
	ELAN log *	Packer Test Data	test interval(s)
	FMI log*	Water level (4/97)	Stiff diagrams
	CMR log*		
	Integrated graphic log *		
	Graphic core log *		
W206AR1	Spectral Gamma Log	Hydrophysical Data	Groundwater Sample from packer
	ELAN log *	Packer Test Data	test interval(s)
	FMI log*	Water level - still	Stiff diagrams
	CMR log*	recovering (4/97)	
	Integrated graphic log *		
	Fracture Data		
W206AR1	Stoneley anomalies		

Table 5-3. Data Used to Construct the GM Cross Section

NCLLRWDF  
Wake County, North Carolina

Boring/Well ID	BOREHOLE DATA		
	Geologic	Hydrologic	Geochemical
W207AR1	Spectral Gamma Log	Hydrophysical Data	Groundwater Sample from packer
	ELAN log *	Packer Test Data	test interval(s)
	FMI log*	Water level (4/97)	Stiff diagrams
	CMR log*		
	Integrated graphic log *		
	Fracture Data		
W208AR1	Stoneley anomalies		
	Spectral Gamma Log	Hydrophysical Data	
	ELAN log *	Packer Test Data	
	FMI log *	Water level - still	
	CMR log*	recovering (4/97)	
	Integrated graphic log *		
	Graphic core log *		
	Fracture Data *		
	Diagenetic Features		
	Biogenic Features		
W104MP18	Lithofacies		
	Fault fabrics		
	Stoneley anomalies		
	Gamma Log	Packer Test data	
	Requalified Graphic Core Log *		
	Acoustic velocity log*		
W32MP14	Temperature Log *		
	Zones of water loss/production		
	Lithofacies		
	Fault fabrics		
	Well construction Information (W32MC39, W32MC40, W32MC41)	Water-level data (4/4/97)	
	Gamma Log		
	Requalified Graphic Core Log *		
W73PM3	Acoustic velocity log*		
	Temperature Log *		
	Zones of water loss/production		
	Lithofacies		
W109VS3	Fault fabrics		
	Requalified Graphic Core Log		
	Gamma log		
	Acoustic velocity log*		
W74PM4	Temperature log *		
	Zones of water loss/production		
	Requalified graphic core log		

Table 5-3. Data Used to Construct the GM Cross Section

NCLLRWDF  
Wake County, North Carolina

Boring/Well ID	BOREHOLE DATA		
	Geologic	Hydrologic	Geochemical
W8OW100	Well completion information Gamma log Acoustic velocity log* Temperature log * Zones of water loss/production	Water level data (4/97)	
W97SW43	Requalified graphic core log *		

**OTHER DATA**

Trench maps

Base of Weathering and casing depth (see Table 5-4)

Start Depth of Coring (I.e., base of severely weathered zone)

Diagenetic features in trench

Lithofacies in trench

Seepage Zones in trench

Locations of potential faults based on interpretations of pre-pilot study seismic by Malin

Map Units

\* Starred data was used for construction and analysis of cross-section but is not directly displayed on section.

Table 5-4. Geophysical Logs used to Construct GM Cross Section and for Associated Interpretations

NCLLRWDF  
Wake County, North Carolina

Geophysical Log	How Used in Construction of Cross Section
Natural Gamma Spectroscopy	stratigraphic correlations, identification of lithologies
Resistivity	stratigraphic correlations, identification of lithologies, physical properties
Neutron/density	porosity and other physical properties, lithologies ("log-sands" and "log-shales"), identification of base of weathering
DSI	identification of base of weathering, stoneley anomalies
FMI	identification of lithologies, contacts, some primary and secondary sedimentary features, stratigraphic and fracture orientations
BIPS	identification of lithologies, contacts, some primary and secondary sedimentary features, stratigraphic and fracture orientations
CMR	porosity, permeability
Acoustic Velocity*	identification of base of weathering, lows may be indicative of producing fractures
Temperature*	anomalies may be indicative of producing fractures

\*Logs available for pre-GM Pilot Study wells/borings only

Table 5-5. Relationship Between Fractures and Water Producing Zones

NCLLRWDF  
Wake County, North Carolina

Well No	Hydrophysical Anomalies Depth (feet)	Flow Rate (gpm)	Packer Intervals Test No.	(feet)	(feet)	T (m <sup>2</sup> /s)	Ti (m <sup>2</sup> /s)	To (m <sup>2</sup> /s)	Fracture Depth (feet)	Fracture Type	Fracture Surface	Fracture Dip	Fracture Dip Direction	Top Lithology	Bottom Lithology	Contact	Bedding Type
W201	45.28	0.0048	1	44.6	64.1	8.51E-07			43.4	Non-Bedding	Irreg	77	295	Med SS	Med SS	None	Massive
	48.88	0.0098							46.8	Bedding	Planar	10	97	VCrsSS	Siltstone	Grad	Massive
									49.4	Bedding	Planar	19	86	Med SS	Med SS	None	Lamin
W202	33.79-39.37	0.013	1	31	215	6.04E-07	6.04E-06		33.2	Bedding	Irreg	28	94	Med SS	Mudstone	Sharp	Massive
									35	Bedding	Planar	16	279	Siltstone	Siltstone	None	Massive
									39.1	Non-Bedding	Planar	51	275	Siltstone	Siltstone	None	Massive
									39.7	Non-Bedding	Irreg	27	79	Siltstone	Siltstone	None	Massive
									40.3	Non-Bedding	Irreg	26	91	Siltstone	Siltstone	None	Massive
	53.38	0.006							53.2	Bedding	Irreg	20	102	Fine SS	Mudstone	Sharp	Massive
	91.86	0.001							88.3	Bedding	Irreg	18	85	Siltstn	Fine SS	Sharp	Massive
W203	44.93	0.002	2	61	70.3	9.42E-09			43.5	Bedding	Planar	30	67	VF SS	VF SS	None	Massive
	53.15-80.05	0.011							58	Non-Bedding	Planar	21.8	134	SiltStone	SiltStone	None	Massive
									65.4	Bedding	Planar	18.5	125	Med SS	Med SS	Sharp	Massive
									79.8	Bedding	Planar	16	64	Mudstone	Mudstone	None	Massive
	108.27-141.08	0.009															
W204	42.98	0.0106	1	117	126.3	5.95E-06	1.98E-07		39.6	Bedding	Planar	34	115	Med SS	Siltstone	Sharp	Interb
	103.02-138.46	1.0077		38.8	55.2				40.8	Non-Bedding	Planar	64	281	Siltstone	Siltstone	None	Massive
W205	61.02	0.013	9			7.70E-07	1.60E-06		57.9	Bedding	Irreg	26	99	V Crs SS	V Crs SS	Sharp	Interb
	80.05	0.053		72	93				59.6	Bedding	Irreg	15	152	V Crs SS	Siltstone	Sharp	Interb
	82.02	0.053							80.9	Bedding	Irreg	18	110	Med SS	Mudstone	Sharp	Massive
	128.94	0.265		118.1	139.1				126.1	Bedding	Irreg	23.1	98	Med SS	Med SS	Sharp	Interb
									126.9	Non-Bedding	Irreg	63.14	252	Med SS	Med SS	None	Interb
									128.6	Bedding	Irreg	21	84	Med SS	Mudstone	Sharp	Massive
	158.14	1.059		148.2	169.2				161.5	Bedding	Planar	24	72	Med SS	Mudstone	Sharp	Laminat
	206.01	0.008		195.6	216.6				203.9	Non-Bedding	Irreg	73	267	Siltstone	Siltstone	None	Massive
	270.01	0.005		258.9	279.9				269.6	Bedding	Irreg	27	63	Med Ss	Crs SS	Irreg	Interb
									271.3	Non-Bedding	Irreg	52	269	Crs SS	Crs SS	None	Interb
	316.93	0.050	4	301.1	715	2.34E-06			314.5	Non-Bedding	Planar	67	296	Fine SS	Fine SS	None	Massive
									329.6	Fault	Planar	56	274	Siltstone	VCrs SS	Unconfor	Massive



Table 5-5. Relationship Between Fractures and Water Producing Zones

NCLLRWDF  
Wake County, North Carolina

Well No.	Hydrophysical Anomalies Depth (feet)	Flow Rate (gpm)	Packer Intervals Test No.	(feet)	(feet)	T (m <sup>2</sup> /s)	T <sub>1</sub> (m <sup>2</sup> /s)	T <sub>0</sub> (m <sup>2</sup> /s)	Fracture Depth (feet)	Fracture Type	Fracture Surface	Fracture Dip	Fracture Dip Direction	Top Lithology	Bottom Lithology	Contact	Bedding Type
W206	36.09-41.01	0.0025							37.1	Bedding	Planar	23	337	Siltstone	V Fine SS	Sharp	Massive
	42.98-43.96	0.0120	1	41.7	57.1		9.54E-07	1.91E-07	38.8	Non-Bedding	Irreg	10	76	V Fine SS	V Fine SS	None	Massive
	46.92	0.0080							46.4	Bedding	Planar	5	275	V Crs SS	V Crs SS	None	Interb
W207									47.1	Bedding	Planar	12	322	V Crs SS	V Crs SS	None	Interb
	38.39-39.37	0.1060	1	35	44.3		2.33E-06	3.33E-08	37.4	Bedding	Planar	6	33	V Crs SS	Med SS	Irreg	Graded
									38.4	Non-Bedding	Irreg	68	265	Med SS	Siltstone	None	Massive
	46.92	0.0397	4	41.5	50.8	4.94E-07			45.8	Bedding	Planar	16	50	Siltstone	Crs SS	Irreg	Massive
	70.54 - 76.44	0.1393	2	67.5	76.8	1.86E-06			68.6	Bedding	Planar	27	127	Med SS	Mudstone	Sharp	Massive
									72.9	Non-Bedding	Planar	81	260	Crs SS	Crs SS	None	Massive
									73.5	Bedding	Planar	13	56	Siltstone	Siltstone	Sharp	Lamin
									76	Bedding	Planar	20	17	Siltstone	Siltstone	Sharp	Massive
	159.12 - 161.09	0.6860	3	153.1	465	3.09E-05			158.6	Bedding	Irreg	14	65	Med Ss	Mudstone	V Irreg	Massive
V Crs SS -	Very Coarse Sand Stone																
VF SS -	Very Fine Sand Stone																
Med SS -	Medium Sand Stone																



KEY:

- = SEISMIC SURVEY LINE LOCATION
- = TRENCH LOCATION
- · - = NCLLRW BOUNDARY LINE
- = UNPAVED ROADS
- = MONITORING WELL LOCATION



**Harding Lawson Associates**

Engineering and  
Environmental Services

DRAWN  
EWS

PROJECT NUMBER  
36595,301

**Site Location Map**

North Carolina Low-Level Radioactive  
Waste Disposal Facility Project  
Wake County, North Carolina

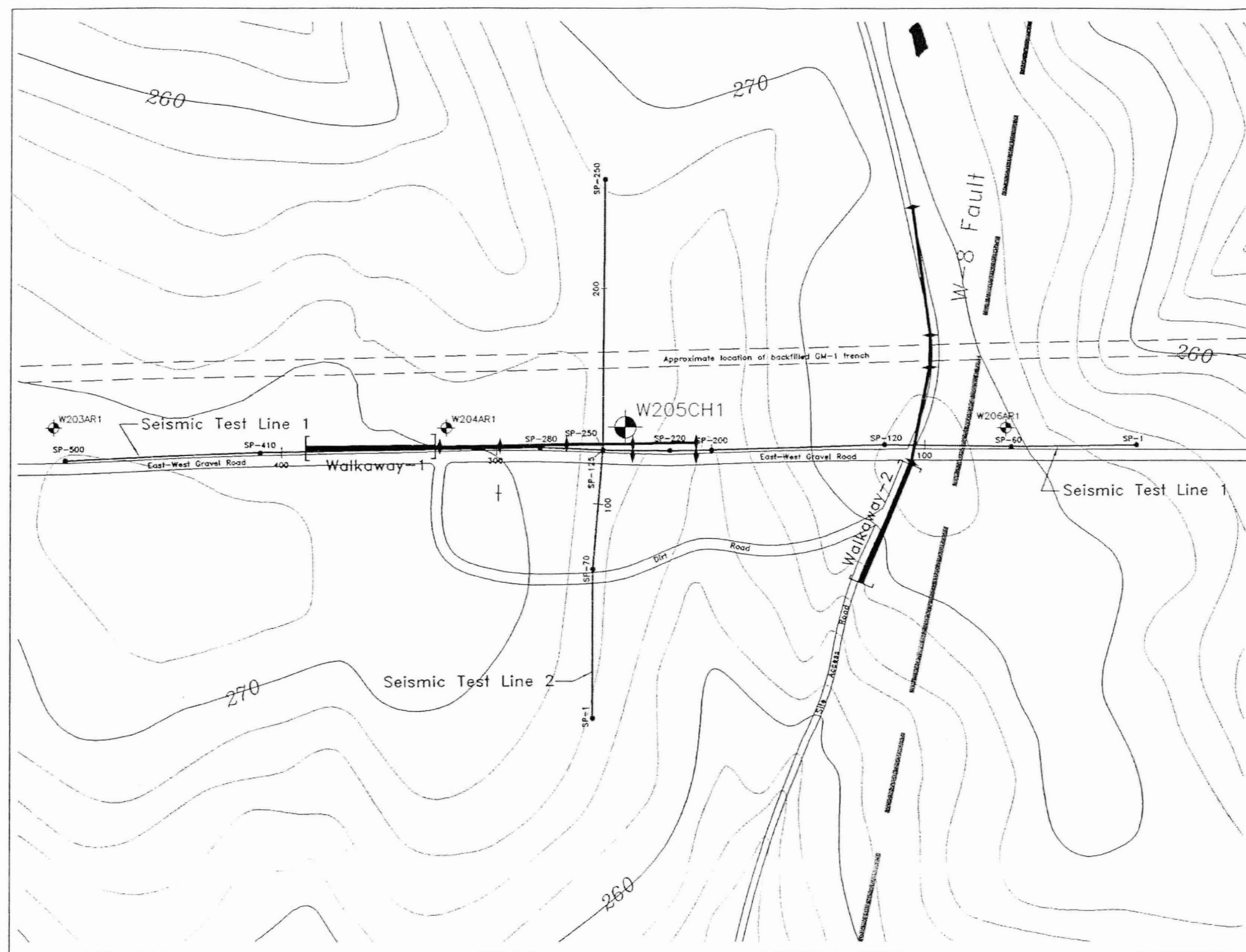
APPROVED

DATE  
10/27/97


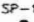





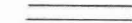
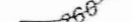
REVISED DATE

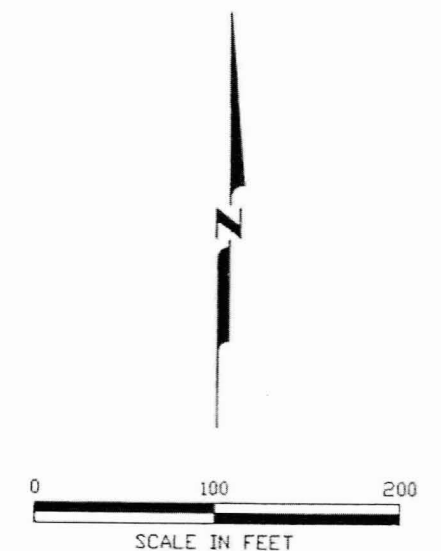
FIGURE

**1-1**



# EXPLANATION

-  SEISMIC REFLECTION/REFRACTION TEST LINE
-  SURVEYED SHOTPOINT LOCATION AND SHOTPOINT DESIGNATION
-  WALKAWAY TEST LINE
-  SHOTPOINT LOCATION RECEIVER ARRAY LOCATION
-  MONITORING WELL
-  MONITORING WELL USED FOR VSP SURVEY
-  GM-1 TRENCH
-  UNPAVED ROAD
-  TOPOGRAPHIC CONTOUR (FEET, MSL)



**Harding Lawson Associates**  
Engineering and  
Environmental Services

DRAWN  
PDA

PROJECT NUMBER  
36595.301

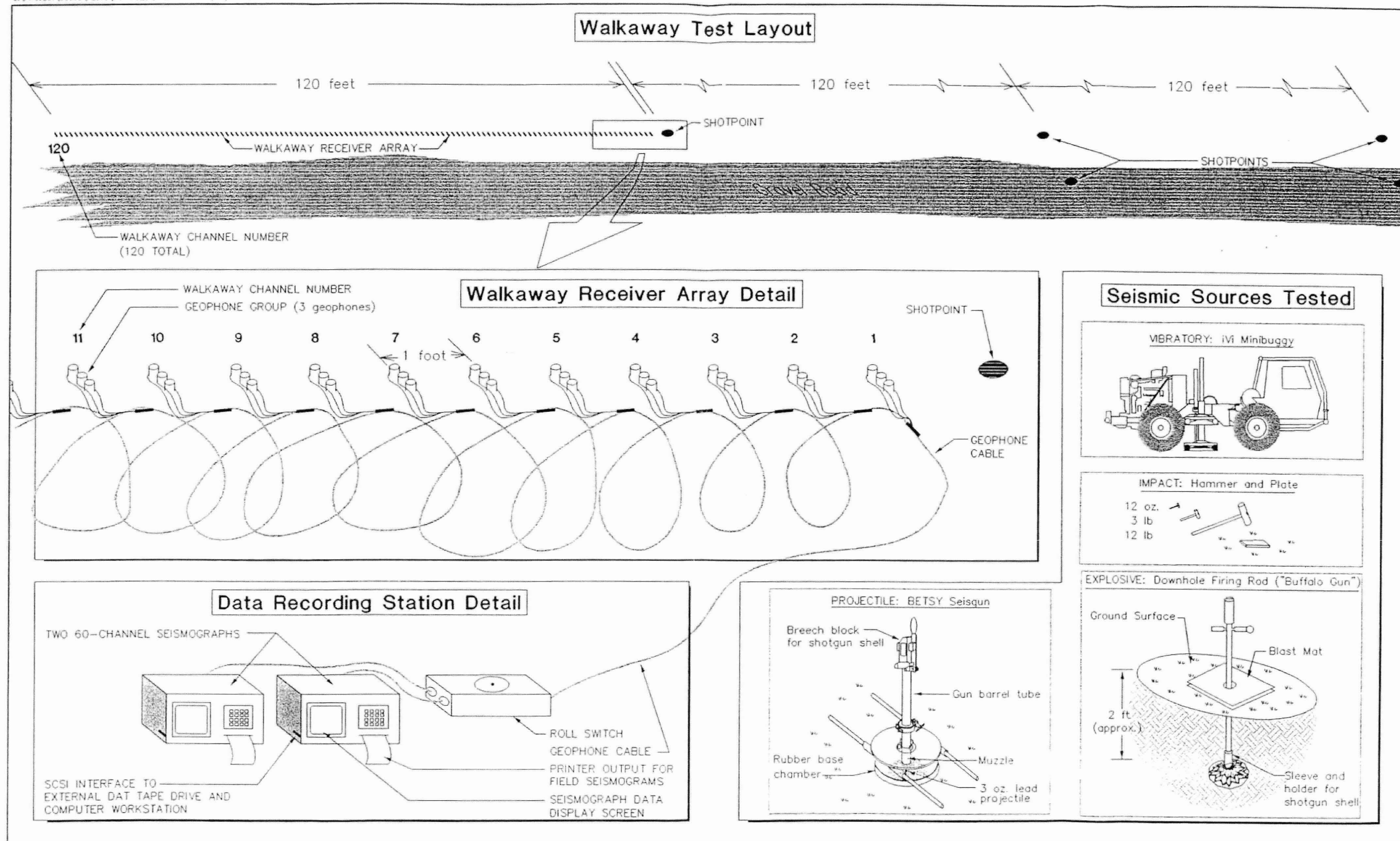
**Seismic Test Line & Walkaway Location Map** FIGURE  
North Carolina Low-Level Radioactive  
Waste Disposal Facility Project  
Wake County, North Carolina

APPROVED

DATE  
10/27/97

REVISED DATE

**3-1**



**Harding Lawson Associates**  
Engineering and  
Environmental Services

DRAWN  
PDA

PROJECT NUMBER  
36595.301

**Walkaway Test Schematic**  
North Carolina Low-Level Radioactive  
Waste Disposal Facility Project  
Wake County, North Carolina

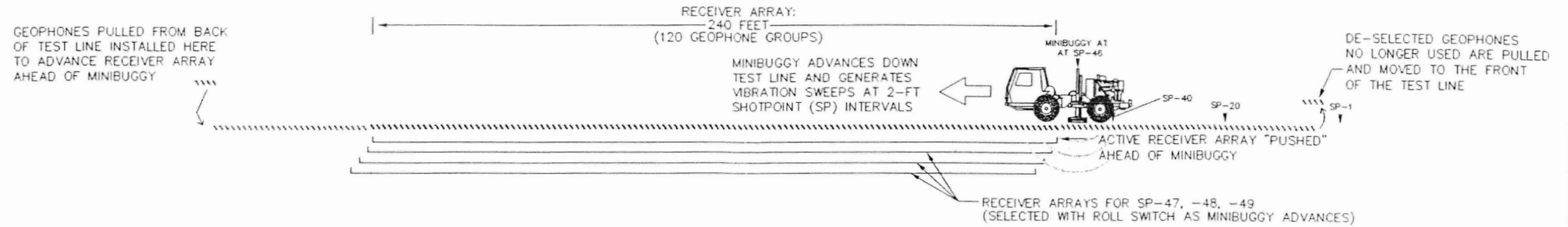
APPROVED

DATE  
10/27/97

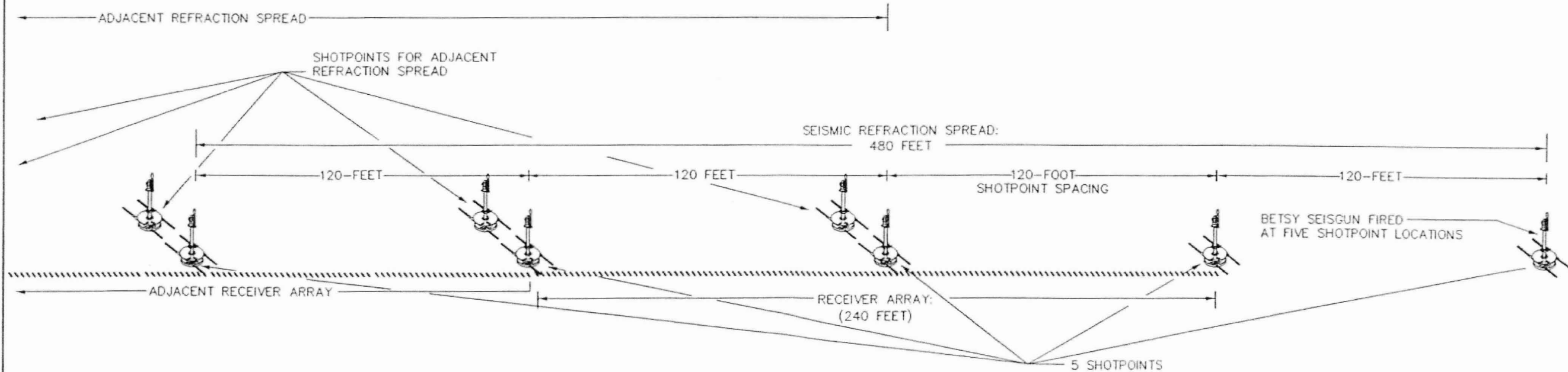
FIGURE  
**3-2**

REVISED DATE

# Seismic Reflection Schematic



# Seismic Refraction Schematic



**Harding Lawson Associates**  
Engineering and  
Environmental Services

DRAWN PDA PROJECT NUMBER 36595.301

**Seismic Reflection & Refraction Schematic**  
North Carolina Low-Level Radioactive  
Waste Disposal Facility Project  
Wake County, North Carolina

APPROVED

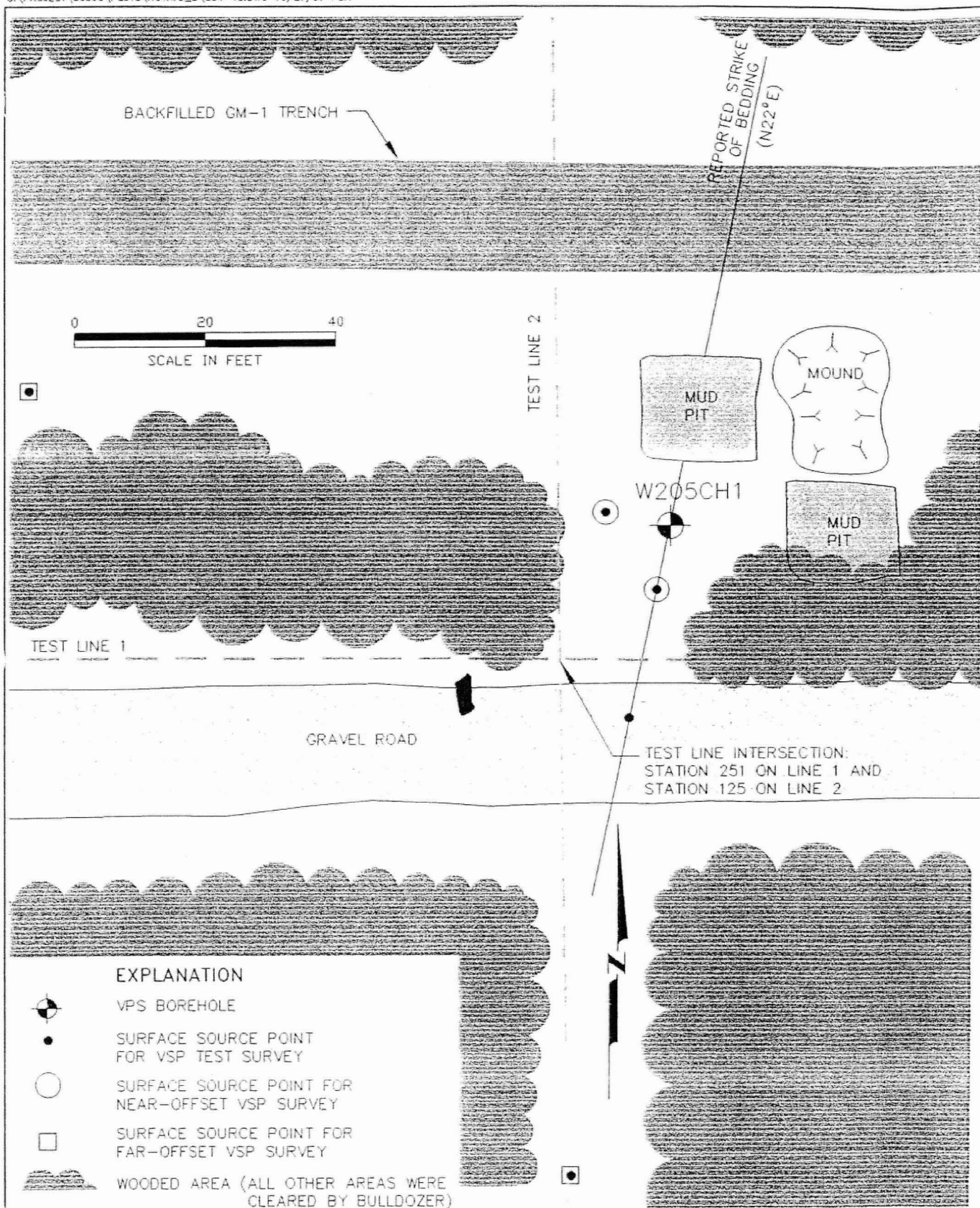
DATE 10/27/97

FIGURE

**3-3**

REVISED DATE





**Harding Lawson Associates**  
Engineering and  
Environmental Services

**VSP SURVEY AREA MAP**

North Carolina Low-Level Radioactive  
Waste Disposal Facility Project  
Wake County, North Carolina

FIGURE

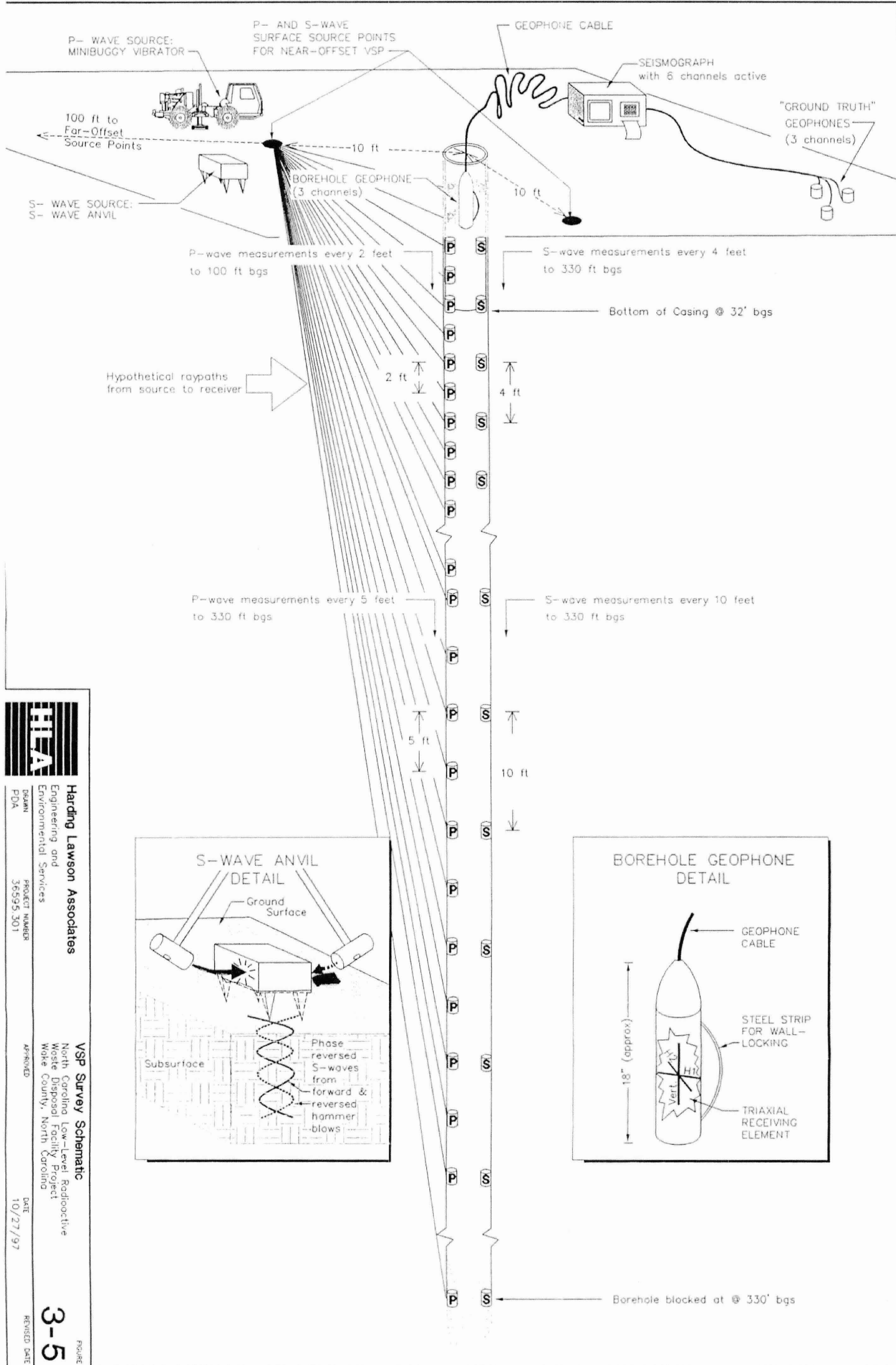
**3-4**

DRAWN PROJECT NUMBER  
PDA 36595.301

APPROVED

DATE  
10/27/97

REVISED DATE



**Harding Lawson Associates**  
Engineering and  
Environmental Services

DESIGN  
PDA

PROJECT NUMBER  
36595.301

**VSP Survey Schematic**  
North Carolina Low-Level Radioactive  
Waste Disposal Facility Project  
Wake County, North Carolina

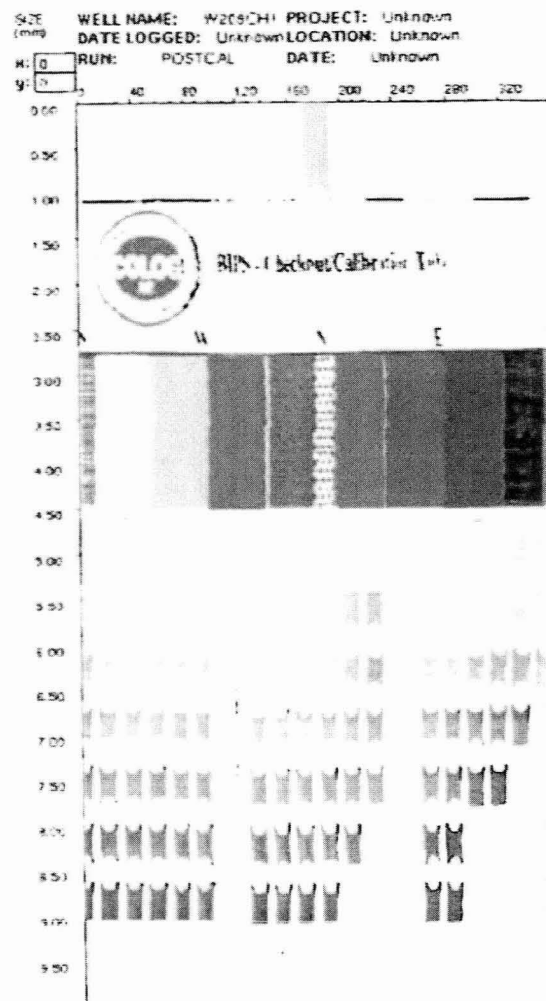
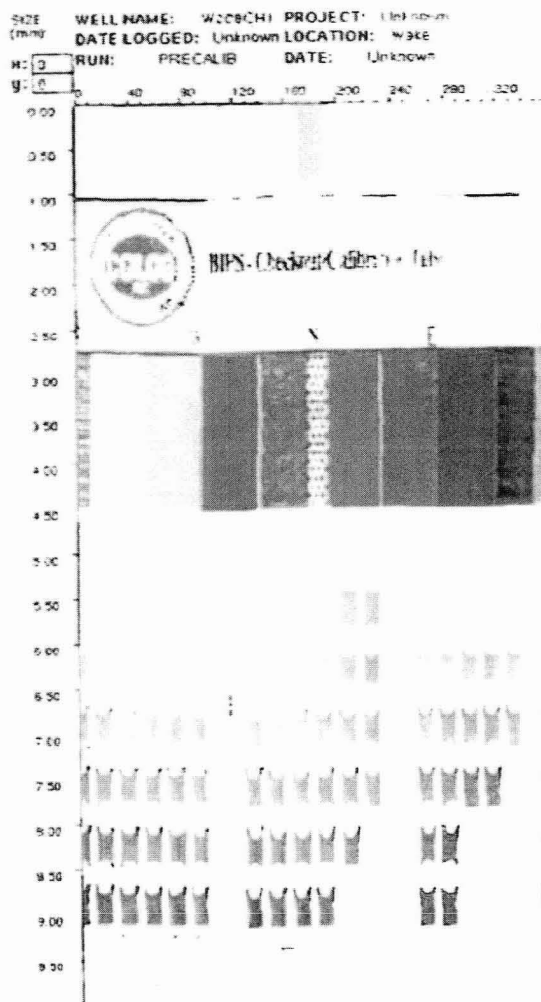
APPROVED

DATE  
10/27/97

REVISED DATE

**3-5**

FIGURE



**Harding Lawson Associates**  
 Engineering and  
 Environmental Services

**Calibration Image For BPS Image Logging**  
 North Carolina Low-Level Radioactive  
 Waste Disposal Facility Project  
 Wake County, North Carolina

FIGURE

**4-1**

DRAWN

PROJECT NUMBER  
 36595,301

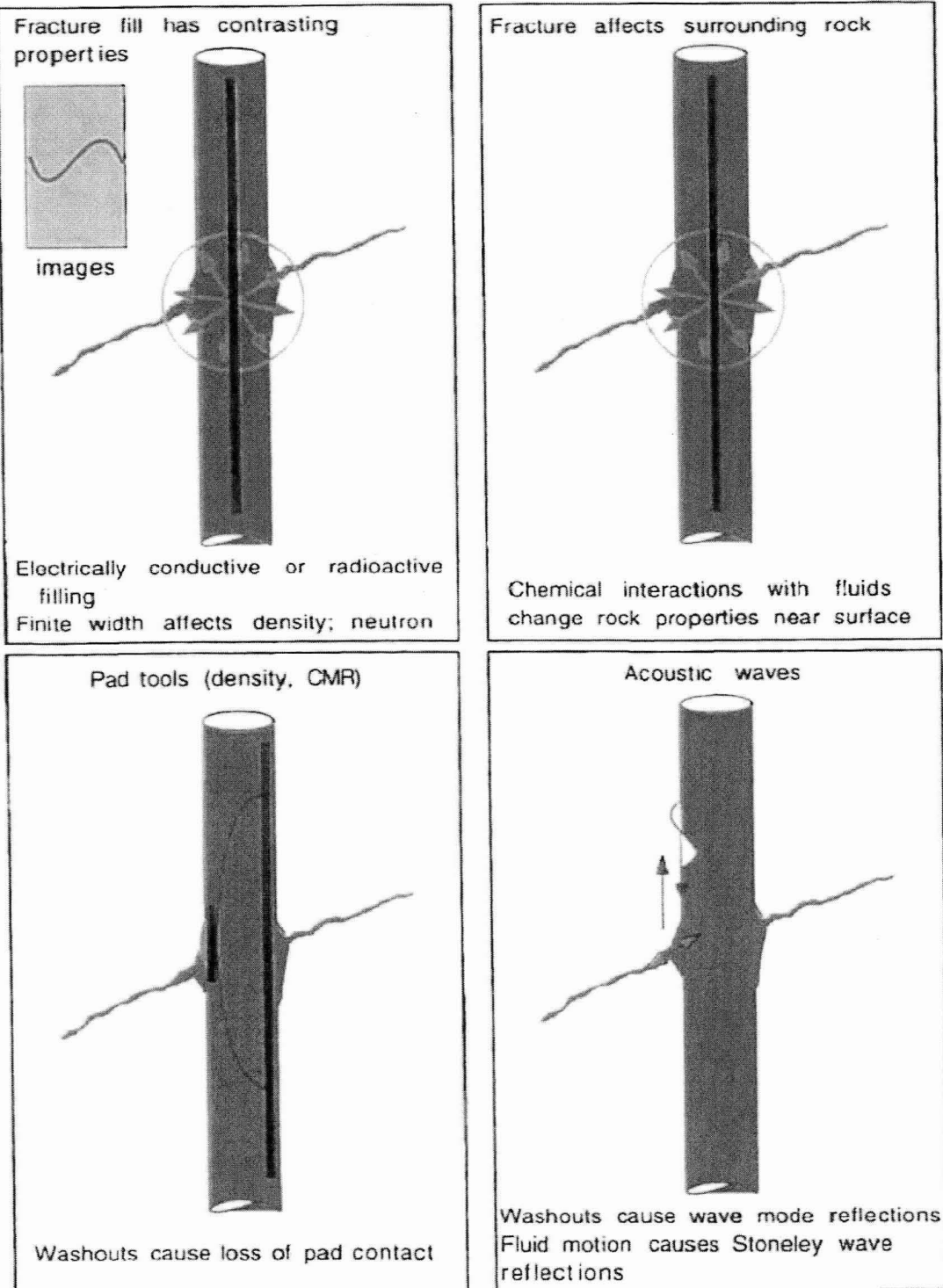
APPROVED

DATE  
 10/97

REVISED DATE



## Effects of Fractures on Logs



**Harding Lawson Associates**

Engineering and  
Environmental Services

**Log Response to Fractures**

North Carolina Low-Level Radioactive  
Waste Disposal Facility Project  
Wake County, North Carolina

FIGURE

**4-2**

DRAWN

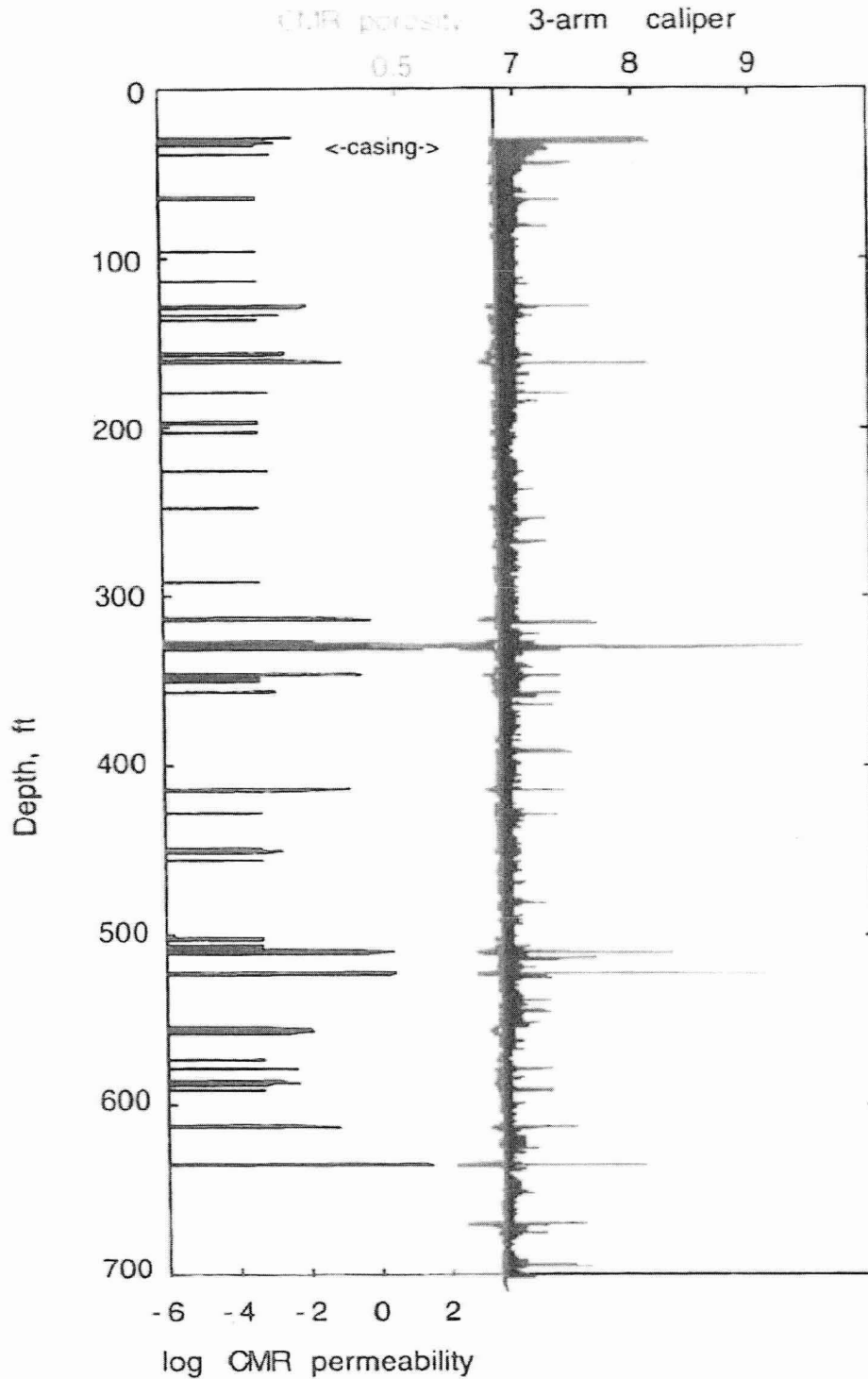
PROJECT NUMBER  
36595.301

APPROVED

DATE  
10/97

REVISED DATE

Comparison  
3-Arm Caliper vs. CMR Permeability  
W205AR1



**Harding Lawson Associates**  
Engineering and  
Environmental Services

DRAWN

PROJECT NUMBER  
36595.301

**Comparison of 3-Arm Caliper vs. CMR  
Permeability**  
North Carolina Low-Level Radioactive  
Waste Disposal Facility Project  
Wake County, North Carolina

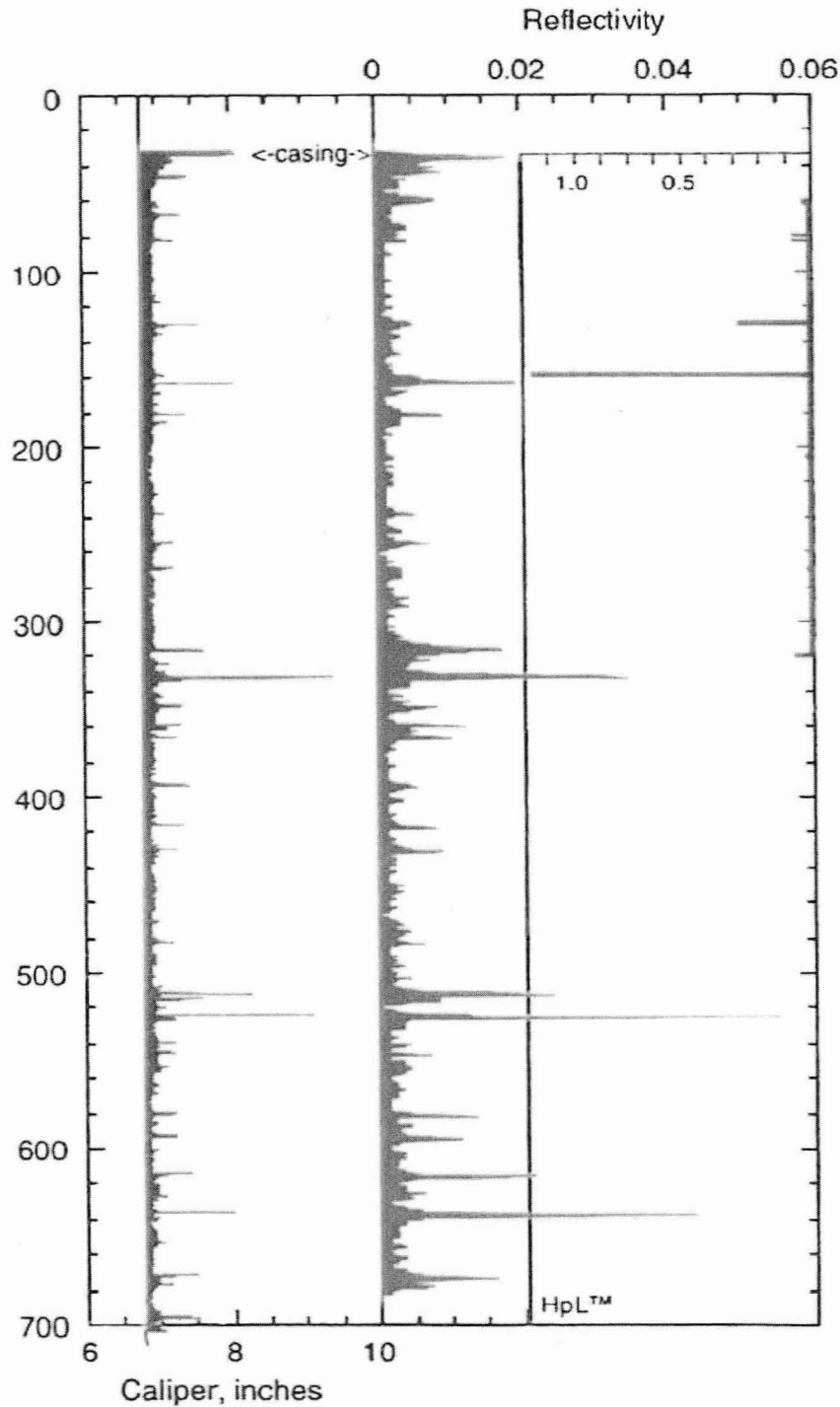
APPROVED

DATE  
10/97

REVISED DATE

FIGURE  
**4-3**

Comparison  
3-Arm Caliper vs. Stoneley Reflectivity  
W205AR1



**Harding Lawson Associates**  
Engineering and  
Environmental Services

**Comparison of 3-Arm Caliper vs. Stoneley  
Reflectivity**  
North Carolina Low-Level Radioactive  
Waste Disposal Facility Project  
Wake County, North Carolina

FIGURE

**4-4**

DRAWN

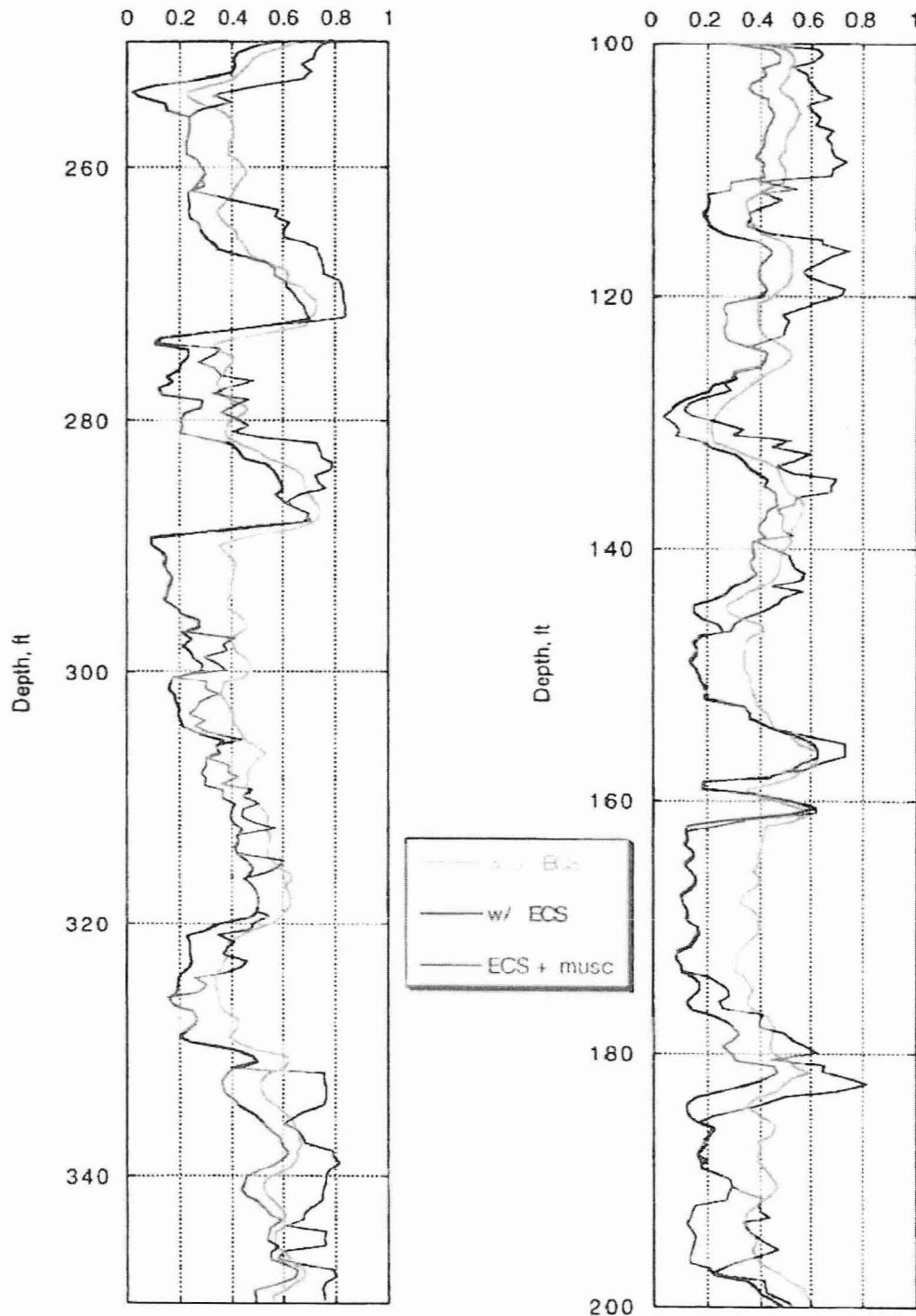
PROJECT NUMBER  
36595,301

APPROVED

DATE  
10/97

REVISED DATE

Comparison - ELAN volumes excluding clay minerals  
("sand mineral" fraction)



Harding Lawson Associates  
Engineering and  
Environmental Services

Comparison of ELAN Volumes  
North Carolina Low-Level Radioactive  
Waste Disposal Facility Project  
Wake County, North Carolina

FIGURE

4-5

DRAWN

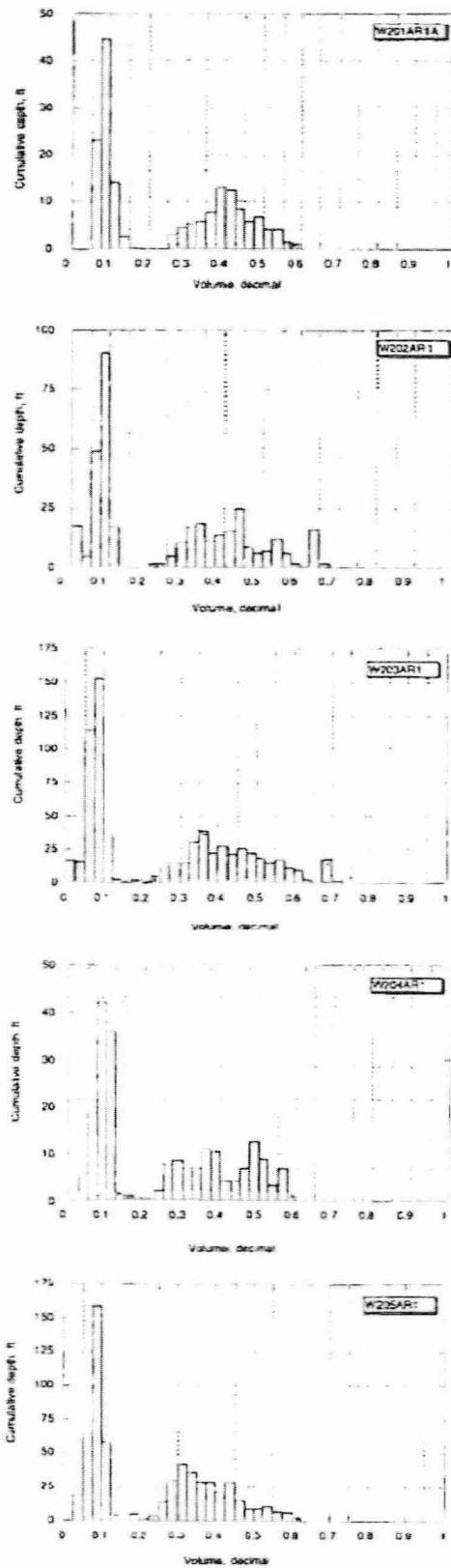
PROJECT NUMBER  
36595,301

APPROVED

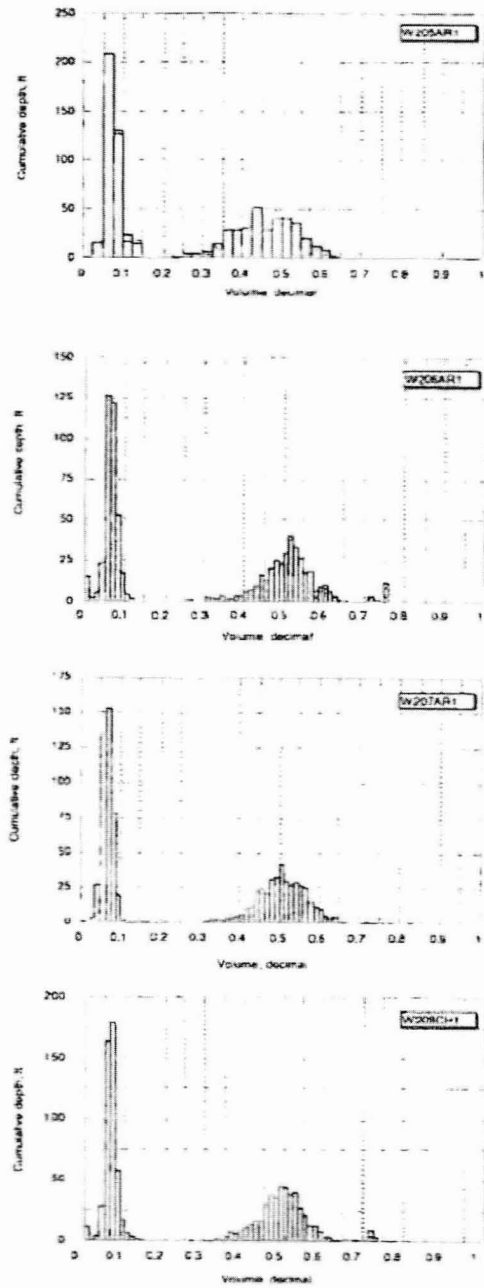
DATE  
10/97

REVISED DATE

## West side of W8 Fault



## East side of W8 Fault



☐ Quartz  
☐ Water Based Slurry



**Harding Lawson Associates**  
 Engineering and  
 Environmental Services

DRAWN: DWN  
 PROJECT NUMBER: 36595.301

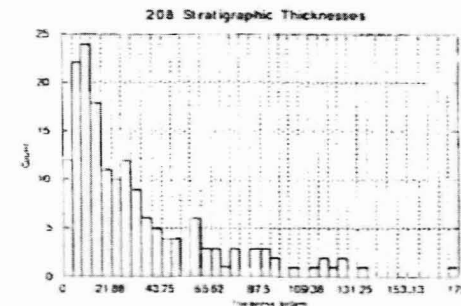
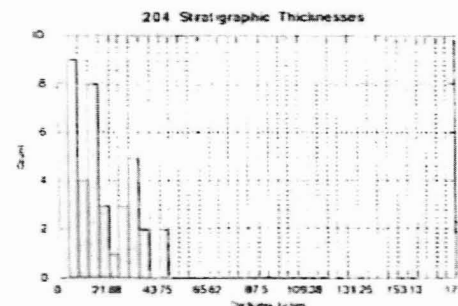
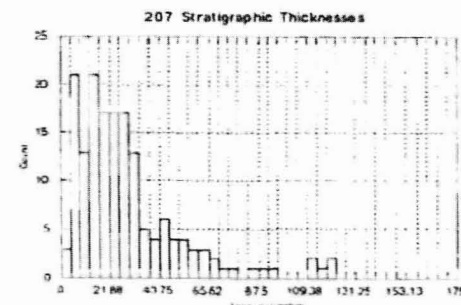
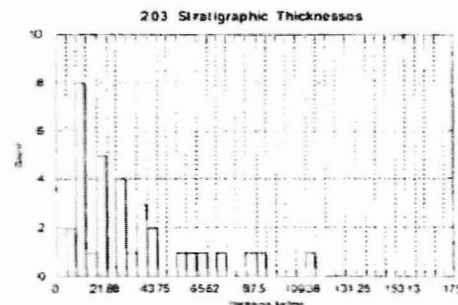
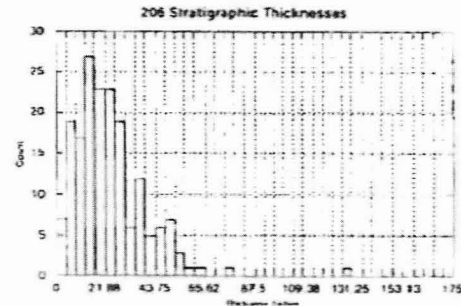
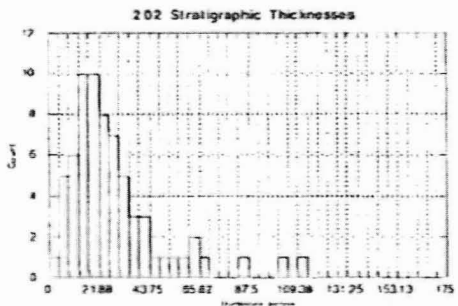
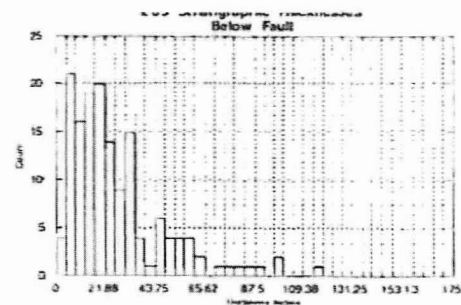
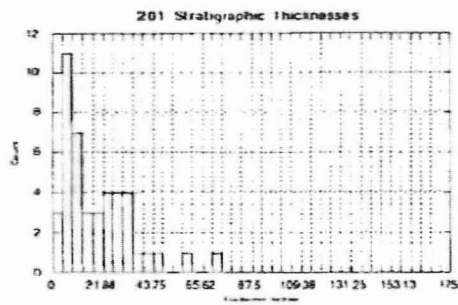
**Histograms of Quartz and Clay Based Water**  
 North Carolina Low-Level Radioactive  
 Waste Disposal Facility Project  
 Wake County, North Carolina

APPROVED:

DATE:  
 10/97

REVISED DATE:

FIGURE  
**4-6**



Harding Lawson Associates  
Engineering and  
Environmental Services

DRAWN: DWN PROJECT NUMBER: 36595-301

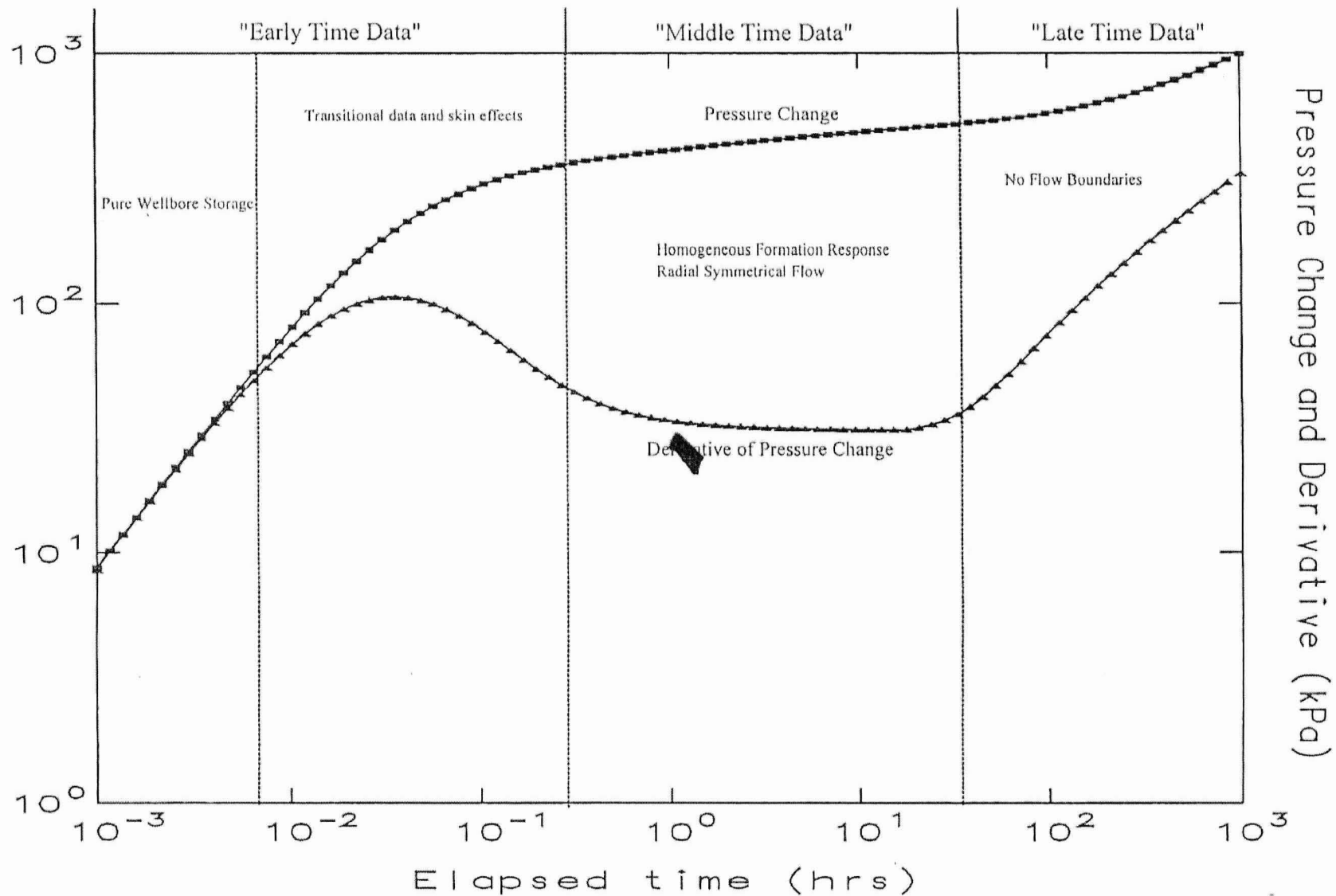
Histograms of Stratigraphic Thicknesses  
North Carolina Low-Level Radioactive  
Waste Disposal Facility Project  
Wake County, North Carolina

APPROVED:

DATE: 10/97

REVISED DATE:

FIGURE  
4-7



**Harding Lawson Associates**  
Engineering and  
Environmental Services

DRAWN  
DWN

PROJECT NUMBER  
36595,301

**Simulated Packer Test Plot of Pressure  
Change and Derivative Vs. Time**  
North Carolina Low-Level Radioactive  
Waste Disposal Facility Project  
Wake County, North Carolina

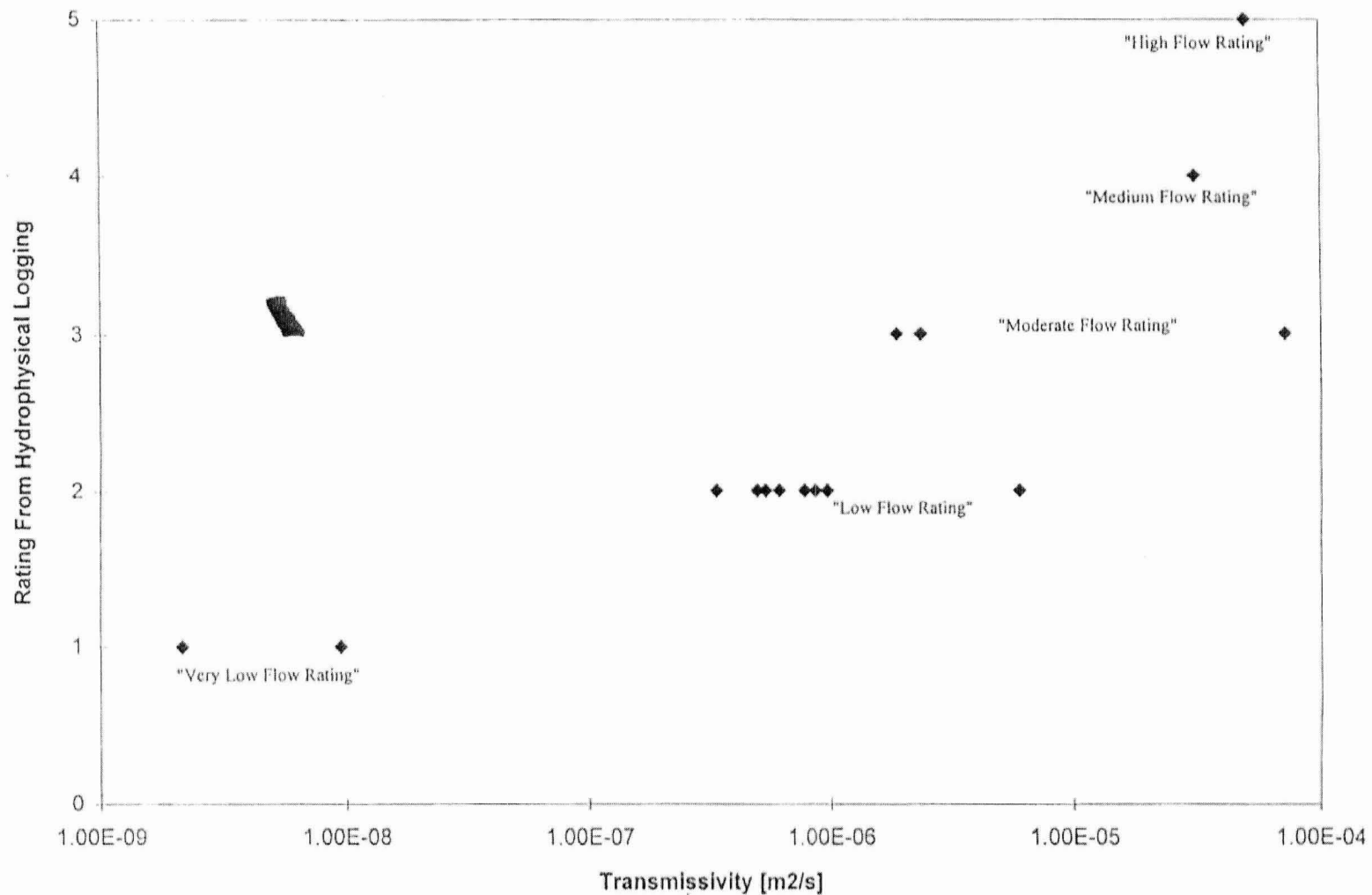
APPROVED

DATE  
10/97

REVISED DATE

FIGURE

**4-8**



**Harding Lawson Associates**  
Engineering and  
Environmental Services

DRAWN  
DWN

PROJECT NUMBER  
36595,301

**Comparison Between Hydrophysical Logging  
and Packer Test Results**  
North Carolina Low-Level Radioactive  
Waste Disposal Facility Project  
Wake County, North Carolina

APPROVED

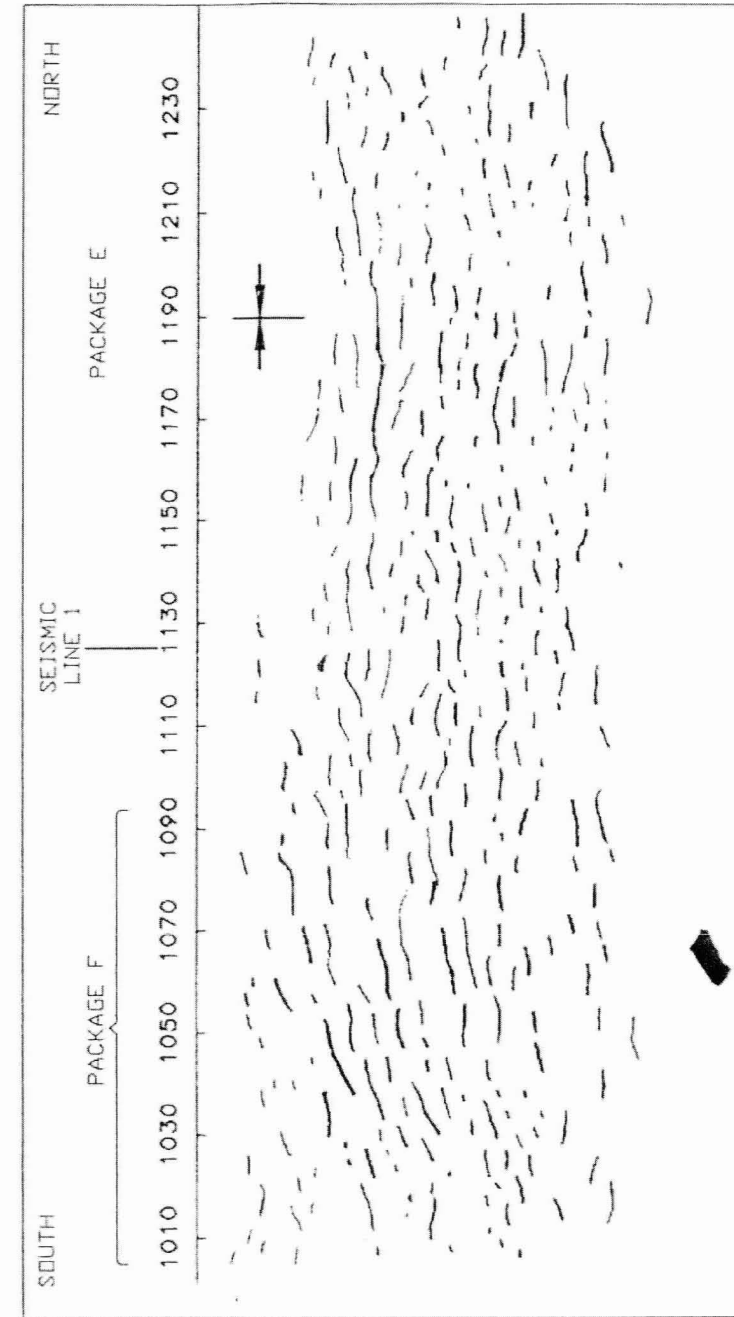
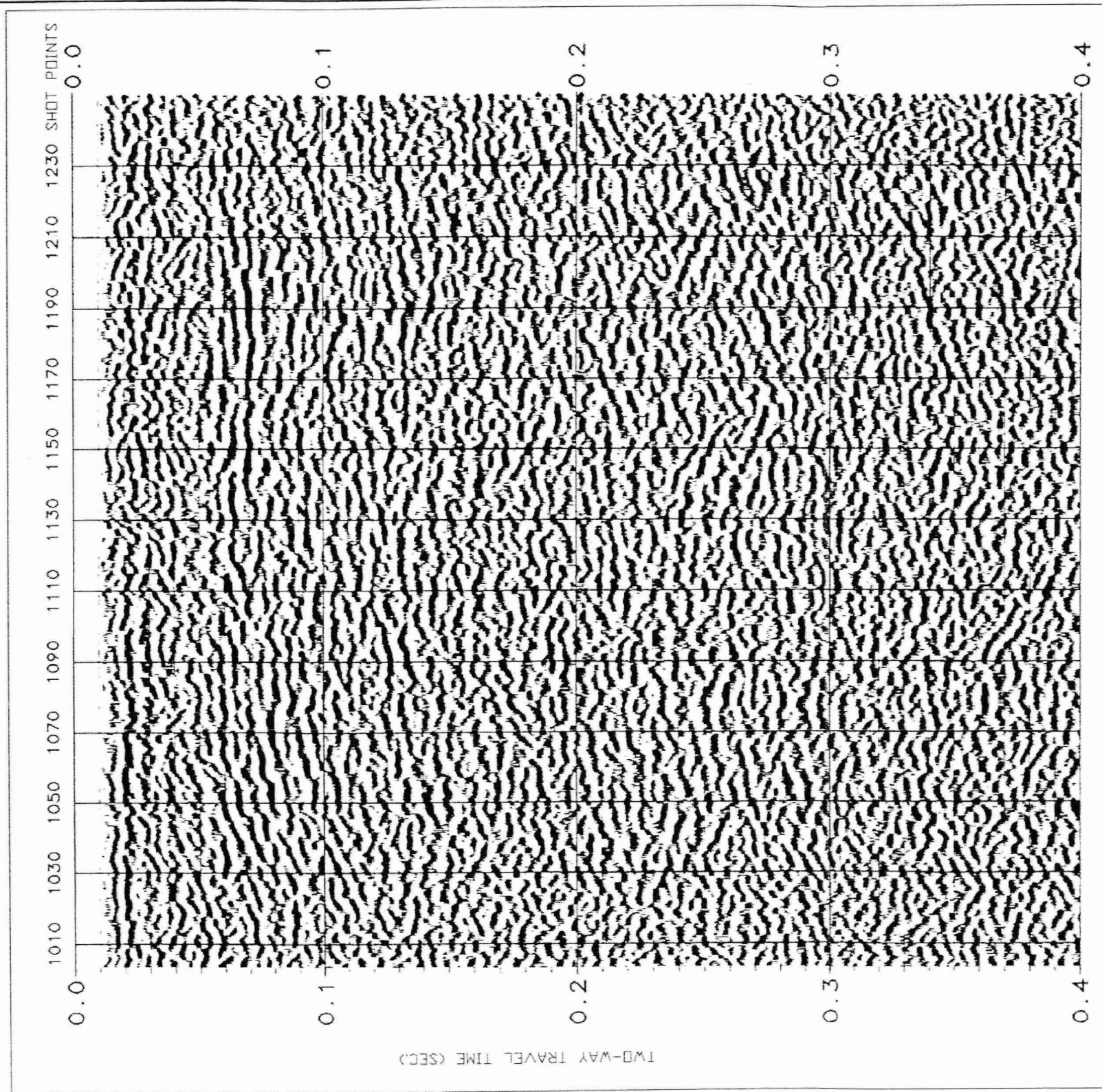
DATE  
10/97

REVISED DATE

FIGURE

**4-9**





Harding Lawson Associates  
Engineering and  
Environmental Services

DRAWN  
EBH

PROJECT NUMBER  
36595 310

Uninterpreted Seismic Section  
Line Drawing - Line 2

APPROVED

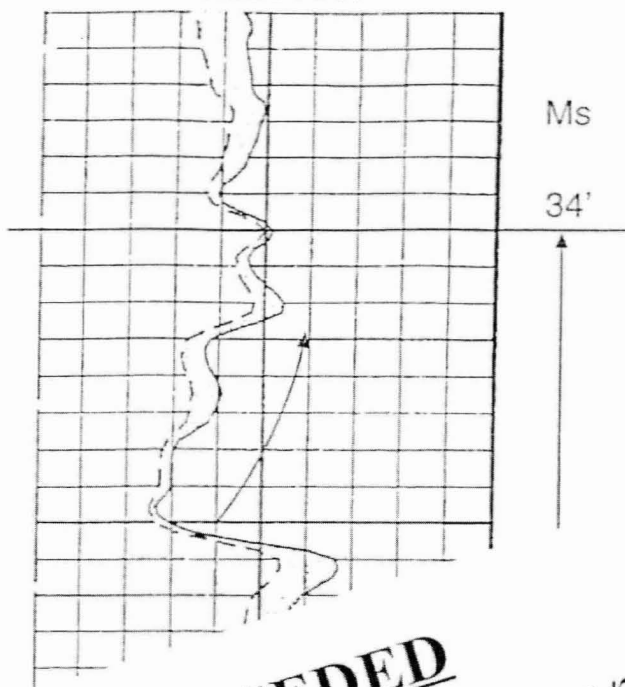
DATE  
10/01/97

FIGURE

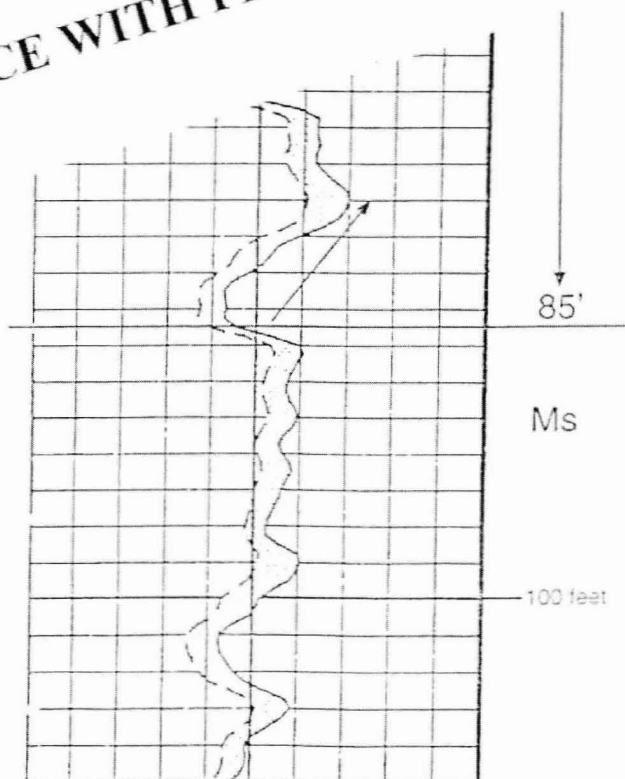
4-11

REVISED DATE

W203 AR1



**SUPERSEDED**  
**REPLACE WITH FIGURE DATED 1/28/98**



Harding Lawson Associates  
 Engineering and  
 Environmental Services

Gamma Log Signature for Upward  
 Fining (UF) Map Unit  
 Proposed North Carolina Low-Level  
 Radioactive Waste Disposal Facility  
 Wake County, North Carolina

FIGURE

**5-1**

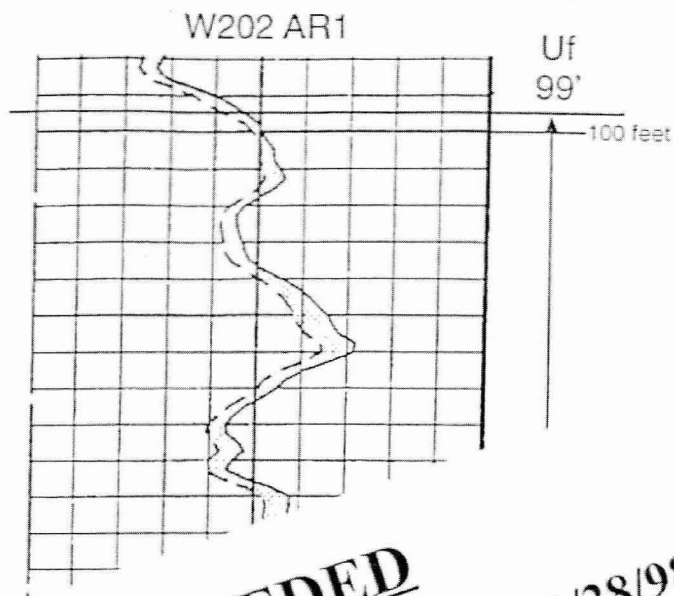
DRAWN  
 GEA

JOB NUMBER  
 36595,301

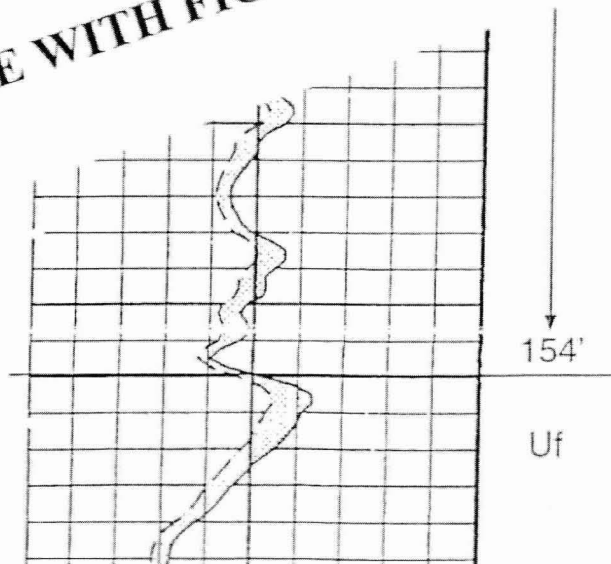
APPROVED

DATE  
 10/97

REVISED DATE



**SUPERSEDED**  
**REPLACE WITH FIGURE DATED 1/28/98**



Harding Lawson Associates  
 Engineering and  
 Environmental Services

Gamma Log Signature for Mudstone/  
 Minor Sandstone (Ms) Map Unit  
 Proposed North Carolina Low-Level  
 Radioactive Waste Disposal Facility  
 Wake County, North Carolina

FIGURE

**5-2**

DRAWN  
 GEA

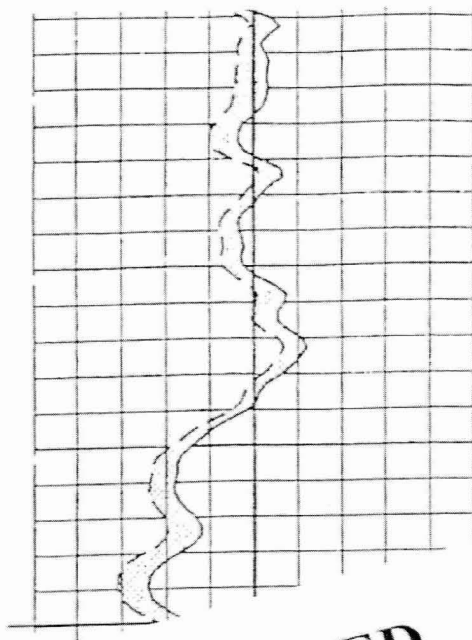
JOB NUMBER  
 36595,301

APPROVED

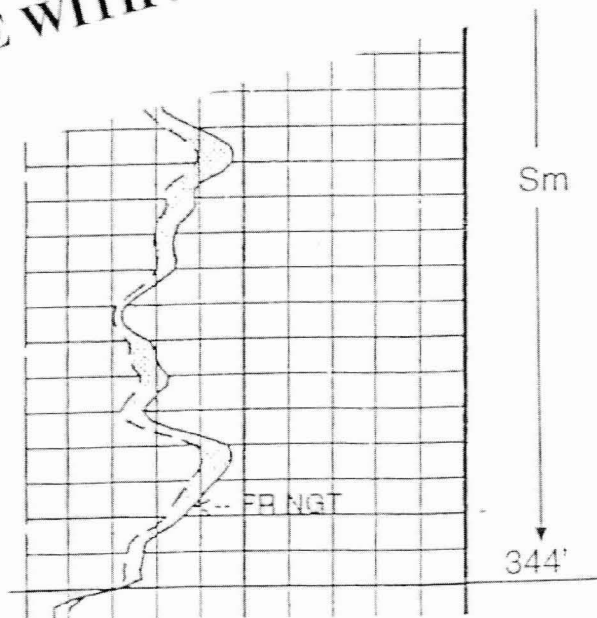
DATE  
 10/97

REVISED DATE

W203 AR1



**SUPERSEDED**  
**REPLACE WITH FIGURE DATED 1/28/98**



Harding Lawson Associates  
 Engineering and  
 Environmental Services

Gamma Log Signature for Sandstone/  
 Minor Mudstone (Sm) Map Unit  
 Proposed North Carolina Low-Level  
 Radioactive Waste Disposal Facility  
 Wake County, North Carolina

FIGURE  
**5-3**

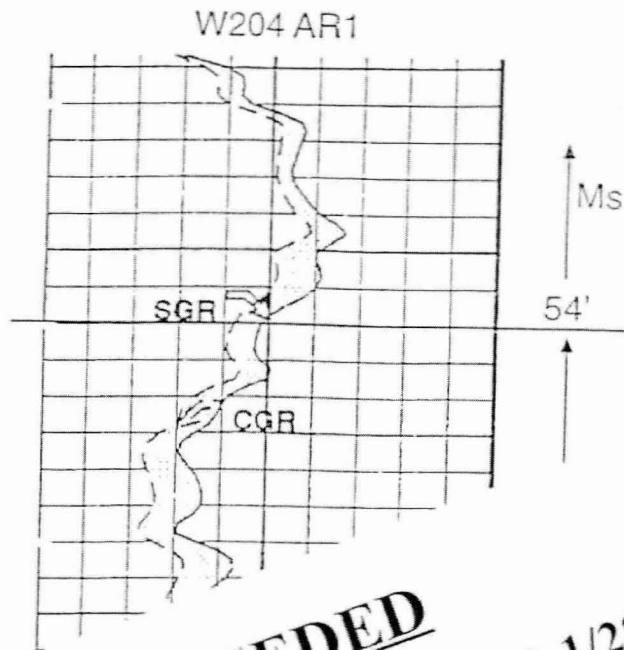
DRAWN  
 GEA

JOB NUMBER  
 36595,301

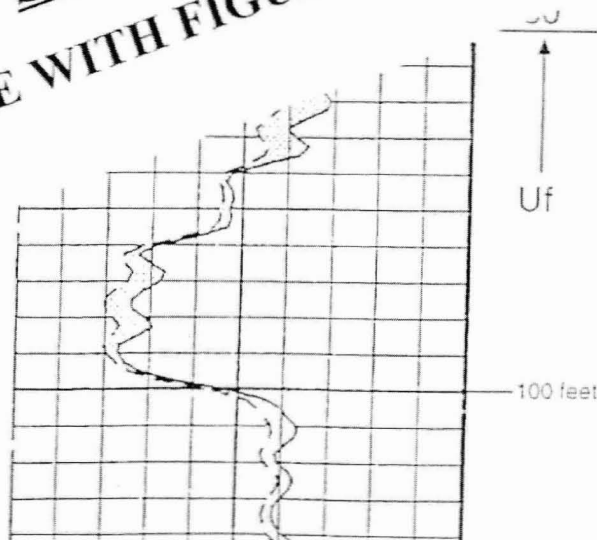
APPROVED

DATE  
 10/97

REVISED DATE



**SUPERSEDED**  
**REPLACE WITH FIGURE DATED 1/28/98**



Harding Lawson Associates  
 Engineering and  
 Environmental Services

DRAWN  
 GEA

PROJECT NUMBER  
 36595,301

Gamma Log Signature for Well-Bedded  
 Sandstone (Swb) Map Unit  
 Proposed North Carolina Low-Level  
 Radioactive Waste Disposal Facility  
 Wake County, North Carolina

APPROVED

DATE  
 10/97

REVISED DATE

FIGURE

5-4



W205CH1 NCLLRWDF  
Wake County, North Carolina

LEGEND

GEOPHYSICAL LOGS

**Hole Size**  
HCAL - 2-arm caliper  
from density log  
3-arm Caliper - 3-arm  
caliper from

**Resistivity**  
RXOZ - "Flushed zone"  
(near-wellbore)  
resistivity  
AHT10 - Shallow  
resistivity  
AHT20 - Intermediate  
resistivity

**Gamma**  
SGR - Standard gamma ray  
(includes K, U,  
and Th)  
CGR - Gamma minus  
energy from Uranium

LITHOLOGY

MUDSTONE  
clay/claystone  
conglomerate  
Very Coarse--Medium  
SANDSTONE  
Very Fine to Fine  
SANDSTONE

CONTACTS

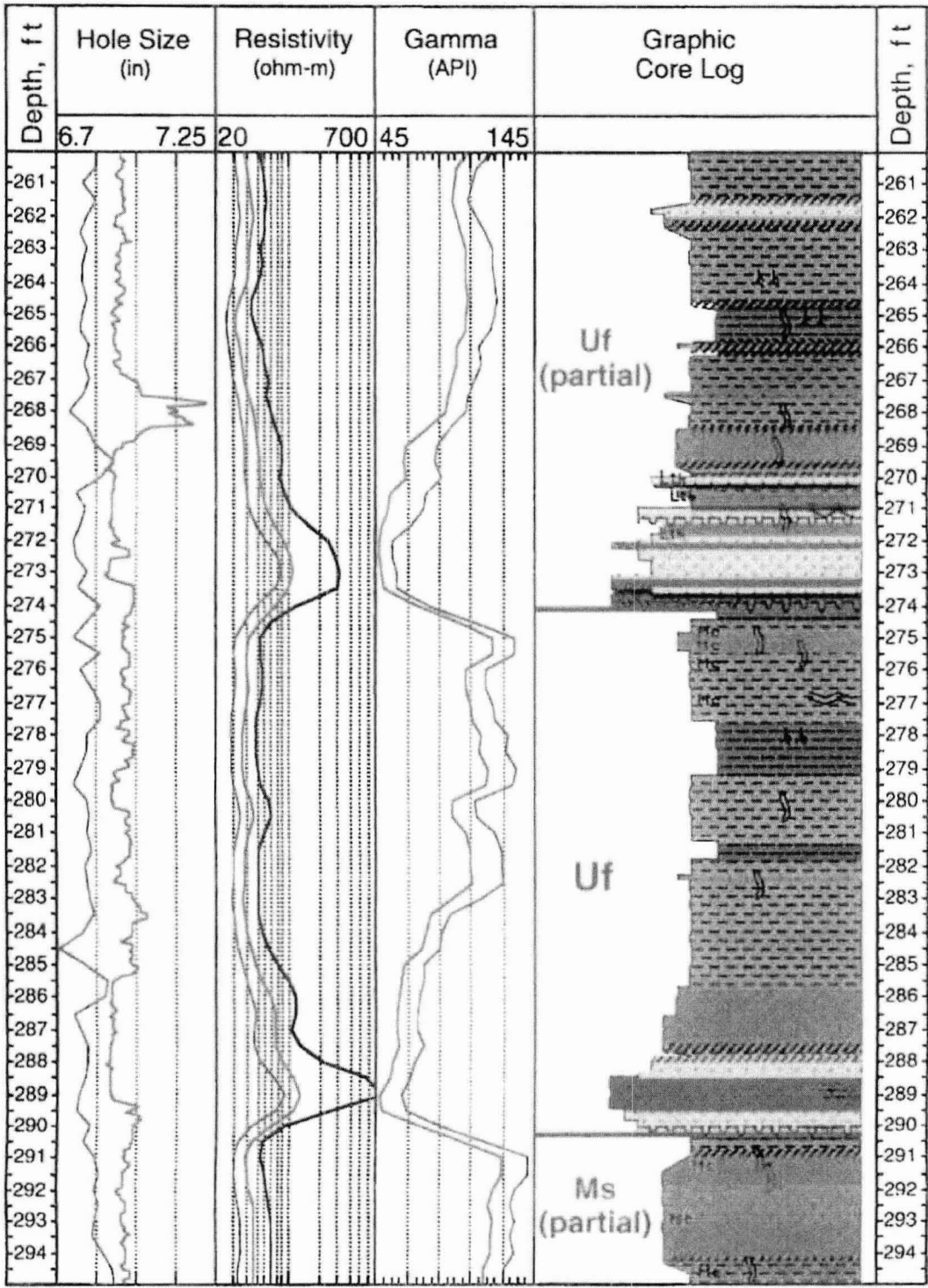
Sharp  
Bioturbated  
Gradational  
Sharp Load  
Vertical Scale 1" = 5'

PHYSICAL STRUCTURES

Trough Cross Bedding  
Lenticular Bedding  
Laminated  
Planar Bedding  
Convolute Bedding  
Wavy Parallel Bedding  
Slickensides

LITHOLOGIC  
ACCESSORIES

Lth - Lithic  
Mg - Manganese  
Mc - Micaceous  
Halo Aureoles  
Root Casts  
Burrow



**HLA** Harding Lawson Associates  
Engineering and Environmental Services  
2000 Aerial Center Parkway  
Suite 106  
Morrisville, N.C. 27560  
(919) 481-1660

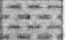


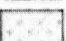
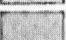




Type Geophysical Signatures  
of Mapping Unit Uf in W205CH1  
Between 260 - 295 Feet.








FIGURE: 5-1  
File Name: 205(260-295)GP/GCL  
REVISION NUMBER: 0  
DATE: 1/28/98

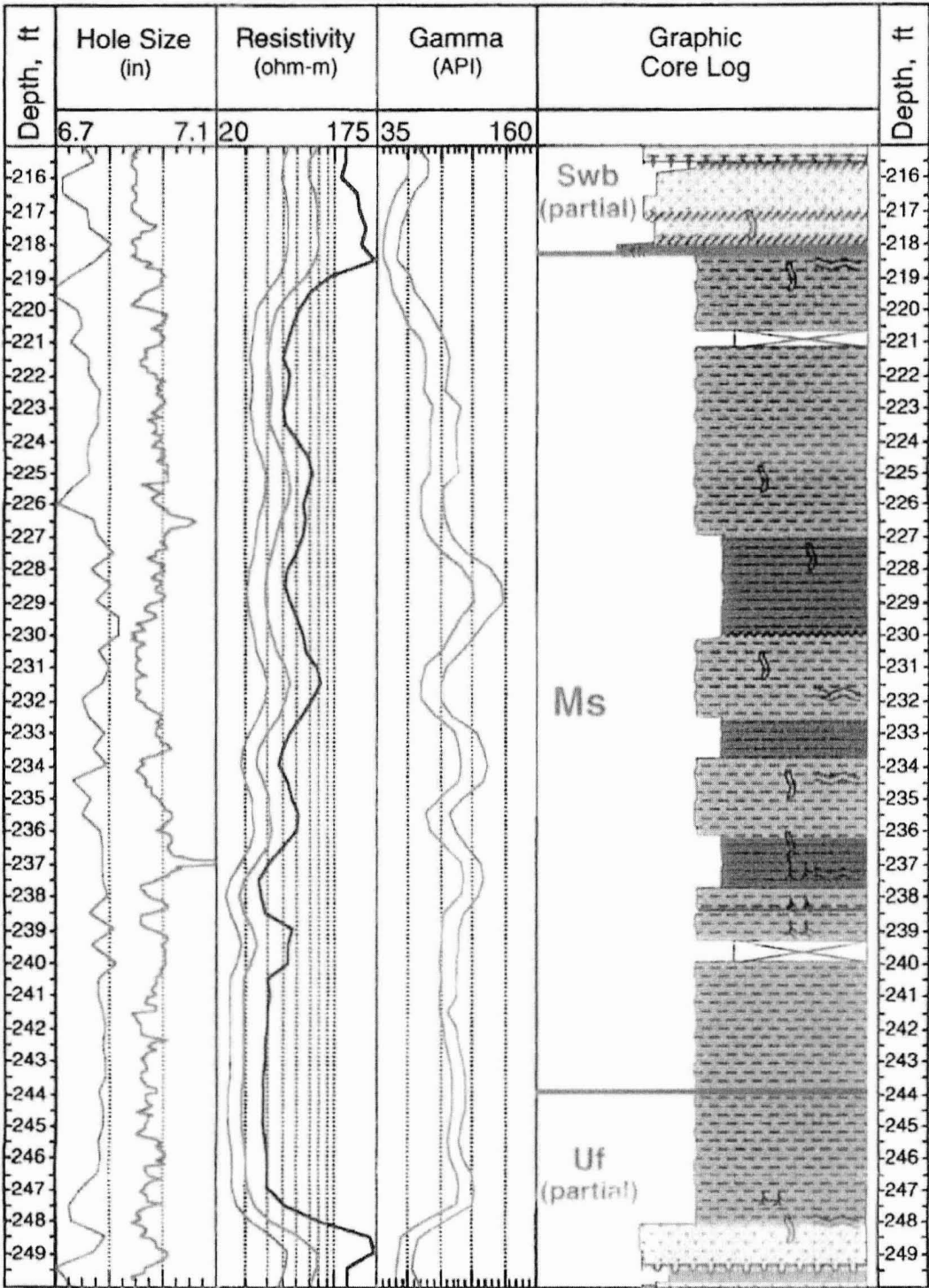
W205CH1 NCLLRWDF  
Wake County, North Carolina


LEGEND

**GEOPHYSICAL LOGS**  
**Hole Size**  
HCAL - 2-arm caliper  
from density log  
3-arm Caliper - 3-arm  
caliper from  
COLOG  
**Resistivity**  
RXOZ - "Flushed zone"  
(near-wellbore)  
resistivity  
AHT10 - Shallow  
resistivity  
AHT20 - Intermediate  
resistivity  
**Gamma**  
SGR - Standard gamma ray  
(includes K, U,  
and Th)  
CGR - Gamma minus  
energy from Uranium

**LITHOLOGY**  
 MUDSTONE  
 clay/claystone  
 conglomerate  
 Coarse to Medium  
SANDSTONE  
 Fine SANDSTONE  
**CONTACTS**  
 Sharp  
 Gradational  
 Sharp Flame  
 Sharp Load  
  
Vertical Scale 1" = 5'

**PHYSICAL STRUCTURES**  
 Trough Cross Bedding  
 Lenticular Bedding  
 Laminated  
 Planar Bedding  
 Convolute Bedding  
 Wavy Parallel Bedding  
 Slickensides  
  
**LITHOLOGIC  
ACCESSORIES**  
Lth - Lithic  
Mg - Manganese  
Mc - Micaceous  
⊙⊙⊙ - Halo Aureoles  
AA - Root Casts  
J - Burrow



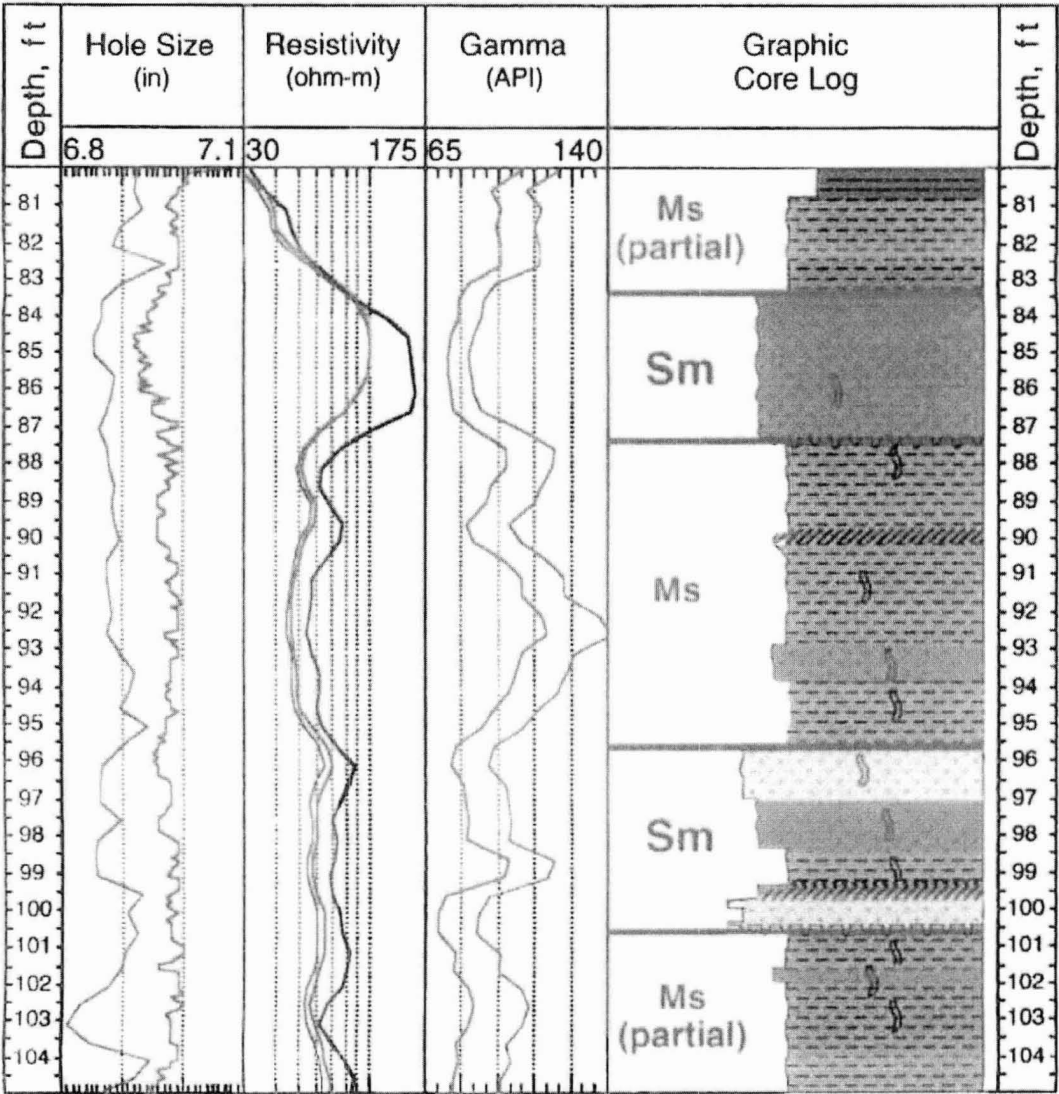
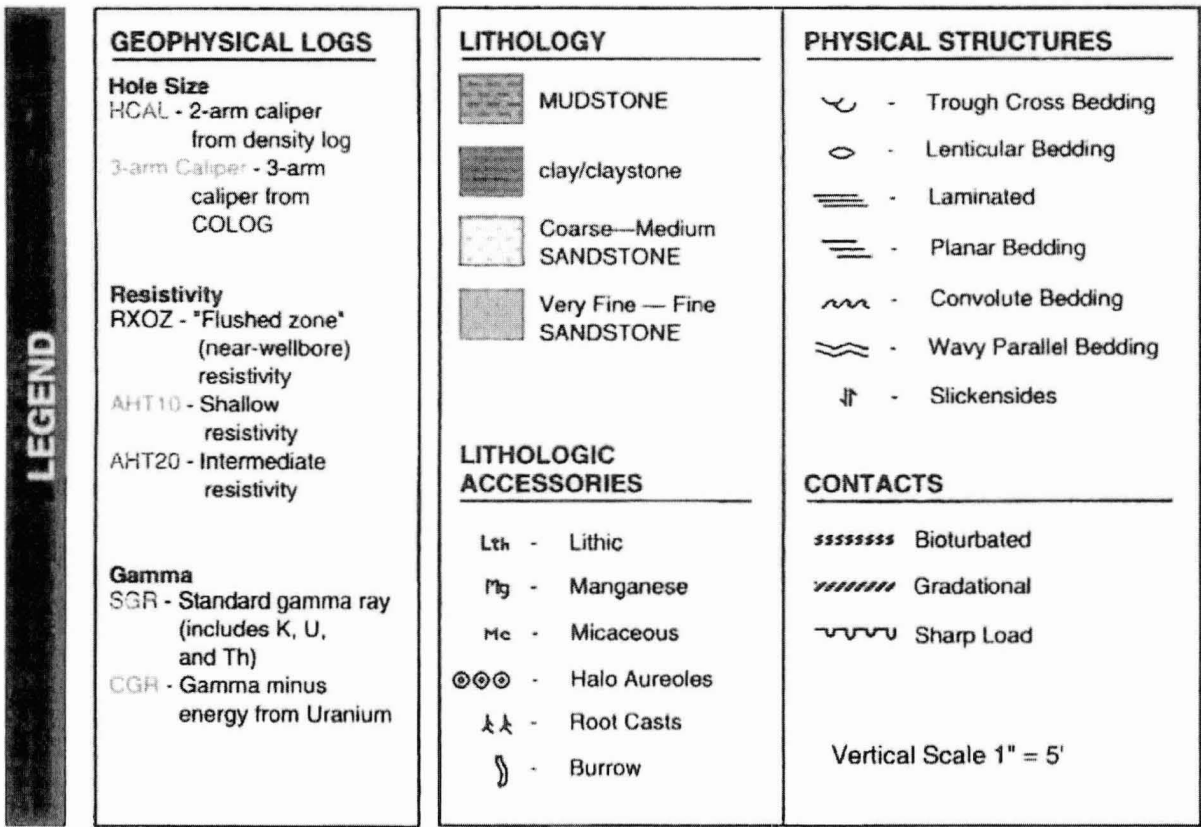
**HLA**

**Harding Lawson Associates**  
Engineering and Environmental Services  
  
2000 Aerial Center Parkway  
Suite 106  
Morrisville, N.C. 27560  
(919) 481-1660

Type Geophysical Signatures  
of Mapping Unit Ms in W205CH1  
Between 215 - 250 Feet.

FIGURE:	5-2
File Name:	205(215-250)GP/GCL
REVISION NUMBER:	0
DATE:	1/28/98

W205CH1 NCLLRWDF  
Wake County, North Carolina



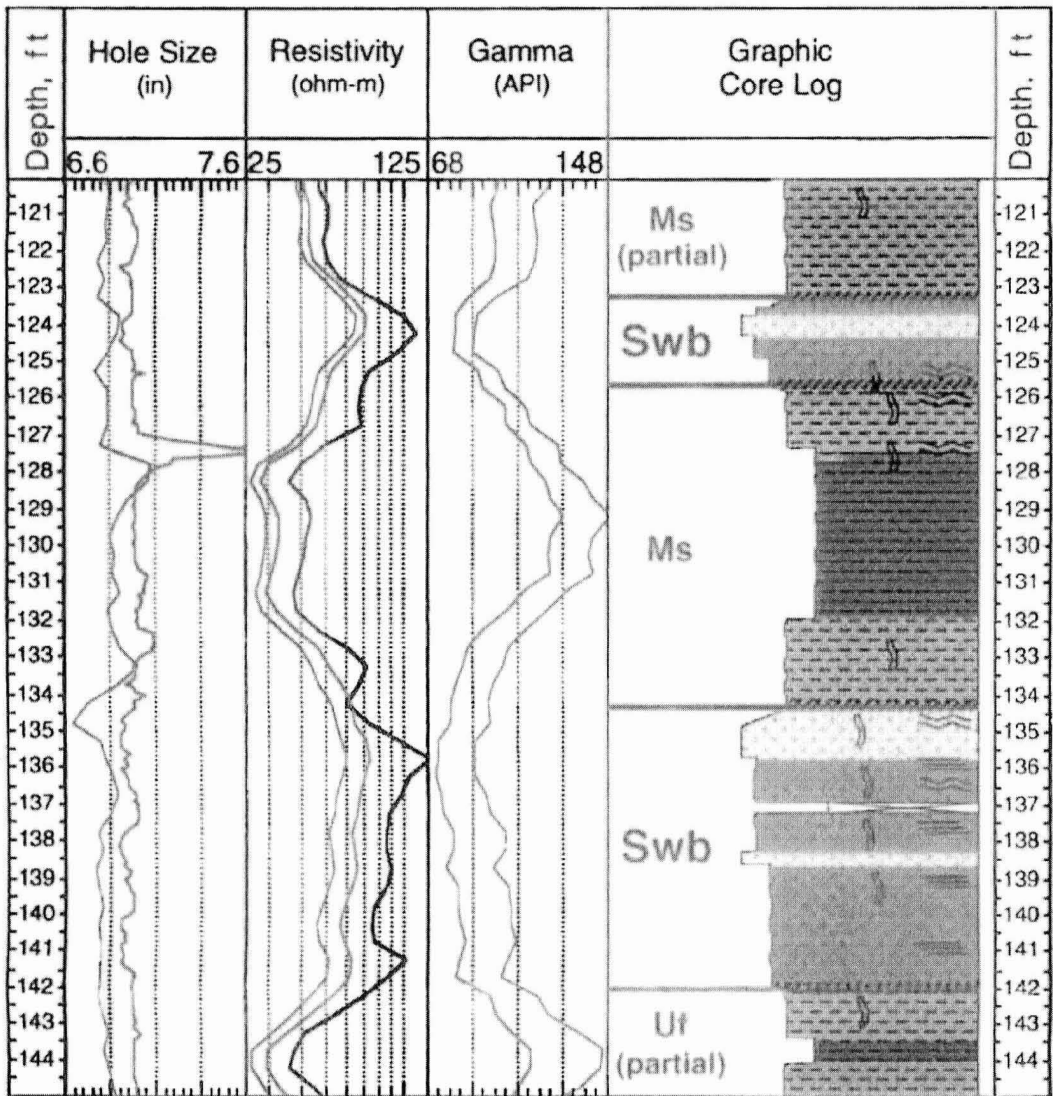
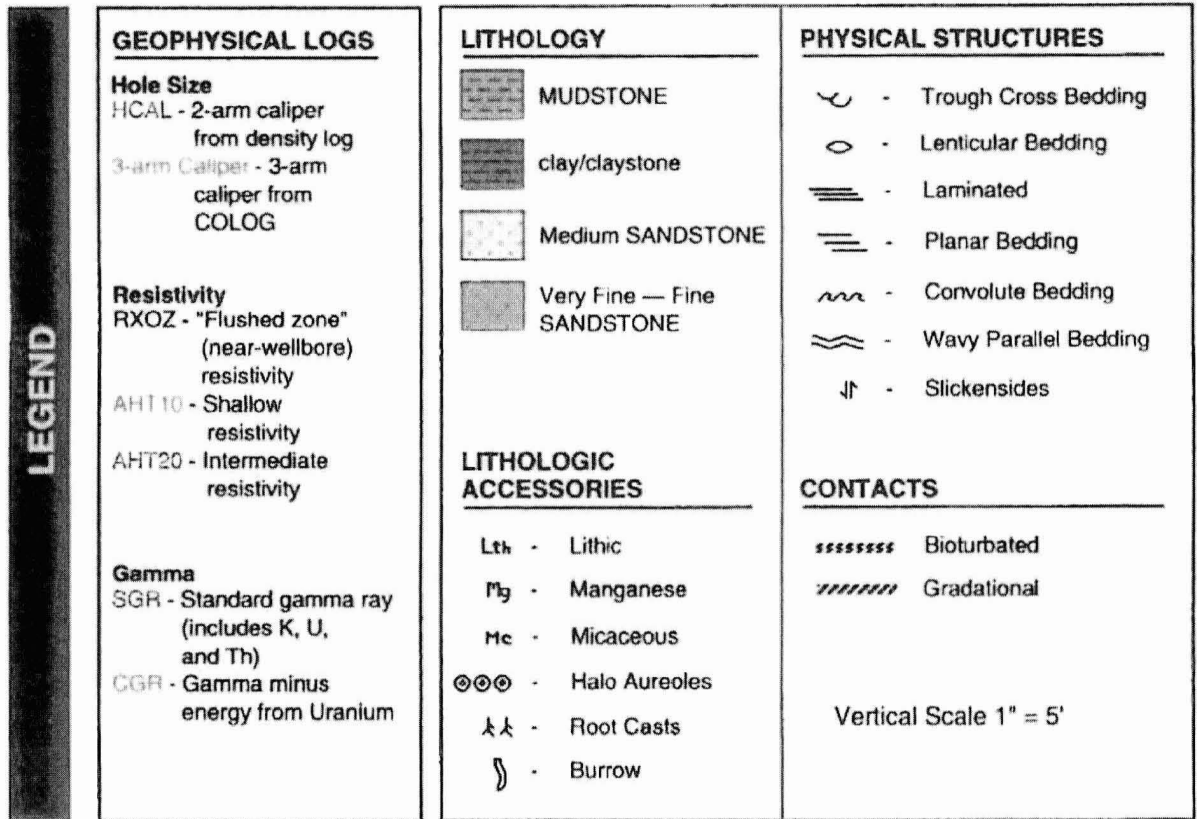
**Harding Lawson Associates**  
Engineering and Environmental Services  
**HLA** 2000 Aerial Center Parkway  
Suite 106  
Morrisville, N.C. 27560  
(919) 481-1660

Type Geophysical Signatures  
of Mapping Unit Sm in W205CH1  
Between 80 - 105 Feet.

FIGURE: 5-3  
File Name: 205(80-105)GP/GCL  
REVISION NUMBER: 0  
DATE: 1/28/98



W205CH1 NCLLRWDF  
Wake County, North Carolina

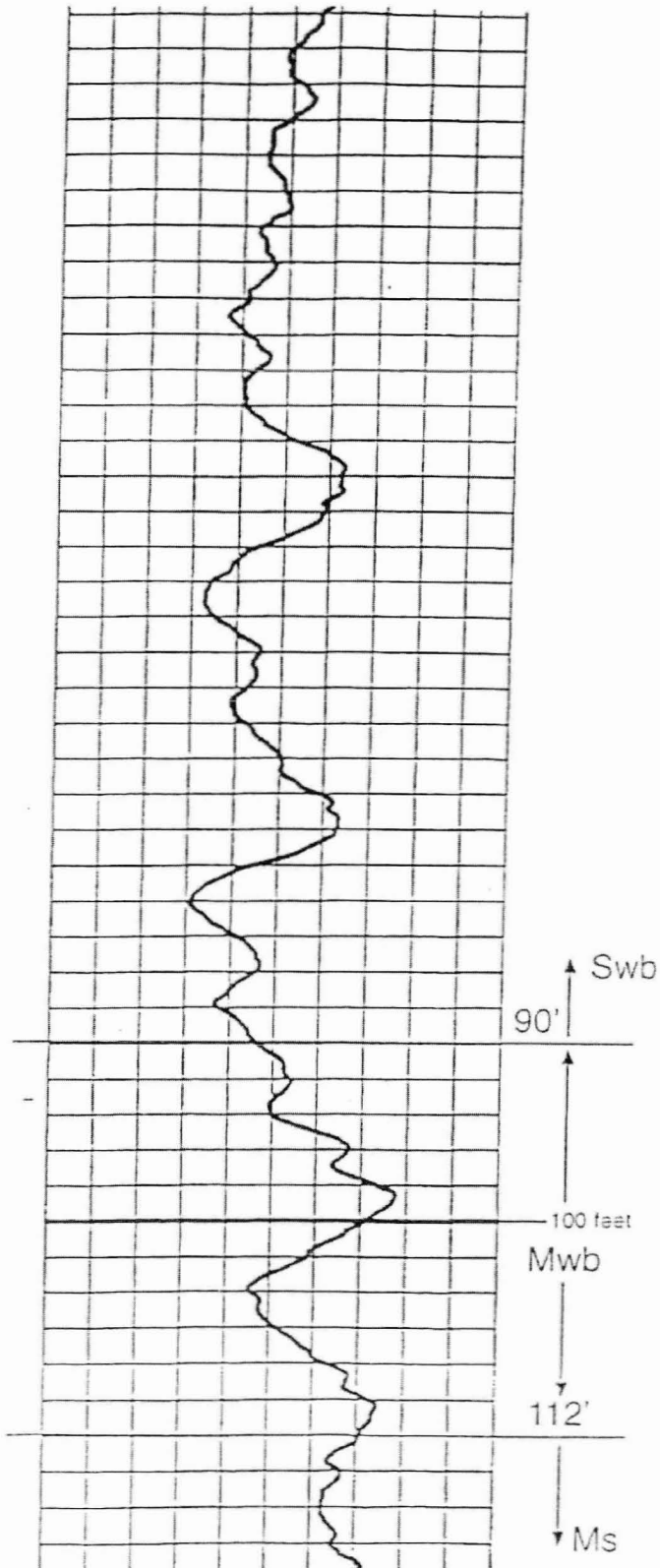


**HLA** Harding Lawson Associates  
Engineering and Environmental Services  
2000 Aerial Center Parkway  
Suite 106  
Morrisville, N.C. 27560  
(919) 481-1660

Type Geophysical Signatures  
of Mapping Unit Swb in W205CH1  
Between 120 - 145 Feet.

FIGURE: 5-4  
File Name: 205(120-145)GP/GCL  
REVISION NUMBER: 0  
DATE: 1/28/98

W104 MP18



Harding Lawson Associates  
Engineering and  
Environmental Services

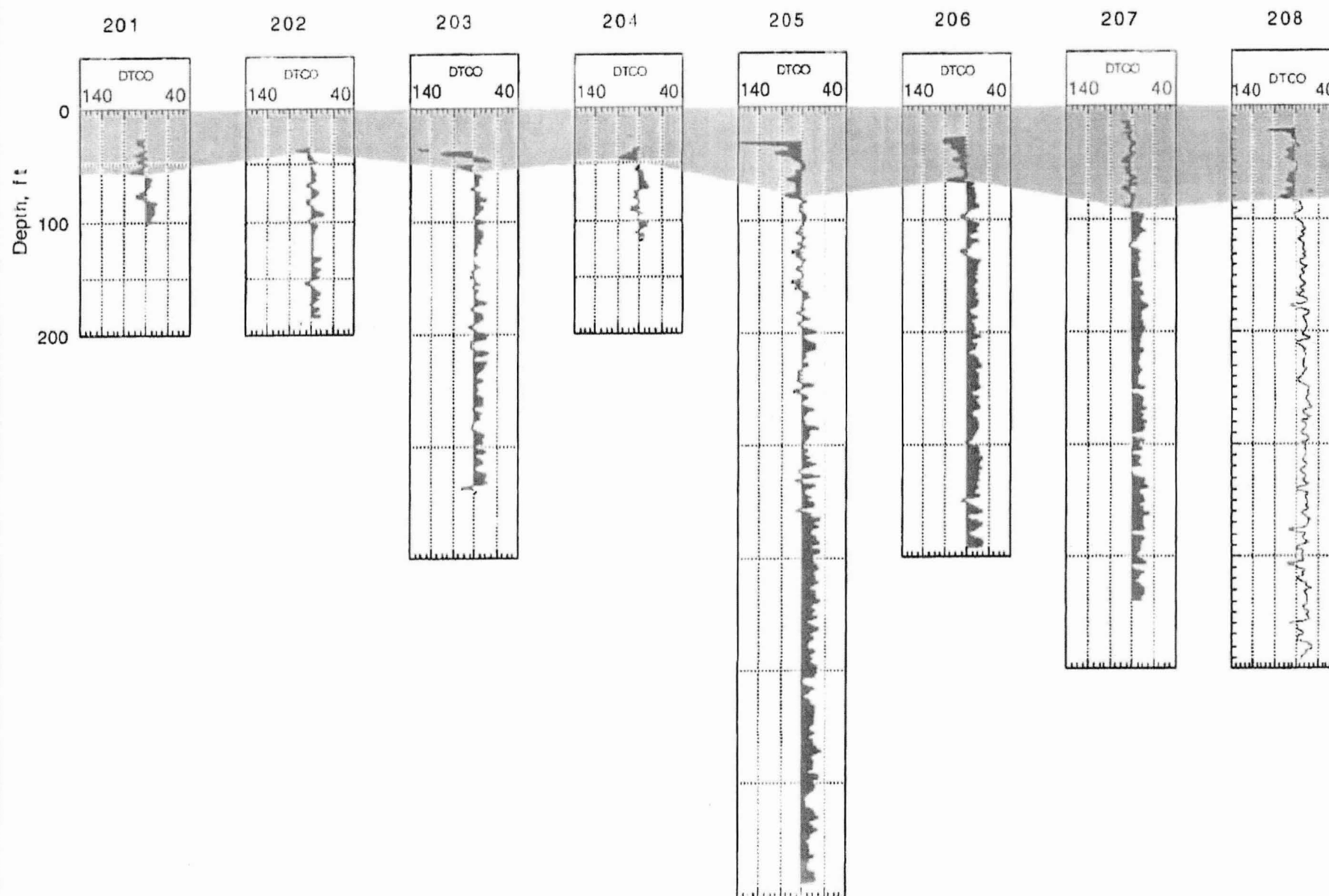
DRAWN PROJECT NUMBER  
GEA 36595.301

Gamma Log Signature for Well-Bedded  
Mudstone (Mwb) Map Unit  
Proposed North Carolina Low-Level  
Radioactive Waste Disposal Facility  
Wake County, North Carolina

APPROVED DATE  
10/97

FIGURE  
5-5

REVISED DATE



**Harding Lawson Associates**  
Engineering and  
Environmental Services

DRAWN  
DWN

PROJECT NUMBER  
36595,301

### Weathering Base / DTCO Curves

North Carolina Low-Level Radioactive  
Waste Disposal Facility Project  
Wake County, North Carolina

APPROVED

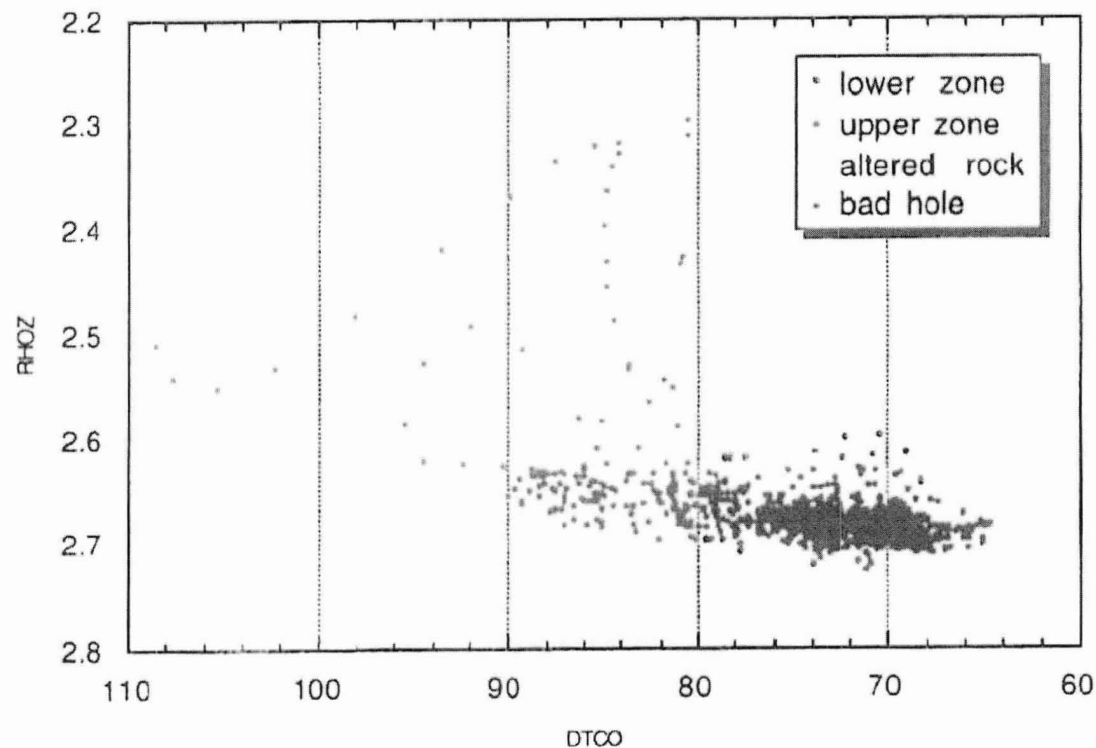
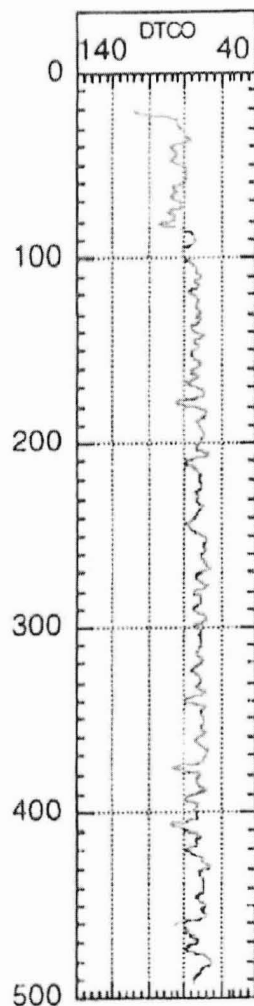
DATE  
10/97

REVISED DATE

FIGURE

**5-6**

# Hole W208CH1



Example - identification of upper zone using velocity and density data: criterion -  $DTCO > 80 \mu s/ft$   
Also illustrates the effect of washouts on density data; velocities are not affected.



Harcing Lawson Associates  
Engineering and  
Environmental Services

DRAWN  
DWN

PROJECT NUMBER  
36595.301

## DTCO versus RH0Z

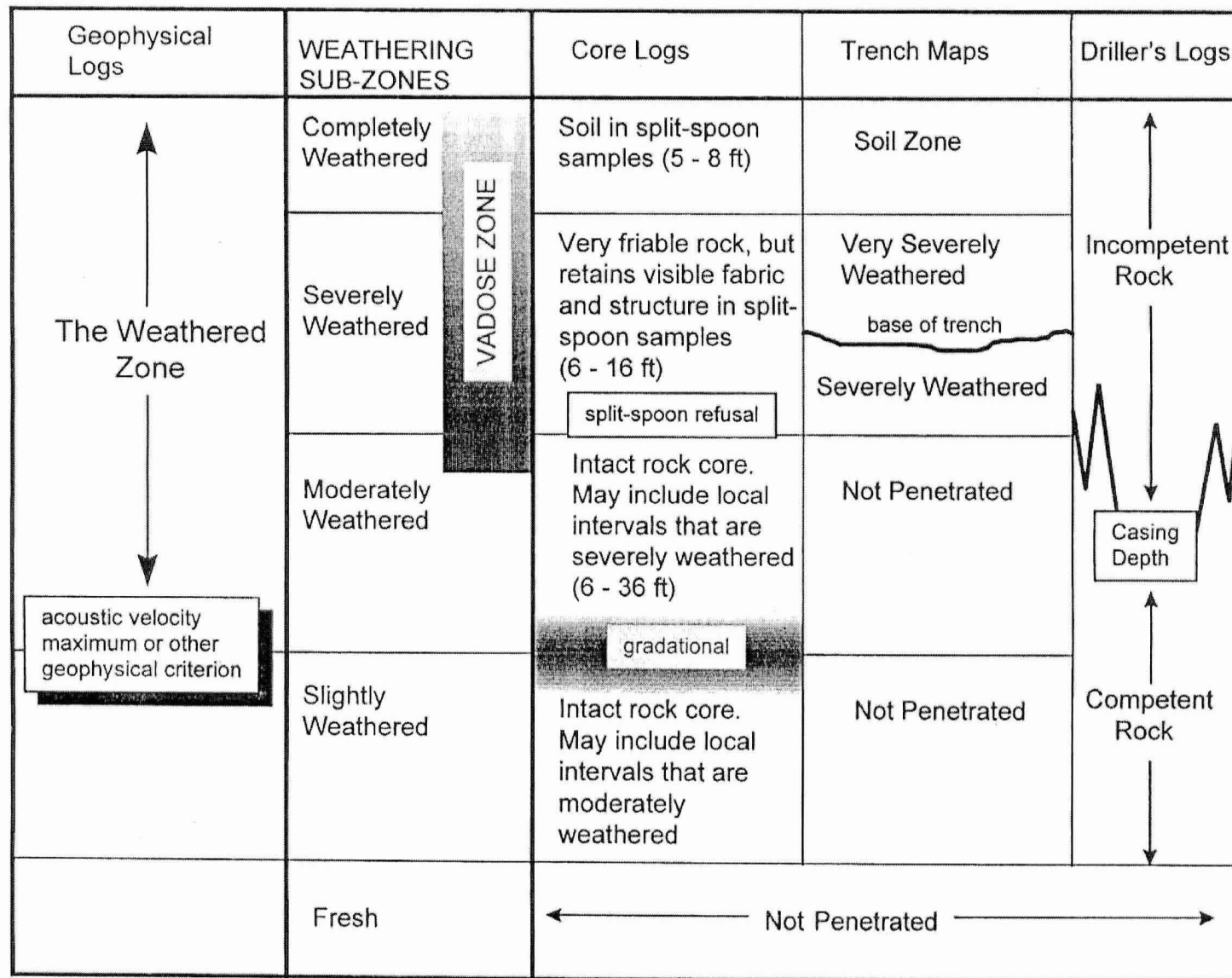
North Carolina Low-Level Radioactive  
Waste Disposal Facility Project  
Wake County, North Carolina

APPROVED

DATE  
10/97

FIGURE  
**5-7**

REVISED DATE



**Harding Lawson Associates**  
Engineering and  
Environmental Services

DRAWN  
DWN

PROJECT NUMBER  
36595,301

**Depth of Weathering Summary**  
North Carolina Low-Level Radioactive  
Waste Disposal Facility Project  
Wake County, North Carolina

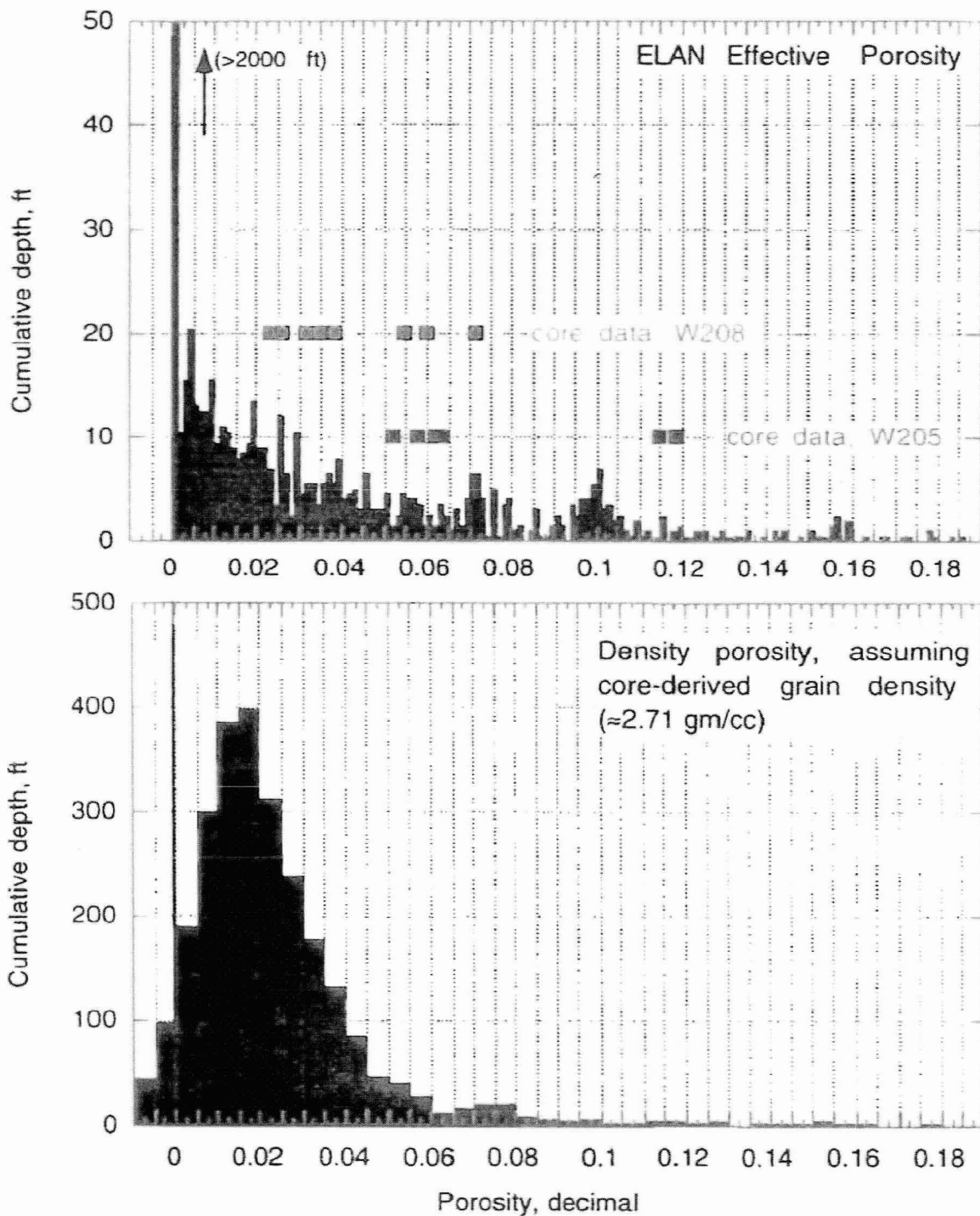
APPROVED

DATE  
10/97

REVISED DATE

FIGURE  
**5-8**

# Porosity Data Summary W201 - W208



**Harding Lawson Associates**  
Engineering and  
Environmental Services

DRAWN

PROJECT NUMBER  
36595,301

**Porosity versus Depth**  
North Carolina Low-Level Radioactive  
Waste Disposal Facility Project  
Wake County, North Carolina

APPROVED

DATE  
10/97

REVISED DATE

FIGURE  
**5-9**



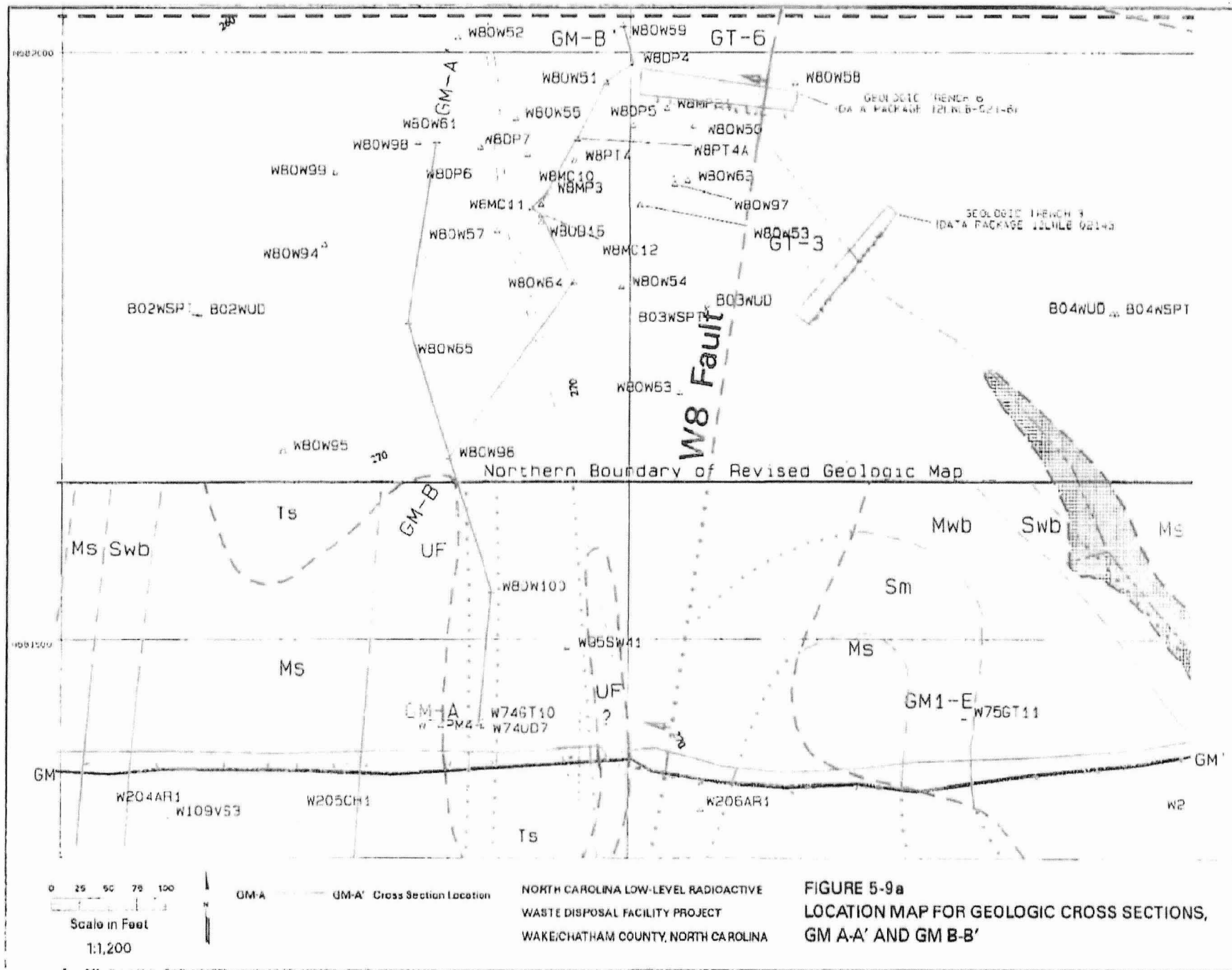
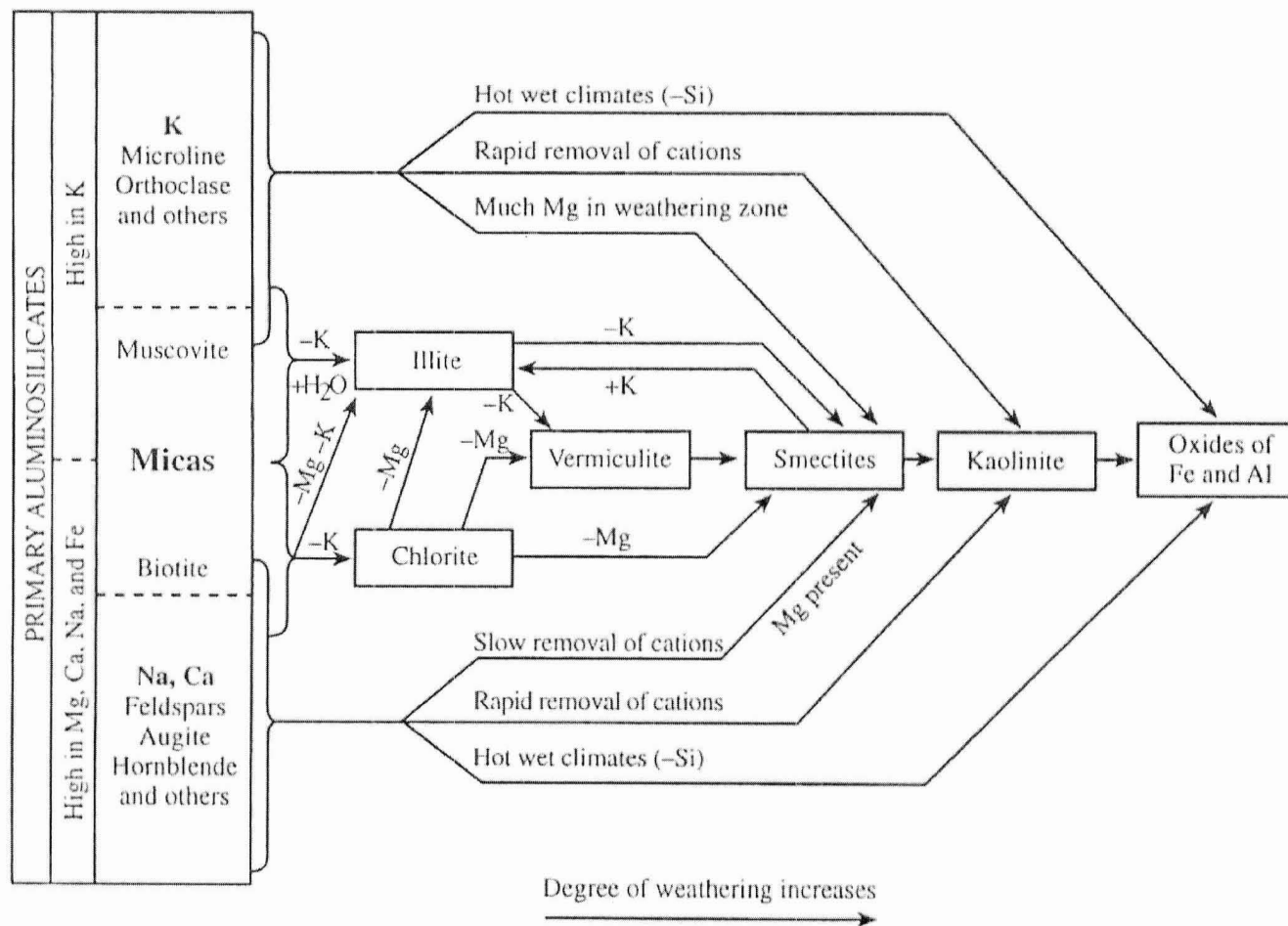


FIGURE 5-9a  
LOCATION MAP FOR GEOLOGIC CROSS SECTIONS,  
GM A-A' AND GM B-B'



Weathering products of primary minerals and sequence of forming clays (Langmuir, 1997)



**Harding Lawson Associates**  
Engineering and  
Environmental Services

**Weathering products**  
North Carolina Low-Level Radioactive  
Waste Disposal Facility Project  
Wake County, North Carolina

FIGURE

**5-10**

DRAWN  
GEA

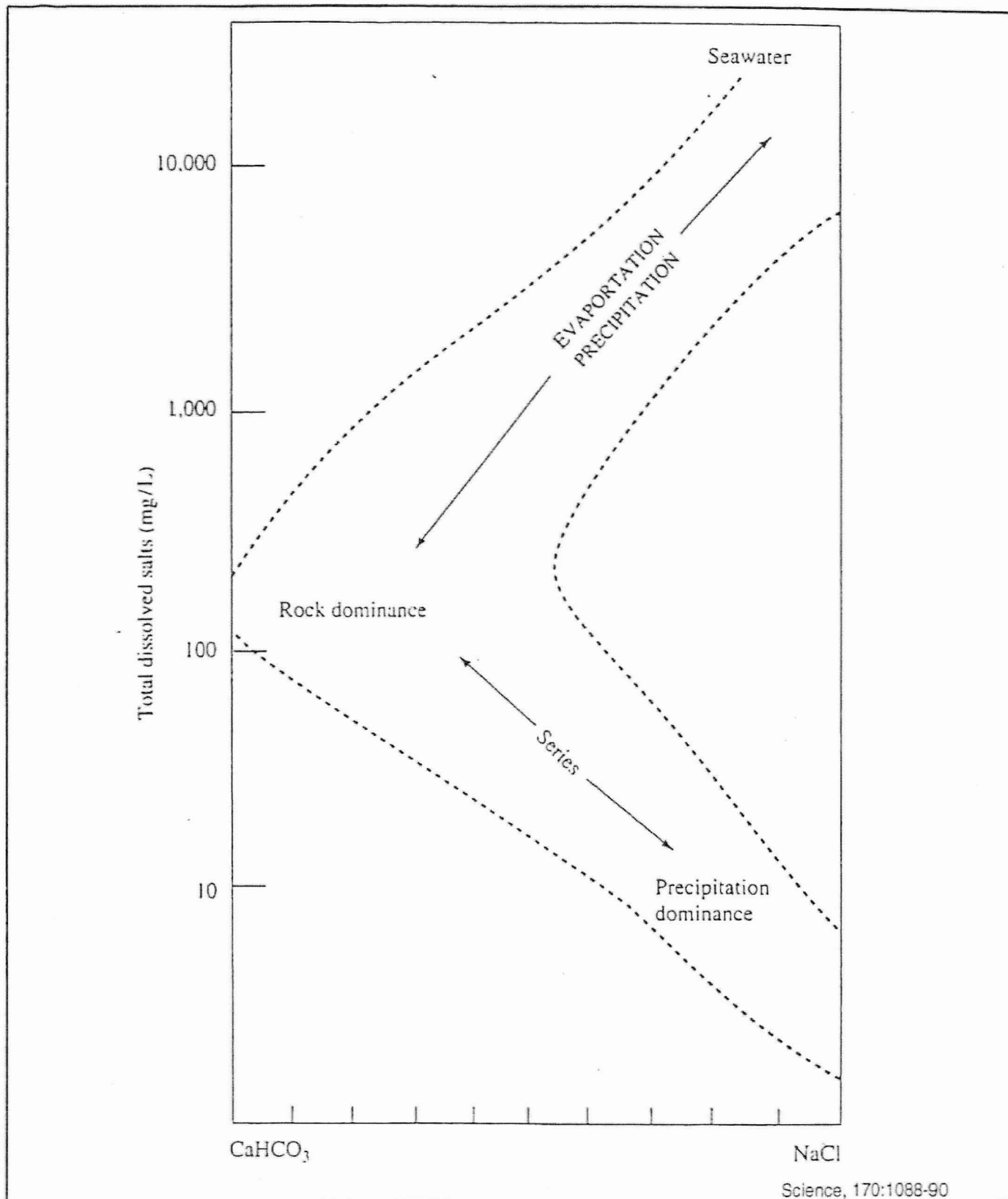
JOB NUMBER  
36595,301

APPROVED  
RAH

DATE  
10/97

REVISED DATE





Harding Lawson Associates  
Engineering and  
Environmental Services

Mechanisms Controlling  
Water Chemistry  
North Carolina Low-Level Radioactive  
Waste Disposal Facility Project  
Wake County, North Carolina

FIGURE

**5-11**

DRAWN  
LDZ

JOB NUMBER  
36595,301

APPROVED

DATE  
10/97

REVISED DATE